THE OXIDATION OF THE ENDOGENOUS CANNABINOID ANANDAMIDE AND THE SYNTHETIC CANNABINOID JWH-018, A DRUG OF ABUSE, BY HUMAN CYTOCHROME P450 2J2

by

Vyvyca J. Walker

A dissertation submitted in partial fulfillment
of the requirements for the degree of
Doctor of Philosophy
(Pharmacology)
in the University of Michigan
2014

Doctoral Committee:

Professor Paul F. Hollenberg, Chair
Professor Yoichi Osawa
Professor Marc Peters-Golden
Professor William L. Smith

DEDICATION

This work is dedicated to my husband. Thank you for your patience and understanding.

TABLE OF CONTENTS

LIST OF FIGURES

FIGURE

LIST OF TABLES

TABLE

LIST OF ABBREVIATIONS

AA-arachidonic acid
AEA-arachidonoyl ethanolamine or anandamide
APAU-1-(1-acetypiperidin-4-yl)-3-adamantanylurea
AUDA-12-(3-admantan-1-yl-ureido) dodecanoic acid
CB1R-cannabinoid 1 receptor
CB2R-cannabinoid 2 receptor
COX-cyclooxygenase
CYP-cytochrome P450
DHA-docosahexaenoic acid
DHET-dihydroxyeicosatrienoic acid
DHET-EA-dihyroxyeicosatrienoic acid ethanolamide
DIC-diphenyliodonium chloride
DIO-diet-induced obesity
DR-diet resistant
ECS-endocannabinoid system
EDP-epoxydocosapentaenoic acid
EET-epoxyeicosatrienoic acid
EET-EA-epoxyeicosatrienoic acid ethanolamide
EEQ-epoxyeicosatetraenoic acid
EH-epoxide hydrolase
EOA-epoxyoctadecenoic acid
EPA- eicosapentaenoic acid
HETE-hydroxyeicosatetraenoic acid
HETE-EA-hydroxyeicosatetraenoic acid ethanolamide
HIM-human intestinal microsomes
HLM-human liver microsomes
JFD-junk food diet
LA-linoleic acid
LOX-lipoxygenase
mEH-microsomal epoxide hydrolase
ND-normal diet
P450-cytochrome P450
PUFA-polyunsaturated fatty acid
RHM-rat heart microsomes
RLM-rat liver microsomes
sEH-soluble epoxide hydrolase
sEHI-soluble epoxide hydrolase inhibitor
SNP-single nucleotide polymorphism
TPPU-1-trifluoromethoxyphenyl-3-(1-propionylpiperidin-4-yl) urea

ABSTRACT

Cytochrome P450s (CYPs) are a superfamily of monooxygenases catalyzing the metabolism of various endogenous and exogenous compounds. CYP2J2 is highly expressed in the cardiovascular system and catalyzes the metabolism of arachidonic acid to give four vasoactive epoxyeicosatrienoic acids (EETs). Similar to the endogenous cannabinoid system, CYP2J2 is also expressed in the gastrointestinal tract, liver, kidney, and the brain. Therefore, we investigated the ability of CYP2J2 to metabolize anandamide (AEA), an endogenous cannabinoid, and JWH-018, a synthetic cannabinoid, thereby contributing to the regulation of the ECS.

We determined that purified CYP2J2 metabolizes AEA to give the 5,6-, 8,9-, 11,12-, and 14,15-epoxyeicosatrienoic acid-ethanolamides (EET-EAs) and 20-hydroxyeicosatrienoic acid-ethanolamide (HETE-EA) and characterized the metabolism in detail. Since AEA plays a role in energy balance, we investigated AEA metabolism by rat liver microsomes from rats bred to be susceptible or resistant to diet-induced obesity and determined that both diet and obesity have significant effects on AEA metabolism. Approaches for increasing the stability of the EET-EAs may aid in understanding their biological actions *in vivo.* Therefore, we tested several inhibitors of soluble epoxide hydrolase (sEH), the enzyme primarily responsible for EET hydrolysis, as inhibitors of the hydrolysis of EET-EAs. Our results indicate that the compounds tested were not

efficacious and that new inhibitors specific for the EET-EAs' epoxide hydrolases need to be developed.

Finally, we determined that JWH-018 is a substrate for CYP2J2 and characterized its metabolism in detail. JWH-018 is a drug of abuse that causes several adverse cardiovascular side effects, but relatively little is known about the metabolism or the pharmacology of this compound. Utilizing an animal model, we determined that JWH-018 causes a significant increase in blood pressure that appears to be only partially mediated by activation of the cannabinoid 1 receptor. Additional studies are required to fully understand the involvement of CYP2J2 in the ECS; however, because CYP2J2 regulates the metabolic fates of at least two ligands for the ECS, it is possible that CYP2J2 may play an important role in the ECS.

CHAPTER I

Introduction

Cytochrome P450s. Cytochrome P450s (P450s or CYPs) are members of a class of heme proteins that catalyze oxidation-reduction reactions. CYPs are distinct from all other members of this group because when the heme iron is reduced, it can bind to carbon monoxide and form a Soret peak with the wavelength for its maximum absorbance near 450, hence the name P450 (pigment absorbing at 450 nm). These P450s form their own superfamily of hemeprotein monooxygenases that are responsible for the metabolism of many exogenous and endogenous compounds. Individual CYPs are named based on their relative sequence homologies. P450s with at least 40% sequence homology are grouped into families and that family is given an Arabic numeral (1, 2, 3, etc.). CYPs with a sequence homology of 55% or greater are assigned to the same subfamily and are differentiated using a letter of the alphabet (A, B, C, etc.). Each member of the subfamily is then given an Arabic numeral corresponding to its sequence in discovery, i.e. CYP1A2. This name also corresponds to the gene, which is written in italics.

P450s can either activate or inactivate compounds and the ultimate outcome of P450-catalyzed metabolism is usually to make a compound more water soluble to aid with excretion from the body. CYPs have the ability to insert one oxygen atom from molecular oxygen (O_2) into a substrate while concurrently reducing the other oxygen atom by two electrons to form water (Ortiz de Montellano, 1995). Using this general

mechanism, P450 enzymes are known to catalyze hydroxylations, epoxidations, *N*-oxidations, dehalogenations, *N*-, *S*-, and *O*-dealkylations, sulfoxidations, and numerous other types of reactions (Ortiz de Montellano, 1995).

When a substrate binds in a substrate binding site of the active site of the P450, it induces a conformation change of the active site that may cause a water molecule to be displaced from the distal axial position of the heme iron (Meunier et al., 2004). This may then cause the heme iron to change from a low spin state to a high spin state which favors the transfer of an electron from nicotinamide adenine dinucleotide phosphate (NADPH) to the heme iron of the P450 by cytochrome P450 reductase (Poulos et al., 1987; Sligar et al., 1979). The electron transfer reduces the ferric heme iron of the resting P450 to the ferrous state allowing molecular oxygen to covalently bind to the distal axial position of the heme iron forming a ferrous P450-dioxygen complex (Ortiz de Montellano, 1995). The environment surrounding the oxygen atom allows the oxygen to be activated to a greater extent than in many other heme proteins which thus facilitates the transfer of a second electron from either cytochrome P450 reductase or cytochrome b_5 to form a peroxoiron(III) complex (Ortiz de Montellano, 1995). At rates too fast to be observed, the negatively charged peroxo group is rapidly protonated, the oxygen-oxygen bond is cleaved, the distal oxygen atom is incorporated into a water molecule, and a reactive iron-oxo complex is formed (Ortiz de Montellano, 1995). The oxygen atom is transferred from this iron-oxo species to the bound substrate followed by the dissociation of the product (Ortiz de Montellano, 1995). After the product is released from the active site, the CYP returns to its original state with a water molecule occupying a position close to the distal position of the heme iron (Guengerich, 2007).

CYPs have been identified in all domains of life, including animals, plants, fungi, and bacteria (Nelson, 2009). There are over 13,000 known P450s, and the genes for 57 have been identified in humans by the Human Genome Project (Nelson, 2009). CYPs are expressed in almost all tissues in the body, but the liver is the tissue with the highest expression levels of P450s. As a result of their high expression and critical roles on drug metabolism, P450s expressed in the liver have been well studied. P450s are also expressed in almost all extrahepatic tissues, including, but not limited to, the lungs, gastrointestinal tract, kidney, heart, and nasal tissue (Chaudhary et al., 2009; Pavek and Dvorak, 2008; Wu et al., 1996). CYP2J2 is one P450 that is mostly expressed in extrahepatic tissues. CYP2J2 is one of the main P450s responsible for the biotransformation of arachidonic acid (AA) to its four regioisomeric epoxyeicosatrienoic acids (5,6-, 8,9-, 11,12-, and 14,15-EET). Because of the importance of the biological actions of the EETs in the body, it is important to study CYP2J2 catalyzed reactions and how other substrates interact with fatty acid metabolism.

Cytochrome P450 2J2. Although this P450 was originally cloned from a cDNA library of the human liver, cytochrome P50 2J2 (CYP2J2) levels are relatively low in the liver compared to other P450s. On the other hand, CYP2J2 is highly expressed in the heart and in the cardiovascular system (Delozier et al., 2007; Wu et al., 1996). CYP2J2 is expressed in large and small coronary arteries, coronary artery smooth muscle cells, the aorta, vascular endothelial cells, and varicose veins (Bertrand-Thiebault et al., 2004; Delozier et al., 2007; Node et al., 1999; Wu et al., 1996). In addition to vascular tissues, CYP2J2 is expressed in the lung, kidney, liver, skeletal muscles, gastrointestinal tract, brain, monocytes, macrophages, and cancer cells and tissues (Bystrom et al., 2011; Chen

et al., 2011; Enayetallah et al., 2004; Jiang et al., 2005; Wu et al., 1996; Zeldin et al., 1997; Zeldin et al., 1996).

Substrates. In addition to arachidonic acid, CYP2J2 metabolizes several other polyunsaturated fatty acids (PUFAs), including eicosapentaenoic acid (EPA), docosahexaenoic acid (DHA), and linoleic acid (LA). CYP2J2 metabolizes EPA to 17,18-epoxyeicosatetraenoic acid (17,18-EEQ) and DHA to 19,20-epoxydocosapentaenoic acid (19,20-EDP)(Arnold et al., 2010). It was reported that at nanomolar concentrations, 17,18-EEQ and 19,20-EDP act as antiarrhythmic agents by inhibiting the Ca^{2+}-induced increased rate of spontaneous beating cardiomyocytes from neonatal rats (Arnold et al., 2010). CYP2J2 metabolizes linoleic acid (LA) to 9,10- and 12,13-epoxyoctadecenoic acids (EOAs) (Moran et al., 2000). These LA metabolites can reach millimolar concentrations in the serum of patients with significant burns (Kosaka et al., 1994). The presence of these compounds is associated with increased mortality in severely burned patients, as well as in patients suffering from systemic shock or adult respiratory distress syndrome (Kosaka et al., 1994; Moran et al., 2000; Ozawa et al., 1986). Moran and coworkers reported that linoleic acid and its monoepoxides induce mitochondrial dysfunction in a concentration dependent manner without causing oxidative stress prior to cell death (Moran et al., 2000). Our lab has investigated the ability of recombinant CYP2J2 to metabolize two other fatty acids, linolenic and dihomo-γ-linoleic acid, but no metabolism was observed (unpublished data).

In addition to PUFAs, CYP2J2 is known to catalyze the metabolism of the non-sedating antihistamines terfenadine, ebastine, and astemizole. CYP2J2 catalyzes the hydroxylation of terfenadine and ebastine (Lafite et al., 2007; Lafite et al., 2006; Liu et

al., 2006), the carboxylation of hydroxyebastine (Liu et al., 2006), and the *O*-demethylation of astemizole (Matsumoto et al., 2002). Several CYP3A4 substrates have been screened to see if they could serve as CYP2J2 substrates because of the similarities of the structures of the active sites of the two proteins. However, due to the relatively narrow channel available for the entry of potential CYP2J2 substrates into the active site, only seven new CYP2J2 substrates were identified from a total of 139 CYP3A4 substrates assayed (Lee et al., 2012). Lee and coworkers determined that the CYP3A4 substrates albendazole, amiodarone, cyclosporine A, danazol, mesoridazine, tamoxifen, and thioridazine were also substrates for CYP2J2 (Lee et al., 2012). More recently, Wu et al. (2013) reported the that CYP2J2 is a major contributor to the hydroxylation of albendazole and fenbendazole (Wu et al., 2013). Data suggest that CYP2J2 is also involved in the ω- and ω-1 hydroxylation of eperisone (Yoo et al., 2009). Similar to various other P450s, CYP2J2 is known to have its *in vivo* activity altered by a variety of inhibitors, inducers, and mutations.

Inhibitors. Several inhibitors of CYP2J2 activity have been investigated, but the inhibition appears to be substrate specific. *N*-Methylsulphonyl-6-(2-proparglyloxy-phenyl)hexanamide (MS-PPOH), 2-(2-propynyloxy)-benzenehexanoic acid (PPOH), and 17-.octadecynoic acid (17-ODA) are routinely used to inhibit CYP2J2 epoxygenase activity in studies of arachidonic acid metabolism (Jiang et al., 2005; Ke et al., 2007; Zhao et al., 2012). Ren and others have studied additional compounds for their ability to inhibit CYP2J2 activity and three were identified (Lee et al., 2012; Ren et al., 2013). Ren et al. (2013) determined that flunarizine is a competitive inhibitor of astemizole *O*-demethylation with a K_i of 0.13 μM (Ren et al., 2013). Telmisartan was also identified

during the same study as a mixed-type inhibitor of astemizole *O*-demethylation with a K_i of 0.19 μM (Ren et al., 2013). Lee and coworkers reported that danazol competitively inhibited both the hydroxylation of terfenadine with an IC_{50} of 77 nM and astemizole O-demethylation with a K_i of 20 nM (Lee et al., 2012). Because the development of a selective CYP2J2 inhibitor would be of great benefit in understanding the role of CYP2J2 in cardiovascular homeostasis, Lafite and others synthesized a number of CYP2J2 inhibitors structurally related to terfenadine and ebastine (Lafite et al., 2007; Lafite et al., 2006). Three compounds were determined to be selective for CYP2J2 inhibition. Compound 4 was identified as a competitive inhibitor of CYP2J2 which exhibited a K_i value of 160 nM (Lafite et al., 2007; Lafite et al., 2006). The other two inhibitors, compounds 5 and 13, where classified as mechanism-based inactivators with k_{inact}/K_i values of about 3000 $Lmol^{-1}s^{-1}$ (Lafite et al., 2007; Lafite et al., 2006).

Inducers. Contrary to the major P450 epoxygenases in the CYP2C family that are induced by nifedifpine, cortisol, and statins (Bauersachs et al., 2002; Fisslthaler et al., 2000; Fisslthaler et al., 2003), none of those compounds induce CYP2J2 mRNA or protein expression (Spiecker and Liao, 2005). However, EPA has been shown to induce CYP2J2 mRNA expression in a time- and dose-dependent manner (Wang et al., 2009). Moreover, EPA increased the cellular concentration of 11,12-EET significantly (Wang et al., 2009). These increases in CYP2J2 mRNA and 11,12-EET levels were significantly inhibited by the peroxisome proliferator-activated receptor γ (PPARγ) antagonist, GW9662, suggesting that PPARγ activity can alter CYP2J2 expression levels (Wang et al., 2009). One group reported that cocaine upregulated the expression of a P450 in the mouse heart that cross-reacted with a CYP2J2-specific antibody (Wang et al., 2002).

Although it was reported as CYP2J2, mice do not express CYP2J2, but they do express several of its homologues, including CYP2J5, CYP2J6, CYP2J8, CYP2J9, CYP2J11 and CYP2J12 that may have cross-reacted with the CYP2J2 antibody (Nelson, 2009).

Polymorphisms. The CYP2J2 gene is located on chromosome 1 and is approximately 40.3 kb in length with nine exons and eight introns (Ma et al., 1998). A considerable number of single nucleotide polymorphisms (SNPs) have been identified for CYP2J2, some of which are nonsynonymous and cause a protein coding change. King and others reported that the CYP2J2 variants D342N (CYP2J2*5) and P351L exhibit catalytic activity similar to that of the wild-type protein (CYP2J2*1) for AA and LA metabolism and astemizole *O*-demethylation and ebastine hydroxylation, respectively (King et al., 2002; Lee et al., 2005). Whereas the I192N (CYP2J2*4) variant exhibits decreased metabolism for AA only, mutants T143A (CYP2J2*2), R158C (CYP2J2*3), and N404Y (CYP2J2*6) exhibit decreased activity for the metabolism of both AA and LA when compared to wild-type (King et al., 2002). Out of 93 Korean subjects, 1.6% expressed the G312R mutant which, compared to wild-type, showed minimal functionality for the catalysis of astemizole *O*-demethylation (Lee et al., 2005). The most functionally relevant mutant discovered so far in humans is thought to be CYP2J2*7. This mutant contains a SNP in the proximal promoter of the CYP2J2 gene where a guanidine is substituted for a thymidine at the -50 position. Carriers of this mutation experience a 50% loss in promotor activity because the Sp1 transcription factor binding site is absent (Spiecker et al., 2004). In a study to determine the effect of the CYP2J2*7 variant, it was determined that subjects expressing this mutation had a significantly higher chance of having a myocardial infarction (Borgel et al., 2008) and coronary artery

disease (Spiecker et al., 2004). The overall importance and actual mechanisms by which these polymorphisms contribute to cardiovascular diseases such as hypertension and coronary artery disease remain to be elucidated; however, there is some evidence that the effects may be dependent on ethnicity (Dreisbach et al., 2005; Fava et al., 2010; Lee et al., 2007; Polonikov et al., 2008).

Arachidonic Acid Metabolism. AA metabolism in the heart occurs in the myocardial, endothelial, and vascular smooth muscle cells. Most of the AA in the heart is esterfied to the *sn*-2 position of phosphotidylethanolamine or phosphotidylcholine. Activation of phospholipases of the A_2 family (PLA_2s) determines the rate of eicosanoid production because they catalyze the release of the arachidonic acid from cellular phospholipids (Jenkins et al., 2009). The three phospholipases that catalyze AA release from cellular membranes are $iPLA_2\beta$, $iPLA_{2\gamma}$, and $cPLA_{2\alpha}$. Although all three of these phospholipases are calcium independent, $iPLA_2\beta$ is catalytically inactive when associated with camodulin, which provides some calcium mediated control (Wolf and Gross, 1996). Once released from cellular phospholipids, the free AA can then be oxidized by cyclooxygenases, lipoxygenases, and cytochrome P450 enzymes (Figure 1.1).

Metabolism of AA by Cylcooxygenase (COX). Prostaglandin synthase (PGS) or COX utilizes its cyclooxygenase activity to catalyze the addition of two oxygen atoms to AA to form prostaglandin G_2 (PGG_2). The enzyme's peroxidase activity subsequently converts PGG_2 to the prostanoid series-2 precursor prostaglandin H_2 (PGH_2). In the heart, PGH_2 is converted to prostaglandin E_2, prostaglandin $F_{2\alpha}$, and prostaglandin I_2 by their respective synthases (Jenkins et al., 2009). Both COX-1 and COX-2 are found in the human heart (Zidar et al., 2007). COX-1 is thought to be involved in the maintenance of

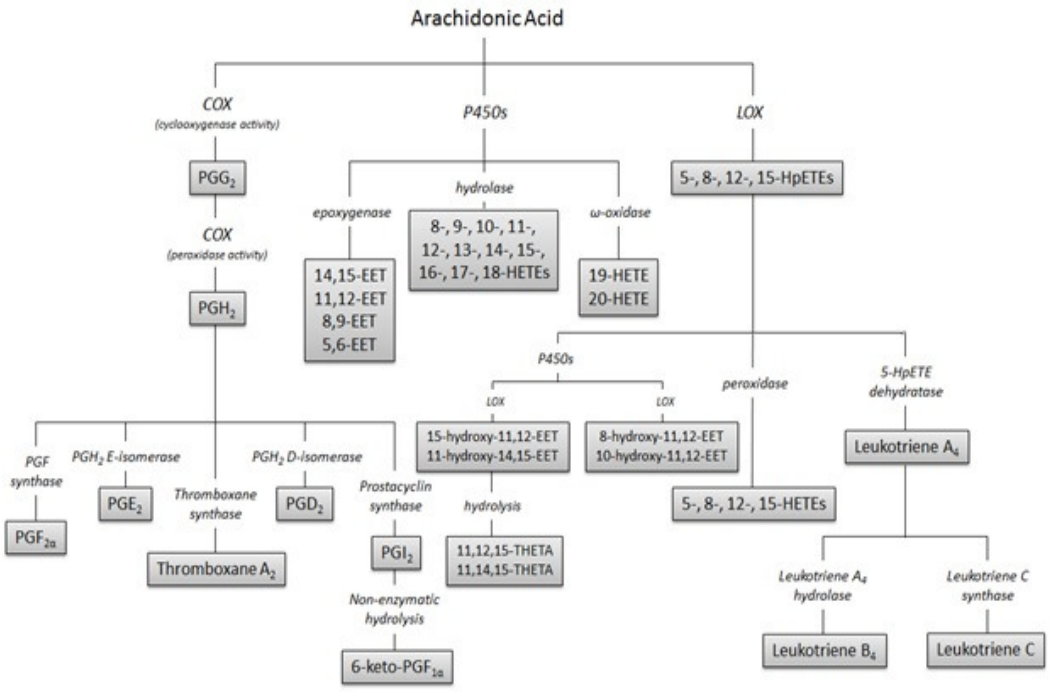

Figure 1.1. Arachidonic acid oxidation in the body. COX, cyclooxygenase; EET, epoxyeicosatrienoic acid; HETE, hydroxyeicosatrienoic acid; HpETE, hydroperoxyeicosatraenoic acid; P450, cytochrome P450; PG, prostaglandin; THETA, trihydroxyeicosatrienoic acid (adapted from Jenkins et al., 2009).

normal cardiovascular function since it is constitutively expressed (Zidar et al., 2007). Conversely, COX-2 is induced in several pathological states and depending on the extent of induction, the pathophysiological condition, and ability of specific cells to form the cardioprotective prostaglandins, PGE_2 and PGI_2, determines if COX-2 mediated inflammation is beneficial or detrimental (Pitt et al., 1983; Shinmura et al., 2000; Wong et al., 1998; Wu, 1998).

Metabolism of AA by Lipoxygenase (LOX). Lipoxygenases produce hydroperoxy-eicosatraenoic acids (HpETEs) by catalyzing the oxidation of olefin linkages in AA. Studies using rat hearts and cultured cardiomyocytes have shown that 12-LOX is responsible for most of the lipoxygenase activity, while 15-LOX only catalyzes a small portion of reactions (Breitbart et al., 1996). HpETEs are subsequently reduced to hydroxyeicosatetraenoic acids (HETEs) by several different enzymes, including phospholipid hydroperoxide glutathione peroxidase and cystolic glutathione peroxidase (Bhatia et al., 2012; Jakobsson et al., 1997; Sutherland et al., 2001). Although the importance of LOX and its metabolites in cardiac function and homeostasis remain relatively unknown, this pathway is believed to be involved in insulin sensitivity and in the development of cardiac fibrosis and hypertrophy (Dransfeld et al., 2002; Wen et al., 2003).

Cytochrome P450-catalyzed Metabolism of AA. Cytochrome P450s metabolize AA to epoxyeicosatrienoic acids (EETs) and HETEs. Due to the relative promiscuity of many of the CYPs, several P450 families are known to metabolize arachidonic acid. Members of the CYP4A, 4B, and 4F families are known to serve as ω-hydrolases and are also responsible for the hydroxylation of arachidonic acid to 17-, 18-, 19-, and 20-HETEs

(Chaudhary et al., 2009; Powell et al., 1998; Roman, 2002). In vascular smooth muscle (VSM) cells, 20-HETE is a potent vasoconstrictor that prevents the depolarization of VSM cells by inhibiting Ca^{2+}-activated K^+ (K_{Ca}) channels (Roman et al., 2000).The vasoconstriction mediated by 20-HETE normally occurs in small arteries and arterioles no larger than 100 µm in diameter (Roman, 2002). Structural analogs of 20-HETE such as 5-, 15-, and 19-HETE block its actions in certain vascular beds (Alonso-Galicia et al., 1999). Although the exact mechanism that 20-HETE utilizes to block K_{Ca} channels has not yet been determined, studies using animal models have reported activation of protein kinase C (PKC), mitogen-activated protein (MAP) kinase signal transduction, extracellular signal-related kinase (ERK), and tyrosine kinase by 20-HETE, depending on the cell type (Lange et al., 1997; Sun et al., 2002). Activation of MAP kinases is the mechanism used by 20-HETE to induce VSM cell proliferation (Muthalif et al., 2001). In addition, 20-HETE is thought to play an influential role in the autoregulation of blood flow, as well as myogenic responses to changes in vascular pressure, and it is thought to act as an oxygen sensor in the microcirculation in certain tissues (Frisbee et al., 2001; Gebremedhin et al., 2000; Harder et al., 1996; Imig et al., 1999; Imig et al., 1994).

Enzymes from P450 families 1A, 2B, 2C, 2E, 2J, 3A, and 4A can catalyze the formation of arachidonic acid epoxide metabolites (Daikh et al., 1994; Laethem et al., 1994; Mitra et al., 2011; Rifkind et al., 1995; Roman, 2002; Scarborough et al., 1999; Wang et al., 1996). There are four potential epoxides that can be formed as a result of P450-mediated AA metabolism; however, the efficiency and metabolite profile by which the various CYP isoforms produce these epoxides are different. The 2C and 2J families are the most efficient at catalyzing the AA epoxygenase pathway. In the liver and kidney,

the CYP2C isoforms are mostly responsible for EET synthesis; however, CYP2J2 is believed to play a major role in the metabolism of AA in the cardiovascular system due to its much higher expression levels relative to CYP2C8 and CYP2C9 in the heart (CYP2J2 > CYP2C8) and in the vascular tissues (CYP2C9 > CYP2J2 > CYP2C8) (Askari et al., 2013; Delozier et al., 2007; Spiecker and Liao, 2005; Wu et al., 1996; Zeldin et al., 1995).

Biological Functions of Epoxyeicosatrienoic Acids. The EETs and other P450-catalyzed metabolites of AA are considered to be autocrine/paracrine mediators because these compounds act on the same cell or a neighboring cell of the cell from which they were secreted. The concentration of EETs is mostly regulated by their lipophilicity, protein binding, and rapid incorporation into the phospholipids of several cell types (Karara et al., 1991; VanRollins et al., 1996; Widstrom et al., 2001; Wu et al., 1996). Thus, these factors keep the tissue concentrations of these eicosanoids higher near their sites of formation than the levels found in plasma, urine, or interstitial fluid (Roman, 2002). Lipid extracts from human tissues have shown that the levels of incorporation of the EETs into membranes may reach micromolar levels (Karara et al., 1991). Biological stimuli that activate phospholipases, such as vasoactive hormones, can trigger the release of the EETs from membrane-bound phospholipids. This evidence may be indicative of the biological fates of structurally similar compounds. Physiologically active EETs have several different effects on the body that include effects on cardiovascular tone, inflammation, thrombolytic activity, and angiogenesis.

EETs regulate vascular tone by activating Ca^{2+}-sensitive K^+ (K_{Ca}) channels and causing vasodilation. They are believed to be the endothelial-derived hyperpolarizing

factors (EDHFs) in vascular smooth muscle cells (Campbell et al., 1996; Fleming, 2004; Harder et al., 1995). Likewise, EETs can directly and indirectly affect other ion channels including L-type Ca^{2+} channels, ATP-sensitive K^+ channels (K(ATP)), and Na^+ channels (Lee et al., 1999; Lu et al., 2001; Seubert et al., 2004; Xiao et al., 1998; Xiao et al., 2004). Xiao and coworkers reported that the EETs increase cardiac L-type Ca^{2+} currents in ventricular myocytes utilizing a mechanism which involves cAMP-protein kinase A-dependent phosphorylation of L-type Ca^{2+} channels (Xiao et al., 1998; Xiao et al., 2004). The 11,12- and 8,9-EET regioisomers are potent activators of (K(ATP)) and can reduce the sensitivity of the channels to ATP in rat cardiomyocytes (Lu et al., 2001). Moreover, the cardioprotection observed in transgenic mice with cardiomyocyte-specific overexpression of CYP2J2 involves the activation of mitochondrial (K(ATP)) channels and the p42/p44 MAPK pathway (Seubert et al., 2004). The EETs, especially 8,9-EET, act as potent Na^+ channel inhibitors by decreasing the probability of the Na^+ channel opening (Lee et al., 1999).

EETs exhibit anti-inflammatory effects similar to those observed for members of the peroxisome proliferator-activated receptor (PPAR) family (Liu et al., 2005; Node et al., 1999). The EETs and PPARα inhibit NF-κB activation and vascular cell adhesion molecule-1 (VCAM-1) expression (Node et al., 1999; Rival et al., 2002). In addition to PPARγ activation, 14,15-, 11,12-, and 8,9-EET have been shown to inhibit cyclooxygenase activity (Fitzpatrick et al., 1986; Mendez and LaPointe, 2003). While 11,12-EET is believed to activate PPARα directly, PPARγ is thought to be an effector of the EETs (Liu et al., 2005; Ng et al., 2007). EETs and their metabolites may, in fact, be the endogenous ligands for PPARα and PPARγ because activation of these receptors has

similar effects as EETs on the inhibition of cell migration and inflammation (Wray and Bishop-Bailey, 2008).

Utilizing several different pathways, epoxyeicosatrienoic acids can modulate thrombolytic activity. At physiological concentrations, EETs, especially 11,12-EET, are known to increase tissue plasminogen activator expression and activity via $G_{\alpha}s$ activation, while having no effect on plasminogen activator inhibitor-1 expression (Node et al., 2001). Using a mechanism that has yet to be determined, all of the EETs inhibit platelet aggregation induced by AA (Fitzpatrick et al., 1986). EETs also inhibit platelet adhesion to endothelial cells through a calcium-activated potassium channel dependent mechanism (Krotz et al., 2004). Moreover, Zhang et al. (2008) reported that 11,12-epoxyeicosatrienoic acid activates the L-arginine/nitric oxide pathway in human platelets (Zhang et al., 2008).

EETs are known to inhibit apoptosis and promote cell proliferation and angiogenesis in several different models (Askari et al., 2013; Fleming, 2011; Panigrahy et al., 2011). EETs employ multiple mechanisms in order to cause these biological outcomes, including crosstalk with the epithelial growth factor receptor (EGFR), activation of mitogen-activated protein kinase (MAPK) and PI3K/Akt signaling pathways, SRC-activation of STAT-3, and increased endothelial nitric oxide synthase (eNOS) expression (Chen et al., 2001; Cheranov et al., 2008; Jiang et al., 2007; Michaelis et al., 2005; Node et al., 2001; Wang et al., 2003; Wang et al., 2005). Incidentally, these same mechanisms that promote cancer-like activities, i.e. cell proliferation and inhibition of apoptosis, allow the CYP epoxygenase CYP2J2 to be protective against cardiac stress, doxorubicin-induced cardiotoxicity, and after hypoxic or ischemic events (Katragadda et

al., 2009; Nithipatikom et al., 2006; Seubert et al., 2004; Yang et al., 2001; Zhang et al., 2009). Only the expression of the cardiac-specific CYP2J2, not the expression of endothelial-specific CYP2J2, is thought to be beneficial in ischemic-reperfusion injury (Askari et al., 2013; Edin et al., 2011; Seubert et al., 2004). However, this benefit in ischemic-reperfusion injury is believed to be mediated only by CYP2J2, because CYP2C8 and CYP2C9 activities have been shown to be detrimental to cardiac recovery due to their production of reactive oxygen species (Edin et al., 2011; Khan et al., 2007).

Secondary Metabolism of Epoxyeicosatrienoic Acids. In addition to causing important biological effects, free epoxyeicosatrienoic acids can undergo secondary reactions including: hydration by soluble epoxide hydrolase (sEH); oxidation by cyclooxygenase, lipoxygenase, and P450 ω-oxidase enzymes; partial β-oxidation; chain-elongation; and glutathione conjugation (Figure 1.2). The epoxide metabolites of P450-catalyzed arachidonic acid metabolism are usually converted by soluble epoxide hydrolase to form dihydroxyeicosatrienoic acids (DHETs), which are generally believed to be less biologically active than the precursory epoxides (Imig et al., 1996; Roman, 2002). However, DHETs are as potent as the EETs in the dilation of canine coronary arteries (Oltman et al., 1998). Moreover, 14,15-DHET can activate PPARα in a COS-7 cell expression system (Fang et al., 2006). The substrate preference for the hydration of EETs by rabbit sEH is 14,15-EET > 11,12-EET > 8,9-EET (Zeldin et al., 1993).

Oxidation. Although 5,6-EET is reported to be a poor substrate for sEH (Sisignano et al., 2012; Zeldin et al., 1993), it is readily oxidized by cyclooxygenase in the vasculature to 5-hydroxy-PGI_1 and 5,6-epoxy-PGE_1 (Carroll et al., 1993; Oliw, 1984).

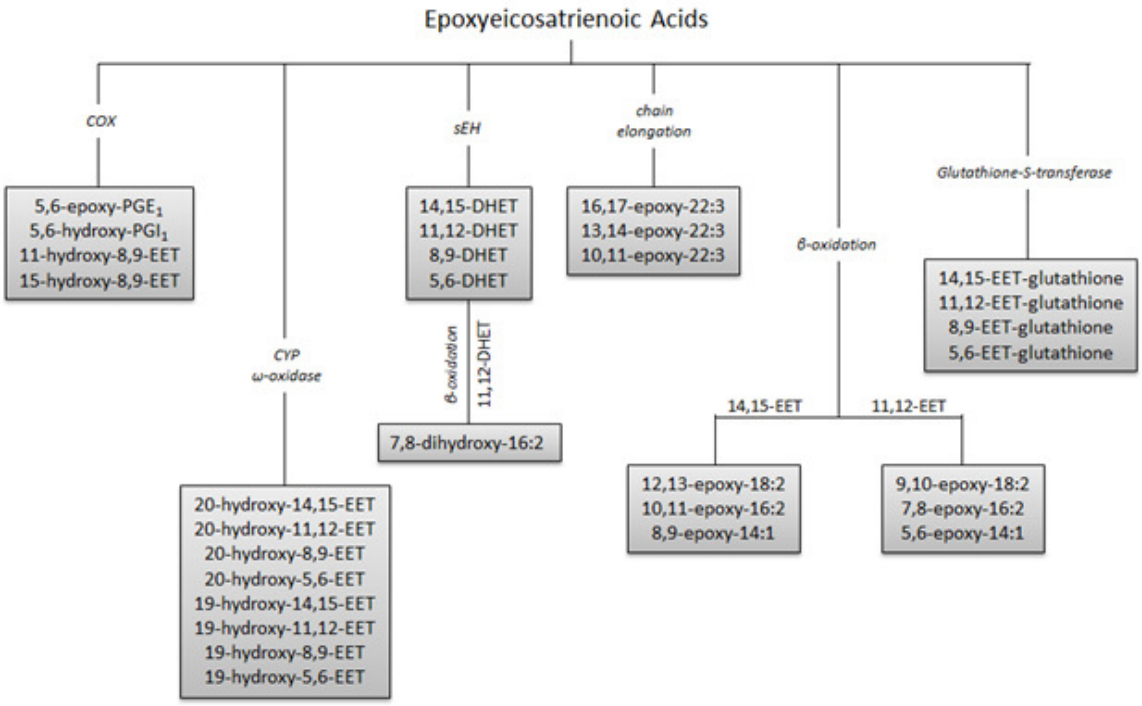

Figure 1.2. Secondary metabolism of epoxyeicosatrienoic acids (EETs). COX, cyclooxygenase; CYP, cytochrome P450; EET, epoxyeicosatrienoic acid; DHET, dihydroxyeicosatrienoic acid; PG, prostaglandin; sEH, soluble epoxide hydrolase (adapted from Spector et al., 2004).

Although 5-hydroxy-PGI_1 lacks vasodilator activity, 5,6-epoxy-PGE_1 is equal to 5,6-EET in its ability to stimulate cyclooxygenase-dependent vasodilation (Carroll et al., 1993; Carroll et al., 1992). Moreover, 8,9-EET can form 11- and 15-hydroxy-8,9-EET products catalyzed by cyclooxygenase (Zhang et al., 1992). The hydroxyepoxyeixosatrienoic acids formed from the 12-lipoxygenase metabolism of 11,12-EET are called hepoxilins and they can induce glucose-dependent insulin secretion in pancreatic islets (Pace-Asciak et al., 1983; Pace-Asciak and Martin, 1984). Likewise, 15-LOX catalyzes the formation of 11-hydroxy-14,15-EET and 15-hydroxy-11,12-EET from 14,15- and 11,12-EET, respectively, and their trihydroxyeicosatrienoic acid derivatives (Pfister et al., 1998). Finally, all four EET isomers can undergo ω- and ω-1 hydroxylation catalyzed by CYP4A1 and CYP4A2 (Cowart et al., 2002). The 20-hydroxylation metabolites of 8,9-, 11,12-, and 14,15-EET all activate PPARα (Cowart et al., 2002). With a K_i of 3 nM at PPARα, the 20-hydroxy-14,15-EET may be an endogenous ligand for this receptor (Cowart et al., 2002).

Alternative Metabolism Routes. In human skin fibroblasts, instead of being metabolized to form DHETs, the 8,9-, 11,12- and 14,15-EETs primarily undergo peroxisomal β-oxidation which shortens the carbon chain of the epoxy fatty acids (Fang et al., 2000; Spector et al., 2004). The 14,15-EET forms the 10,11-epoxy-16:2 β-oxidation product that can relax coronary microvessels that have been contracted with endothelin (Fang et al., 2002). In the presence of the sEH inhibitor *N,N'*-dicyclohexylurea, porcine coronary endothelial cells produce a chain-elongation product of 14,15-EET, 16,17-epoxy-$\Delta^{7,10,13}$-22:3 which is then incorporated into the lipids of the cells (Fang et al., 2001). Glutathione S-transferase prefers the 14,15-EET over the other

three epoxidated isomers for further conjugation with glutathione; however, the biological significance of this pathway has not been investigated (Spearman et al., 1985).

Drug-Drug Interactions. A drug-drug interaction occurs when the efficacy or toxicity of one drug is altered by the administration of a second compound. There are two types of drug-drug interactions, pharmacokinetic and pharmacodynamic. Pharmacokinetic interactions occur when one drug alters the absorption, distribution, metabolism, or excretion of another drug whereas pharmacodynamic interactions occur when two drugs have more than additive or opposing effects on the efficacy of one or both of the administered drugs. CYPs normally are responsible for pharmacokinetic interactions because the metabolizing ability of the respective P450 for one of the two drugs is either induced or inhibited by the other drug. For example, grapefruit juice contains furanocoumarins that inhibit CYP3A4 activity (Lin et al., 2012). Co-administration of grapefruit juice with any drug that is metabolized by CYP3A4 will result in an increase in the bioavailability of that drug due to the inhibition of CYP3A4-catalyzed metabolism by the grapefruit juice. Because the EETs are deeply involved in the maintenance of normal cardiac function, a drug interaction that disrupts arachidonic acid metabolism may alter the bioavailability of these eicosanoids in the cardiovascular system and have the potential to cause adverse or to enhance beneficial effects.

The Endogenous Cannabinoid System (ECS). The ECS is a lipid signaling system which consists of specific receptors, ligands, and the enzymes required to regulate the degradation of those ligands (Mouslech and Valla, 2009). Two seven transmembrane G-protein coupled receptors have been designated as members of this system, cannabinoid 1receptor (CBR1) and the CB2R (Mackie, 2008). The ligands for these

receptors can be exogenous, plant-derived or synthetic, or endogenous (DiMarzo et al., 2004). Moreover, several enzymes are known to participate in the synthesis and degradation of cannabinoid ligands (Di Marzo and Deutsch, 1998). Interestingly, the ECS and CYP2J2 are coexpressed in several organs including, but not limited to, the brain, liver, bladder, and the intestine (Mackie, 2008; Pacher et al., 2006). Because CYP2J2 can catalyze the oxidation of a variety of different compounds, its vicinity to ECS ligands such as anandamide may allow it to regulate the physiological fates of ECS ligands via oxidation.

The research described in this thesis is primarily focused on the ability of CYP2J2 to participate in the regulation of the endogenous cannabinoid system (ECS) by participating in the metabolic fates of some of its ligands. To complete this task, we investigated the metabolism of the endogenous cannabinoid anandamide (AEA) and the synthetic cannabinoid JWH-018 by purified CYP2J2 and microsomes prepared from drug metabolizing organs reported to express CYP2J2 or other members of the CYP2J family. The ECS, including AEA, is known to play a role in energy balance (Matias et al., 2006). Due to the connection between AEA and food intake, we have also investigated the effect of diet and obesity on the metabolism of AEA. Moreover, in order to better understand the possible importance of the epoxyeicosatrienoic acid ethanolamides (EET-EAs), the products formed from AEA metabolism by CYP2J2 and other P450s, we studied several soluble epoxide hydrolase inhibitors for their ability to prevent the hydrolysis of EET-EAs. Likewise, we also investigated the cardiovascular effects of JWH-18 administration in rats and its metabolism in microsomes isolated from several rat and human organs in

order to identify metabolites that can potentially contribute to the adverse effects seen *in vivo*.

References

Alonso-Galicia, M., Falck, J.R., Reddy, K.M., and Roman, R.J. (1999). 20-HETE agonists and antagonists in the renal circulation. Am J Physiol *277*, F790-796.

Arnold, C., Markovic, M., Blossey, K., Wallukat, G., Fischer, R., Dechend, R., Konkel, A., von Schacky, C., Luft, F.C., Muller, D.N., Rothe, M., and Schunck, W.H. (2010). Arachidonic acid-metabolizing cytochrome P450 enzymes are targets of {omega}-3 fatty acids. J Biol Chem *285*, 32720-32733.

Askari, A., Thomson, S.J., Edin, M.L., Zeldin, D.C., and Bishop-Bailey, D. (2013). Roles of the epoxygenase CYP2J2 in the endothelium. Prostaglandins Other Lipid Mediat.

Bhatia, S., Knoch, B., Wong, J., Kim, W.S., Else, P.L., Oakley, A.J., and Garner, B. (2012). Selective reduction of hydroperoxyeicosatetraenoic acids to their hydroxy derivatives by apolipoprotein D: implications for lipid antioxidant activity and Alzheimer's disease. Biochem J *442*, 713-721.

Bauersachs, J., Christ, M., Ertl, G., Michaelis, U.R., Fisslthaler, B., Busse, R., and Fleming, I. (2002). Cytochrome P450 2C expression and EDHF-mediated relaxation in porcine coronary arteries is increased by cortisol. Cardiovasc Res *54*, 669-675.

Bertrand-Thiebault, C., Ferrari, L., Boutherin-Falson, O., Kockx, M., Desquand-Billiald, S., Fichelle, J.M., Nottin, R., Renaud, J.F., Batt, A.M., and Visvikis, S. (2004). Cytochromes P450 are differently expressed in normal and varicose human saphenous veins: linkage with varicosis. Clin Exp Pharmacol Physiol *31*, 295-301.

Bieche, I., Narjoz, C., Asselah, T., Vacher, S., Marcellin, P., Lidereau, R., Beaune, P., and de Waziers, I. (2007). Reverse transcriptase-PCR quantification of mRNA levels from cytochrome (CYP)1, CYP2 and CYP3 families in 22 different human tissues. Pharmacogenet Genomics *17*, 731-742.

Borgel, J., Bulut, D., Hanefeld, C., Neubauer, H., Mugge, A., Epplen, J.T., Holland-Letz, T., and Spiecker, M. (2008). The CYP2J2 G-50T polymorphism and myocardial infarction in patients with cardiovascular risk profile. BMC Cardiovasc Disord *8*, 41.

Breitbart, E., Sofer, Y., Shainberg, A., and Grossman, S. (1996). Lipoxygenase activity in heart cells. FEBS Lett *395*, 148-152.

Bystrom, J., Wray, J.A., Sugden, M.C., Holness, M.J., Swales, K.E., Warner, T.D., Edin, M.L., Zeldin, D.C., Gilroy, D.W., and Bishop-Bailey, D. (2011). Endogenous epoxygenases are modulators of monocyte/macrophage activity. PLoS One *6*, e26591.

Campbell, W.B., Gebremedhin, D., Pratt, P.F., and Harder, D.R. (1996). Identification of epoxyeicosatrienoic acids as endothelium-derived hyperpolarizing factors. Circ Res *78*, 415-423.

Carroll, M.A., Balazy, M., Margiotta, P., Falck, J.R., and McGiff, J.C. (1993). Renal vasodilator activity of 5,6-epoxyeicosatrienoic acid depends upon conversion by cyclooxygenase and release of prostaglandins. J Biol Chem *268*, 12260-12266.

Carroll, M.A., Garcia, M.P., Falck, J.R., and McGiff, J.C. (1992). Cyclooxygenase dependency of the renovascular actions of cytochrome P450-derived arachidonate metabolites. J Pharmacol Exp Ther *260*, 104-109.

Chaudhary, K.R., Batchu, S.N., and Seubert, J.M. (2009). Cytochrome P450 enzymes and the heart. IUBMB Life *61*, 954-960.

Chen, C., Wei, X., Rao, X., Wu, J., Yang, S., Chen, F., Ma, D., Zhou, J., Dackor, R.T., Zeldin, D.C.*, et al.* (2011). Cytochrome P450 2J2 is highly expressed in hematologic malignant diseases and promotes tumor cell growth. J Pharmacol Exp Ther *336*, 344-355.

Chen, J.K., Capdevila, J., and Harris, R.C. (2001). Cytochrome p450 epoxygenase metabolism of arachidonic acid inhibits apoptosis. Mol Cell Biol *21*, 6322-6331.

Cheranov, S.Y., Karpurapu, M., Wang, D., Zhang, B., Venema, R.C., and Rao, G.N. (2008). An essential role for SRC-activated STAT-3 in 14,15-EET-induced VEGF expression and angiogenesis. Blood *111*, 5581-5591.

Cowart, L.A., Wei, S., Hsu, M.H., Johnson, E.F., Krishna, M.U., Falck, J.R., and Capdevila, J.H. (2002). The CYP4A isoforms hydroxylate epoxyeicosatrienoic acids to form high affinity peroxisome proliferator-activated receptor ligands. J Biol Chem *277*, 35105-35112.

Daikh, B.E., Lasker, J.M., Raucy, J.L., and Koop, D.R. (1994). Regio- and stereoselective epoxidation of arachidonic acid by human cytochromes P450 2C8 and 2C9. J Pharmacol Exp Ther *271*, 1427-1433.

Delozier, T.C., Kissling, G.E., Coulter, S.J., Dai, D., Foley, J.F., Bradbury, J.A., Murphy, E., Steenbergen, C., Zeldin, D.C., and Goldstein, J.A. (2007). Detection of human CYP2C8, CYP2C9, and CYP2J2 in cardiovascular tissues. Drug Metab Dispos *35*, 682-688.

Di Marzo, V., Bifulco, M., and De Petrocellis, L. (2004). The endocannabinoid system and its therapeutic exploitation. Nat Rev Drug Discov *3*, 771-784.

Di Marzo, V., and Deutsch, D.G. (1998). Biochemistry of the endogenous ligands of cannabinoid receptors. Neurobiol Dis *5*, 386-404.

Dransfeld, O., Rakatzi, I., Sasson, S., and Eckel, J. (2002). Eicosanoids and the regulation of cardiac glucose transport. Ann N Y Acad Sci *967*, 208-216.

Dreisbach, A.W., Japa, S., Sigel, A., Parenti, M.B., Hess, A.E., Srinouanprachanh, S.L., Rettie, A.E., Kim, H., Farin, F.M., Hamm, L.L., and Lertora, J.J. (2005). The Prevalence of CYP2C8, 2C9, 2J2, and soluble epoxide hydrolase polymorphisms in African Americans with hypertension. Am J Hypertens *18*, 1276-1281.

Edin, M.L., Wang, Z., Bradbury, J.A., Graves, J.P., Lih, F.B., DeGraff, L.M., Foley, J.F., Torphy, R., Ronnekleiv, O.K., Tomer, K.B., Lee, C.R., and Zeldin, D.C. (2011). Endothelial expression of human cytochrome P450 epoxygenase CYP2C8 increases susceptibility to ischemia-reperfusion injury in isolated mouse heart. FASEB J *25*, 3436-3447.

Elbekai, R.H., and El-Kadi, A.O. (2006). Cytochrome P450 enzymes: central players in cardiovascular health and disease. Pharmacol Ther *112*, 564-587.

Enayetallah, A.E., French, R.A., Thibodeau, M.S., and Grant, D.F. (2004). Distribution of soluble epoxide hydrolase and of cytochrome P450 2C8, 2C9, and 2J2 in human tissues. J Histochem Cytochem *52*, 447-454.

Fang, X., Hu, S., Xu, B., Snyder, G.D., Harmon, S., Yao, J., Liu, Y., Sangras, B., Falck, J.R., Weintraub, N.L., and Spector, A.A. (2006). 14,15-Dihydroxyeicosatrienoic acid activates peroxisome proliferator-activated receptor-alpha. Am J Physiol Heart Circ Physiol *290*, H55-63.

Fang, X., Kaduce, T.L., VanRollins, M., Weintraub, N.L., and Spector, A.A. (2000). Conversion of epoxyeicosatrienoic acids (EETs) to chain-shortened epoxy fatty acids by human skin fibroblasts. J Lipid Res *41*, 66-74.

Fang, X., Kaduce, T.L., Weintraub, N.L., Harmon, S., Teesch, L.M., Morisseau, C., Thompson, D.A., Hammock, B.D., and Spector, A.A. (2001). Pathways of epoxyeicosatrienoic acid metabolism in endothelial cells. Implications for the vascular effects of soluble epoxide hydrolase inhibition. J Biol Chem *276*, 14867-14874.

Fang, X., Weintraub, N.L., Oltman, C.L., Stoll, L.L., Kaduce, T.L., Harmon, S., Dellsperger, K.C., Morisseau, C., Hammock, B.D., and Spector, A.A. (2002). Human coronary endothelial cells convert 14,15-EET to a biologically active chain-shortened epoxide. Am J Physiol Heart Circ Physiol *283*, H2306-2314.

Fava, C., Montagnana, M., Almgren, P., Hedblad, B., Engstrom, G., Berglund, G., Minuz, P., and Melander, O. (2010). The common functional polymorphism -50G>T of the CYP2J2 gene is not associated with ischemic coronary and cerebrovascular events in an urban-based sample of Swedes. J Hypertens *28*, 294-299.

Fisslthaler, B., Hinsch, N., Chataigneau, T., Popp, R., Kiss, L., Busse, R., and Fleming, I. (2000). Nifedipine increases cytochrome P4502C expression and endothelium-derived hyperpolarizing factor-mediated responses in coronary arteries. Hypertension *36*, 270-275.

Fisslthaler, B., Michaelis, U.R., Randriamboavonjy, V., Busse, R., and Fleming, I. (2003). Cytochrome P450 epoxygenases and vascular tone: novel role for HMG-CoA reductase inhibitors in the regulation of CYP 2C expression. Biochim Biophys Acta *1619*, 332-339.

Fitzpatrick, F.A., Ennis, M.D., Baze, M.E., Wynalda, M.A., McGee, J.E., and Liggett, W.F. (1986). Inhibition of cyclooxygenase activity and platelet aggregation by epoxyeicosatrienoic acids. Influence of stereochemistry. J Biol Chem *261*, 15334-15338.

Fleming, I. (2004). Cytochrome P450 epoxygenases as EDHF synthase(s). Pharmacol Res *49*, 525-533.

Fleming, I. (2011). The cytochrome P450 pathway in angiogenesis and endothelial cell biology. Cancer Metastasis Rev *30*, 541-555.

Frisbee, J.C., Roman, R.J., Falck, J.R., Krishna, U.M., and Lombard, J.H. (2001). 20-HETE contributes to myogenic activation of skeletal muscle resistance arteries in Brown Norway and Sprague-Dawley rats. Microcirculation *8*, 45-55.

Gebremedhin, D., Lange, A.R., Lowry, T.F., Taheri, M.R., Birks, E.K., Hudetz, A.G., Narayanan, J., Falck, J.R., Okamoto, H., Roman, R.J., Nithipatikom, K., Campbell, W.B., and Harder, D.R. (2000). Production of 20-HETE and its role in autoregulation of cerebral blood flow. Circ Res *87*, 60-65.

Guengerich, F.P. (2007). Mechanisms of cytochrome P450 substrate oxidation: MiniReview. J Biochem Mol Toxicol *21*, 163-168.

Harder, D.R., Campbell, W.B., and Roman, R.J. (1995). Role of cytochrome P-450 enzymes and metabolites of arachidonic acid in the control of vascular tone. J Vasc Res *32*, 79-92.

Harder, D.R., Narayanan, J., Birks, E.K., Liard, J.F., Imig, J.D., Lombard, J.H., Lange, A.R., and Roman, R.J. (1996). Identification of a putative microvascular oxygen sensor. Circ Res *79*, 54-61.

Imig, J.D., Falck, J.R., and Inscho, E.W. (1999). Contribution of cytochrome P450 epoxygenase and hydroxylase pathways to afferent arteriolar autoregulatory responsiveness. Br J Pharmacol *127*, 1399-1405.

Imig, J.D., Navar, L.G., Roman, R.J., Reddy, K.K., and Falck, J.R. (1996). Actions of epoxygenase metabolites on the preglomerular vasculature. J Am Soc Nephrol *7*, 2364-2370.

Imig, J.D., Zou, A.P., Ortiz de Montellano, P.R., Sui, Z., and Roman, R.J. (1994). Cytochrome P-450 inhibitors alter afferent arteriolar responses to elevations in pressure. Am J Physiol *266*, H1879-1885.

Jakobsson, P.J., Mancini, J.A., Riendeau, D., and Ford-Hutchinson, A.W. (1997). Identification and characterization of a novel microsomal enzyme with glutathione-dependent transferase and peroxidase activities. J Biol Chem *272*, 22934-22939.

Jenkins, C.M., Cedars, A., and Gross, R.W. (2009). Eicosanoid signalling pathways in the heart. Cardiovasc Res *82*, 240-249.

Jiang, J.G., Chen, C.L., Card, J.W., Yang, S., Chen, J.X., Fu, X.N., Ning, Y.G., Xiao, X., Zeldin, D.C., and Wang, D.W. (2005). Cytochrome P450 2J2 promotes the neoplastic phenotype of carcinoma cells and is up-regulated in human tumors. Cancer Res *65*, 4707-4715.

Jiang, J.G., Chen, R.J., Xiao, B., Yang, S., Wang, J.N., Wang, Y., Cowart, L.A., Xiao, X., Wang, D.W., and Xia, Y. (2007). Regulation of endothelial nitric-oxide synthase activity through phosphorylation in response to epoxyeicosatrienoic acids. Prostaglandins Other Lipid Mediat *82*, 162-174.

Karara, A., Dishman, E., Falck, J.R., and Capdevila, J.H. (1991). Endogenous epoxyeicosatrienoyl-phospholipids. A novel class of cellular glycerolipids containing epoxidized arachidonate moieties. J Biol Chem *266*, 7561-7569.

Katragadda, D., Batchu, S.N., Cho, W.J., Chaudhary, K.R., Falck, J.R., and Seubert, J.M. (2009). Epoxyeicosatrienoic acids limit damage to mitochondrial function following stress in cardiac cells. J Mol Cell Cardiol *46*, 867-875.

Ke, Q., Xiao, Y.F., Bradbury, J.A., Graves, J.P., Degraff, L.M., Seubert, J.M., and Zeldin, D.C. (2007). Electrophysiological properties of cardiomyocytes isolated from CYP2J2 transgenic mice. Mol Pharmacol *72*, 1063-1073.

Khan, M., Mohan, I.K., Kutala, V.K., Kumbala, D., and Kuppusamy, P. (2007). Cardioprotection by sulfaphenazole, a cytochrome p450 inhibitor: mitigation of ischemia-reperfusion injury by scavenging of reactive oxygen species. J Pharmacol Exp Ther *323*, 813-821.

King, L.M., Ma, J., Srettabunjong, S., Graves, J., Bradbury, J.A., Li, L., Spiecker, M., Liao, J.K., Mohrenweiser, H., and Zeldin, D.C. (2002). Cloning of CYP2J2 gene and identification of functional polymorphisms. Mol Pharmacol *61*, 840-852.

Kosaka, K., Suzuki, K., Hayakawa, M., Sugiyama, S., and Ozawa, T. (1994). Leukotoxin, a linoleate epoxide: its implication in the late death of patients with extensive burns. Mol Cell Biochem *139*, 141-148.

Krotz, F., Riexinger, T., Buerkle, M.A., Nithipatikom, K., Gloe, T., Sohn, H.Y., Campbell, W.B., and Pohl, U. (2004). Membrane-potential-dependent inhibition of platelet adhesion to endothelial cells by epoxyeicosatrienoic acids. Arterioscler Thromb Vasc Biol *24*, 595-600.

Laethem, R.M., Halpert, J.R., and Koop, D.R. (1994). Epoxidation of arachidonic acid as an active-site probe of cytochrome P-450 2B isoforms. Biochim Biophys Acta *1206*, 42-48.

Lafite, P., Andre, F., Zeldin, D.C., Dansette, P.M., and Mansuy, D. (2007). Unusual regioselectivity and active site topology of human cytochrome P450 2J2. Biochemistry *46*, 10237-10247.

Lafite, P., Dijols, S., Buisson, D., Macherey, A.C., Zeldin, D.C., Dansette, P.M., and Mansuy, D. (2006). Design and synthesis of selective, high-affinity inhibitors of human cytochrome P450 2J2. Bioorg Med Chem Lett *16*, 2777-2780.

Lange, A., Gebremedhin, D., Narayanan, J., and Harder, D. (1997). 20-Hydroxyeicosatetraenoic acid-induced vasoconstriction and inhibition of potassium current in cerebral vascular smooth muscle is dependent on activation of protein kinase C. J Biol Chem *272*, 27345-27352.

Lee, C.A., Jones, J.P., 3rd, Katayama, J., Kaspera, R., Jiang, Y., Freiwald, S., Smith, E., Walker, G.S., and Totah, R.A. (2012). Identifying a selective substrate and inhibitor pair for the evaluation of CYP2J2 activity. Drug Metab Dispos *40*, 943-951.

Lee, C.R., North, K.E., Bray, M.S., Couper, D.J., Heiss, G., and Zeldin, D.C. (2007). CYP2J2 and CYP2C8 polymorphisms and coronary heart disease risk: the Atherosclerosis Risk in Communities (ARIC) study. Pharmacogenet Genomics *17*, 349-358.

Lee, H.C., Lu, T., Weintraub, N.L., VanRollins, M., Spector, A.A., and Shibata, E.F. (1999). Effects of epoxyeicosatrienoic acids on the cardiac sodium channels in isolated rat ventricular myocytes. J Physiol *519 Pt 1*, 153-168.

Lee, S.S., Jeong, H.E., Liu, K.H., Ryu, J.Y., Moon, T., Yoon, C.N., Oh, S.J., Yun, C.H., and Shin, J.G. (2005). Identification and functional characterization of novel CYP2J2 variants: G312R variant causes loss of enzyme catalytic activity. Pharmacogenet Genomics *15*, 105-113.

Lin, H.L., Kenaan, C., and Hollenberg, P.F. (2012). Identification of the residue in human CYP3A4 that is covalently modified by bergamottin and the reactive intermediate that contributes to the grapefruit juice effect. Drug Metab Dispos *40*, 998-1006.

Liu, K.H., Kim, M.G., Lee, D.J., Yoon, Y.J., Kim, M.J., Shon, J.H., Choi, C.S., Choi, Y.K., Desta, Z., and Shin, J.G. (2006). Characterization of ebastine, hydroxyebastine, and carebastine metabolism by human liver microsomes and expressed cytochrome P450 enzymes: major roles for CYP2J2 and CYP3A. Drug Metab Dispos *34*, 1793-1797.

Liu, Y., Zhang, Y., Schmelzer, K., Lee, T.S., Fang, X., Zhu, Y., Spector, A.A., Gill, S., Morisseau, C., Hammock, B.D., and Shyy, J.Y. (2005). The antiinflammatory effect of

laminar flow: the role of PPARgamma, epoxyeicosatrienoic acids, and soluble epoxide hydrolase. Proc Natl Acad Sci U S A *102*, 16747-16752.

Lu, T., Hoshi, T., Weintraub, N.L., Spector, A.A., and Lee, H.C. (2001). Activation of ATP-sensitive K(+) channels by epoxyeicosatrienoic acids in rat cardiac ventricular myocytes. J Physiol *537*, 811-827.

Ma, J., Ramachandran, S., Fiedorek, F.T., Jr., and Zeldin, D.C. (1998). Mapping of the CYP2J cytochrome P450 genes to human chromosome 1 and mouse chromosome 4. Genomics *49*, 152-155.

Mackie, K. (2008). Cannabinoid receptors: where they are and what they do. J Neuroendocrinol *20 Suppl 1*, 10-14.

Matias, I., Bisogno, T., and Di Marzo, V. (2006). Endogenous cannabinoids in the brain and peripheral tissues: regulation of their levels and control of food intake. Int J Obes (Lond) *30 Suppl 1*, S7-S12.

Matsumoto, S., Hirama, T., Matsubara, T., Nagata, K., and Yamazoe, Y. (2002). Involvement of CYP2J2 on the intestinal first-pass metabolism of antihistamine drug, astemizole. Drug Metab Dispos *30*, 1240-1245.

Mendez, M., and LaPointe, M.C. (2003). PPARgamma inhibition of cyclooxygenase-2, PGE2 synthase, and inducible nitric oxide synthase in cardiac myocytes. Hypertension *42*, 844-850.

Meunier, B., de Visser, S.P., and Shaik, S. (2004). Mechanism of oxidation reactions catalyzed by cytochrome p450 enzymes. Chem Rev *104*, 3947-3980.

Michaelis, U.R., Falck, J.R., Schmidt, R., Busse, R., and Fleming, I. (2005). Cytochrome P4502C9-derived epoxyeicosatrienoic acids induce the expression of cyclooxygenase-2 in endothelial cells. Arterioscler Thromb Vasc Biol *25*, 321-326.

Mitra, R., Guo, Z., Milani, M., Mesaros, C., Rodriguez, M., Nguyen, J., Luo, X., Clarke, D., Lamba, J., Schuetz, E., Donner, D.B., Puli, N., Falck, J.R., Capdevila, J., Gupta, K., Blair, I.A., and Potter, D.A. (2011). CYP3A4 mediates growth of estrogen receptor-positive breast cancer cells in part by inducing nuclear translocation of phospho-Stat3 through biosynthesis of (+/-)-14,15-epoxyeicosatrienoic acid (EET). J Biol Chem *286*, 17543-17559.

Moran, J.H., Mitchell, L.A., Bradbury, J.A., Qu, W., Zeldin, D.C., Schnellmann, R.G., and Grant, D.F. (2000). Analysis of the cytotoxic properties of linoleic acid metabolites produced by renal and hepatic P450s. Toxicol Appl Pharmacol *168*, 268-279.

Mouslech, Z., and Valla, V. (2009). Endocannabinoid system: An overview of its potential in current medical practice. Neuro Endocrinol Lett *30*, 153-179.

Muthalif, M.M., Uddin, M.R., Fatima, S., Parmentier, J.H., Khandekar, Z., and Malik, K.U. (2001). Small GTP binding protein Ras contributes to norepinephrine-induced mitogenesis of vascular smooth muscle cells. Prostaglandins Other Lipid Mediat *65*, 33-43.

Nelson, D.R. (2009). The cytochrome p450 homepage. Hum Genomics *4*, 59-65.

Ng, V.Y., Huang, Y., Reddy, L.M., Falck, J.R., Lin, E.T., and Kroetz, D.L. (2007). Cytochrome P450 eicosanoids are activators of peroxisome proliferator-activated receptor alpha. Drug Metab Dispos *35*, 1126-1134.

Nithipatikom, K., Moore, J.M., Isbell, M.A., Falck, J.R., and Gross, G.J. (2006). Epoxyeicosatrienoic acids in cardioprotection: ischemic versus reperfusion injury. Am J Physiol Heart Circ Physiol *291*, H537-542.

Node, K., Huo, Y., Ruan, X., Yang, B., Spiecker, M., Ley, K., Zeldin, D.C., and Liao, J.K. (1999). Anti-inflammatory properties of cytochrome P450 epoxygenase-derived eicosanoids. Science *285*, 1276-1279.

Node, K., Ruan, X.L., Dai, J., Yang, S.X., Graham, L., Zeldin, D.C., and Liao, J.K. (2001). Activation of Galpha s mediates induction of tissue-type plasminogen activator gene transcription by epoxyeicosatrienoic acids. J Biol Chem *276*, 15983-15989.

Oliw, E.H. (1984). Metabolism of 5(6)Oxidoeicosatrienoic acid by ram seminal vesicles. Formation of two stereoisomers of 5-hydroxyprostaglandin I1. J Biol Chem *259*, 2716-2721.

Oltman, C.L., Weintraub, N.L., VanRollins, M., and Dellsperger, K.C. (1998). Epoxyeicosatrienoic acids and dihydroxyeicosatrienoic acids are potent vasodilators in the canine coronary microcirculation. Circ Res *83*, 932-939.

Ortiz de Montellano, P.R., ed. (1995). Cytochrome P450: Structure, Mechanism, and Biochemistry (Second Edition), 2nd edn (New York, Plenum Press).

Ozawa, T., Hayakawa, M., Takamura, T., Sugiyama, S., Suzuki, K., Iwata, M., Taki, F., and Tomita, T. (1986). Biosynthesis of leukotoxin, 9,10-epoxy-12 octadecenoate, by leukocytes in lung lavages of rat after exposure to hyperoxia. Biochem Biophys Res Commun *134*, 1071-1078.

Pace-Asciak, C.R., Granstrom, E., and Samuelsson, B. (1983). Arachidonic acid epoxides. Isolation and structure of two hydroxy epoxide intermediates in the formation of 8,11,12- and 10,11,12-trihydroxyeicosatrienoic acids. J Biol Chem *258*, 6835-6840.

Pace-Asciak, C.R., and Martin, J.M. (1984). Hepoxilin, a new family of insulin secretagogues formed by intact rat pancreatic islets. Prostaglandins Leukot Med *16*, 173-180.

Pacher, P., Batkai, S., and Kunos, G. (2006). The endocannabinoid system as an emerging target of pharmacotherapy. Pharmacol Rev *58*, 389-462.

Panigrahy, D., Greene, E.R., Pozzi, A., Wang, D.W., and Zeldin, D.C. (2011). EET signaling in cancer. Cancer Metastasis Rev *30*, 525-540.

Pavek, P., and Dvorak, Z. (2008). Xenobiotic-induced transcriptional regulation of xenobiotic metabolizing enzymes of the cytochrome P450 superfamily in human extrahepatic tissues. Curr Drug Metab *9*, 129-143.

Pfister, S.L., Spitzbarth, N., Nithipatikom, K., Edgemond, W.S., Falck, J.R., and Campbell, W.B. (1998). Identification of the 11,14,15- and 11,12, 15-trihydroxyeicosatrienoic acids as endothelium-derived relaxing factors of rabbit aorta. J Biol Chem *273*, 30879-30887.

Pitt, B., Shea, M.J., Romson, J.L., and Lucchesi, B.R. (1983). Prostaglandins and prostaglandin inhibitors in ischemic heart disease. Ann Intern Med *99*, 83-92.

Polonikov, A.V., Ivanov, V.P., Solodilova, M.A., Khoroshaya, I.V., Kozhuhov, M.A., Ivakin, V.E., Katargina, L.N., and Kolesnikova, O.E. (2008). A common polymorphism G-50T in cytochrome P450 2J2 gene is associated with increased risk of essential hypertension in a Russian population. Dis Markers *24*, 119-126.

Poulos, T.L., Finzel, B.C., and Howard, A.J. (1987). High-resolution crystal structure of cytochrome P450cam. J Mol Biol *195*, 687-700.

Powell, P.K., Wolf, I., Jin, R., and Lasker, J.M. (1998). Metabolism of arachidonic acid to 20-hydroxy-5,8,11, 14-eicosatetraenoic acid by P450 enzymes in human liver: involvement of CYP4F2 and CYP4A11. J Pharmacol Exp Ther *285*, 1327-1336.

Ren, S., Zeng, J., Mei, Y., Zhang, J.Z., Yan, S.F., Fei, J., and Chen, L. (2013). Discovery and characterization of novel, potent, and selective cytochrome P450 2J2 inhibitors. Drug Metab Dispos *41*, 60-71.

Rifkind, A.B., Lee, C., Chang, T.K., and Waxman, D.J. (1995). Arachidonic acid metabolism by human cytochrome P450s 2C8, 2C9, 2E1, and 1A2: regioselective oxygenation and evidence for a role for CYP2C enzymes in arachidonic acid epoxygenation in human liver microsomes. Arch Biochem Biophys *320*, 380-389.

Rival, Y., Beneteau, N., Taillandier, T., Pezet, M., Dupont-Passelaigue, E., Patoiseau, J.F., Junquero, D., Colpaert, F.C., and Delhon, A. (2002). PPARalpha and PPARdelta activators inhibit cytokine-induced nuclear translocation of NF-kappaB and expression of VCAM-1 in EAhy926 endothelial cells. Eur J Pharmacol *435*, 143-151.

Roman, R.J. (2002). P-450 metabolites of arachidonic acid in the control of cardiovascular function. Physiol Rev *82*, 131-185.

Roman, R.J., Maier, K.G., Sun, C.W., Harder, D.R., and Alonso-Galicia, M. (2000). Renal and cardiovascular actions of 20-hydroxyeicosatetraenoic acid and epoxyeicosatrienoic acids. Clin Exp Pharmacol Physiol *27*, 855-865.

Scarborough, P.E., Ma, J., Qu, W., and Zeldin, D.C. (1999). P450 subfamily CYP2J and their role in the bioactivation of arachidonic acid in extrahepatic tissues. Drug Metab Rev *31*, 205-234.

Seubert, J., Yang, B., Bradbury, J.A., Graves, J., Degraff, L.M., Gabel, S., Gooch, R., Foley, J., Newman, J., Mao, L., Rockman, H.A., Hammock, B.D., Murphy, E., and Zeldin, D.C. (2004). Enhanced postischemic functional recovery in CYP2J2 transgenic hearts involves mitochondrial ATP-sensitive K+ channels and p42/p44 MAPK pathway. Circ Res *95*, 506-514.

Shinmura, K., Tang, X.L., Wang, Y., Xuan, Y.T., Liu, S.Q., Takano, H., Bhatnagar, A., and Bolli, R. (2000). Cyclooxygenase-2 mediates the cardioprotective effects of the late phase of ischemic preconditioning in conscious rabbits. Proc Natl Acad Sci U S A *97*, 10197-10202.

Sisignano, M., Park, C.K., Angioni, C., Zhang, D.D., von Hehn, C., Cobos, E.J., Ghasemlou, N., Xu, Z.Z., Kumaran, V., Lu, R., Grant, A., Fischer, M.J., Schmidtko, A., Reeh, P., Ji, R.R., Woolf, C.J., Geisslinger, G., Scholich, K., and Brenneis, C. (2012). 5,6-EET is released upon neuronal activity and induces mechanical pain hypersensitivity via TRPA1 on central afferent terminals. J Neurosci *32*, 6364-6372.

Sligar, S.G., Cinti, D.L., Gibson, G.G., and Schenkman, J.B. (1979). Spin state control of the hepatic cytochrome P450 redox potential. Biochem Biophys Res Commun *90*, 925-932.

Spearman, M.E., Prough, R.A., Estabrook, R.W., Falck, J.R., Manna, S., Leibman, K.C., Murphy, R.C., and Capdevila, J. (1985). Novel glutathione conjugates formed from epoxyeicosatrienoic acids (EETs). Arch Biochem Biophys *242*, 225-230.

Spector, A.A., Fang, X., Snyder, G.D., and Weintraub, N.L. (2004). Epoxyeicosatrienoic acids (EETs): metabolism and biochemical function. Prog Lipid Res *43*, 55-90.

Spiecker, M., Darius, H., Hankeln, T., Soufi, M., Sattler, A.M., Schaefer, J.R., Node, K., Borgel, J., Mugge, A., Lindpaintner, K., Huesing, A., Maisch, B., Zeldin, D.C., and Liao, J.K. (2004). Risk of coronary artery disease associated with polymorphism of the cytochrome P450 epoxygenase CYP2J2. Circulation *110*, 2132-2136.

Spiecker, M., and Liao, J.K. (2005). Vascular protective effects of cytochrome p450 epoxygenase-derived eicosanoids. Arch Biochem Biophys *433*, 413-420.

Sun, J., Sui, X., Bradbury, J.A., Zeldin, D.C., Conte, M.S., and Liao, J.K. (2002). Inhibition of vascular smooth muscle cell migration by cytochrome p450 epoxygenase-derived eicosanoids. Circ Res *90*, 1020-1027.

Sutherland, M., Shankaranarayanan, P., Schewe, T., and Nigam, S. (2001). Evidence for the presence of phospholipid hydroperoxide glutathione peroxidase in human platelets: implications for its involvement in the regulatory network of the 12-lipoxygenase pathway of arachidonic acid metabolism. Biochem J *353*, 91-100.

Thum, T., and Borlak, J. (2000). Gene expression in distinct regions of the heart. Lancet *355*, 979-983.

VanRollins, M., Kaduce, T.L., Fang, X., Knapp, H.R., and Spector, A.A. (1996). Arachidonic acid diols produced by cytochrome P-450 monooxygenases are incorporated into phospholipids of vascular endothelial cells. J Biol Chem *271*, 14001-14009.

Wang, D., Hirase, T., Nitto, T., Soma, M., and Node, K. (2009). Eicosapentaenoic acid increases cytochrome P-450 2J2 gene expression and epoxyeicosatrienoic acid production via peroxisome proliferator-activated receptor gamma in endothelial cells. J Cardiol *54*, 368-374.

Wang, H., Lin, L., Jiang, J., Wang, Y., Lu, Z.Y., Bradbury, J.A., Lih, F.B., Wang, D.W., and Zeldin, D.C. (2003). Up-regulation of endothelial nitric-oxide synthase by endothelium-derived hyperpolarizing factor involves mitogen-activated protein kinase and protein kinase C signaling pathways. J Pharmacol Exp Ther *307*, 753-764.

Wang, J.F., Yang, Y., Sullivan, M.F., Min, J., Cai, J., Zeldin, D.C., Xiao, Y.F., and Morgan, J.P. (2002). Induction of cardiac cytochrome p450 in cocaine-treated mice. Exp Biol Med (Maywood) *227*, 182-188.

Wang, M.H., Stec, D.E., Balazy, M., Mastyugin, V., Yang, C.S., Roman, R.J., and Schwartzman, M.L. (1996). Cloning, sequencing, and cDNA-directed expression of the rat renal CYP4A2: arachidonic acid omega-hydroxylation and 11,12-epoxidation by CYP4A2 protein. Arch Biochem Biophys *336*, 240-250.

Wang, Y., Wei, X., Xiao, X., Hui, R., Card, J.W., Carey, M.A., Wang, D.W., and Zeldin, D.C. (2005). Arachidonic acid epoxygenase metabolites stimulate endothelial cell growth and angiogenesis via mitogen-activated protein kinase and phosphatidylinositol 3-kinase/Akt signaling pathways. J Pharmacol Exp Ther *314*, 522-532.

Wen, Y., Gu, J., Peng, X., Zhang, G., and Nadler, J. (2003). Overexpression of 12-lipoxygenase and cardiac fibroblast hypertrophy. Trends Cardiovasc Med *13*, 129-136.

Widstrom, R.L., Norris, A.W., and Spector, A.A. (2001). Binding of cytochrome P450 monooxygenase and lipoxygenase pathway products by heart fatty acid-binding protein. Biochemistry *40*, 1070-1076.

Wolf, M.J., and Gross, R.W. (1996). The calcium-dependent association and functional coupling of calmodulin with myocardial phospholipase A2. Implications for cardiac cycle-dependent alterations in phospholipolysis. J Biol Chem *271*, 20989-20992.

Wong, S.C., Fukuchi, M., Melnyk, P., Rodger, I., and Giaid, A. (1998). Induction of cyclooxygenase-2 and activation of nuclear factor-kappaB in myocardium of patients with congestive heart failure. Circulation *98*, 100-103.

Wray, J., and Bishop-Bailey, D. (2008). Epoxygenases and peroxisome proliferator-activated receptors in mammalian vascular biology. Exp Physiol *93*, 148-154.

Wu, K.K. (1998). Cyclooxygenase-2 induction in congestive heart failure: friend or foe? Circulation *98*, 95-96.

Wu, S., Moomaw, C.R., Tomer, K.B., Falck, J.R., and Zeldin, D.C. (1996). Molecular cloning and expression of CYP2J2, a human cytochrome P450 arachidonic acid epoxygenase highly expressed in heart. J Biol Chem *271*, 3460-3468.

Wu, Z., Lee, D., Joo, J., Shin, J.H., Kang, W., Oh, S., Lee, D.Y., Lee, S.J., Yea, S.S., Lee, H.S., Lee, T., and Liu, K.H. (2013). CYP2J2 and CYP2C19 are the Major Enzymes Responsible for Metabolism of Albendazole and Fenbendazole in Human Liver Microsomes and Recombinant P450 Assay Systems. Antimicrob Agents Chemother *50*, 5448-5456.

Xiao, Y.F., Huang, L., and Morgan, J.P. (1998). Cytochrome P450: a novel system modulating Ca2+ channels and contraction in mammalian heart cells. J Physiol *508 (Pt 3)*, 777-792.

Xiao, Y.F., Ke, Q., Seubert, J.M., Bradbury, J.A., Graves, J., Degraff, L.M., Falck, J.R., Krausz, K., Gelboin, H.V., Morgan, J.P., and Zeldin, D.C. (2004). Enhancement of cardiac L-type Ca2+ currents in transgenic mice with cardiac-specific overexpression of CYP2J2. Mol Pharmacol *66*, 1607-1616.

Yang, B., Graham, L., Dikalov, S., Mason, R.P., Falck, J.R., Liao, J.K., and Zeldin, D.C. (2001). Overexpression of cytochrome P450 CYP2J2 protects against hypoxia-reoxygenation injury in cultured bovine aortic endothelial cells. Mol Pharmacol *60*, 310-320.

Yoo, H.H., Kim, N.S., Lee, J., Sohn, D.R., Jin, C., and Kim, D.H. (2009). Characterization of human cytochrome P450 enzymes involved in the biotransformation of eperisone. Xenobiotica *39*, 1-10.

Zeldin, D.C., DuBois, R.N., Falck, J.R., and Capdevila, J.H. (1995). Molecular cloning, expression and characterization of an endogenous human cytochrome P450 arachidonic acid epoxygenase isoform. Arch Biochem Biophys *322*, 76-86.

Zeldin, D.C., Foley, J., Goldsworthy, S.M., Cook, M.E., Boyle, J.E., Ma, J., Moomaw, C.R., Tomer, K.B., Steenbergen, C., and Wu, S. (1997). CYP2J subfamily cytochrome P450s in the gastrointestinal tract: expression, localization, and potential functional significance. Mol Pharmacol *51*, 931-943.

Zeldin, D.C., Foley, J., Ma, J., Boyle, J.E., Pascual, J.M., Moomaw, C.R., Tomer, K.B., Steenbergen, C., and Wu, S. (1996). CYP2J subfamily P450s in the lung: expression, localization, and potential functional significance. Mol Pharmacol *50*, 1111-1117.

Zeldin, D.C., Kobayashi, J., Falck, J.R., Winder, B.S., Hammock, B.D., Snapper, J.R., and Capdevila, J.H. (1993). Regio- and enantiofacial selectivity of epoxyeicosatrienoic acid hydration by cytosolic epoxide hydrolase. J Biol Chem *268*, 6402-6407.

Zhang, J.Y., Prakash, C., Yamashita, K., and Blair, I.A. (1992). Regiospecific and enantioselective metabolism of 8,9-epoxyeicosatrienoic acid by cyclooxygenase. Biochem Biophys Res Commun *183*, 138-143.

Zhang, L., Cui, Y., Geng, B., Zeng, X., and Tang, C. (2008). 11,12-Epoxyeicosatrienoic acid activates the L-arginine/nitric oxide pathway in human platelets. Mol Cell Biochem *308*, 51-56.

Zhang, Y., El-Sikhry, H., Chaudhary, K.R., Batchu, S.N., Shayeganpour, A., Jukar, T.O., Bradbury, J.A., Graves, J.P., DeGraff, L.M., Myers, P., Rouse, D.C., Foley, J., Nyska, A., Zeldin, D.C., and Seubert, J.M. (2009). Overexpression of CYP2J2 provides protection against doxorubicin-induced cardiotoxicity. Am J Physiol Heart Circ Physiol *297*, H37-46.

Zhao, G., Wang, J., Xu, X., Jing, Y., Tu, L., Li, X., Chen, C., Cianflone, K., Wang, P., Dackor, R.T., Zeldin, D.C., and Wang, D.W. (2012). Epoxyeicosatrienoic acids protect rat hearts against tumor necrosis factor-alpha-induced injury. J Lipid Res *53*, 456-466.

Zidar, N., Dolenc-Strazar, Z., Jeruc, J., Jerse, M., Balazic, J., Gartner, U., Jermol, U., Zupanc, T., and Stajer, D. (2007). Expression of cyclooxygenase-1 and cyclooxygenase-2 in the normal human heart and in myocardial infarction. Cardiovasc Pathol *16*, 300-304.

CHAPTER II

Cytochrome P450 2J2-Catalyzed Metabolism of Anandamide and the Effects of Obesity and Diet on Anandamide Metabolism in the Liver

Abstract

One in three adults in America is obese. Obesity contributes to the development of several other medical conditions such as diabetes and atherosclerosis. Increased plasma concentrations of the endogenous cannabinoid anandamide (AEA) have been observed in obese individuals. Moreover, fatty acid amide hydrolase (FAAH), the enzyme responsible for the hydrolysis of AEA, exhibits decreased activity in obesity. As a result, the probability of AEA being metabolized by other drug metabolizing enzymes such as cytochrome P450s is increased. The role of AEA in energy balance involves the brain and the peripheral organs associated with energy intake including the intestine and the liver. Because of this, it is important to investigate AEA metabolism in these relevant drug metabolizing organs. CYP2J2 is involved in the metabolism of various antihistamines and other drugs in the intestines and may also contribute to intestinal metabolism of AEA. The studies reported here demonstrate that purified human CYP2J2 metabolizes AEA to form the 20-hydroxyeicosatetraenoic acid ethanolamide (HETE-EA) and several epoxygenated products including the 5,6-, 8,9-, 11,12-, and 14,15-epoxyeicosatrienoic acid ethanolamides (EET-EAs) in the reconstituted system. Kinetic studies suggest that the K_M values for these products range from approximately 10-468

μM and that the k_{cat} values range from 0.2-23.3 pmol/min/pmol of CYP450. The catalytic turnover was 7.12 pmol of total product formed/pmol of CYP450/min at 37°C. Human intestinal microsomes metabolize AEA to 20-HETE-EA, 5,6-, 8,9-, and 11,12-EET-EAs with apparent K_m values of 141, 312, 495, and 1700 μM and V_{max} values of 602, 4.4, 4.3, and 30 pmols/min/mg of protein, respectively; however, inhibition studies suggest that CYP2J2 is not a major contributor to intestinal AEA metabolism. In addition, studies using rat liver microsomes suggest that obesity and diet may have significant effects on AEA metabolism in the liver.

Introduction

According to the Centers for Disease Control and Prevention, a little over 35% of the adults in the United States are obese. Moreover, it is estimated that 17% of children, aged 2-19 years, are obese. Obesity contributes to several health concerns including heart disease, type 2 diabetes, stroke, and some cancers. Obesity occurs when an imbalance between food intake and energy expenditure exists and this energy imbalance results in excessive fat accumulation in organs involved in metabolism (Ahima, 2008). Evidence suggests that modifications in the endocannabinoid system (ECS), consisting of the cannabinoid receptors, their endogenous ligands, and the enzymes that regulate the synthesis and degradation of those ligands, can be correlated with several pathological conditions, including a variety of immunological, cardiovascular, gastrointestinal, and metabolic disorders that exhibit altered tissue concentrations of anandamide (AEA) or 2-arachidonoyl glycerol (2-AG), the two most prominent endocannabinoids (ECBs) (Alpini

and Demorrow, 2009; Ashton and Smith, 2007; Bifulco et al., 2007; Di Marzo, 2008; Di Marzo et al., 2004; Lambert, 2007; Storr and Sharkey, 2007).

AEA and other ECBs are signaling mediators that increase appetite by activating the cannabinoid 1 receptor (CB1R) (Matias et al., 2006a). The ECS has been identified in the brain and peripheral tissues involved in energy balance including, but not limited to, the hypothalamus, skeletal muscles, myenteric neurons and epithelial cells of the intestine, and the liver (Pertwee, 1999). In the hypothalamus, ECBs activate CB1Rs to inhibit excitatory and inhibitory neurotransmission in several areas of the brain including those associated with food consumption and leptin signaling (Cota et al., 2003b; Di Marzo et al., 2001; Schlicker and Kathmann, 2001). Activation of the ECS leads to increased body weight, lipogenesis, and defective glucose uptake into skeletal muscle (Cota et al., 2003a; Eckardt et al., 2009). Likewise, activation of presynaptic CB1Rs in neurons and nerve fibers of the stomach, small intestine, and colon decreases gastric acid secretion and intestinal motility and secretion through inhibition of acetylcholine release (Di Carlo and Izzo, 2003; Kulkarni-Narla and Brown, 2000, 2001; Mascolo et al., 2002; Pinto et al., 2002). Overactivation of the ECS in the liver increases liver fat and lipogenesis, in particular VLDL (very low density lipoprotein) which is consider to be "bad" cholesterol (Nesto and Mackie, 2008).

Several studies have shown that overweight and obese individuals have higher levels of circulating endocannabinoids, e.g. AEA and 2-AG (Annuzzi et al., 2010; Engeli et al., 2005; Naughton et al., 2013). In general, the Western diet is considered to be a high-fat diet that is rich in linoleic acid (LA), the biosynthetic precursor to arachidonic acid (AA) (Nagai et al., 2005). It has been shown that increased dietary intake of LA can

lead to elevated levels of endogenous endocannabinoids and induce weight gain and inflammation (Alvheim et al., 2012; Alvheim et al., 2013; Kim et al., 2013; Matias et al., 2008). The elevated endogenous cannabinoid levels are believed to contribute to the overactivation of the ECS observed in obesity and to aggravate the severity of obesity-related complications (Cote et al., 2007; Matias et al., 2006b).

AEA normally undergoes hydrolysis by fatty acid amide hydrolase (FAAH) to form AA and ethanolamide. However, the elevated levels of AEA observed in obese subjects are correlated with a decrease in FAAH activity (Engeli et al., 2005). As a result, it is likely that other mechanisms of anandamide metabolism may be more important in obesity. AEA can also be oxidized by cyclooxygenases (COX) (Kozak et al., 2002; Yu et al., 1997), lipoxygenases (LOX) (Hampson et al., 1995; Ueda et al., 1995), and cytochrome P450s (CYP450s) (Snider et al., 2007; Snider et al., 2008; Sridar et al., 2011; Stark et al., 2008).

CYP450s are a superfamily of mono-oxygenases that are involved in the metabolism of a wide variety of endogenous and exogenous compounds. The metabolism of AEA by human cytochrome P450s is known to give the following metabolites: 19- and 20-hydroxyeicosatetraenoic acid ethanolamides (HETE-EAs) and 5,6-, 8,9-, 11,12-, and 14,15-epoxyeicosatrienoic acid ethanolamides (EET-EAs) (Alberich Jorda et al., 2004; Pratt-Hyatt et al., 2010; Snider et al., 2007; Snider et al., 2009; Snider et al., 2008; Sridar et al., 2011; Stark et al., 2008). CYP2J2 is a CYP450 epoxygenase that is mainly expressed in the cardiovascular system (Wu et al., 1996), but it is also expressed in the intestines (Paine et al., 2006; Wu et al., 1996), lung (Zeldin et al., 1996), pancreas (Zeldin et al., 1997), kidney (Ma et al., 1999), liver (Nishimura et al., 2003; Wu et al., 1996),

brain (Dutheil et al., 2009), salivary ducts, and stomach (Enayetallah et al., 2004). CYP2J2 metabolizes arachidonic acid (AA) to give 5,6-, 8,9-, 11,12-, 14,15-epoxyeicosatrienoic acids (EETs) and several minor hydroxyeicosatetraenoic acids (HETEs) (Wu et al., 1996); however, its ability to metabolize AEA has not yet been investigated. CYP2J2 is involved in the intestinal metabolism of the non-sedating antihistamines ebastine and astemizole and may contribute to AEA metabolism in the intestine (Hashizume et al., 2002; Matsumoto et al., 2002). This chapter provides information on the metabolism of AEA by purified CYP2J2 in the reconstituted system. Because our lab has previously investigated AEA metabolism by human liver microsomes, we investigated AEA metabolism by human intestine microsomes in order to study AEA metabolism in peripheral organs involved in energy balance (Snider et al., 2007). In order to determine if obesity and diet affect AEA metabolism, we also compared AEA metabolism by liver microsomes derived from rats susceptible or resistant to diet-induced obesity. This rat model was developed by Dr. Barry E. Levin (Rutgers New Jersey Medical School, Newark, NJ) by selectively breeding rats for the propensity to gain weight when fed a moderately fatty diet (Levin et al., 1997).

Methods and Materials

Materials. AEA, AEA-d_8, 5,6-EET-EA, 8,9-EET-EA, 11,12-EET-EA, 14,15-EET-EA, 20-HETE-EA, and 12-(3-admantan-1-yl-ureido) dodecanoic acid (AUDA) were purchased from Cayman Chemical (Ann Arbor, MI). Danazol was purchased from Steraloids, Inc. (Newport, RI). Ketoconazole, sulfaphenazole, 1-aminobenzatriazole, and

diphenyliodonium chloride were purchased from Sigma (St. Louis, MO). All other reagents were of the highest quality and were obtained from commercial sources.

Enzymes. The human CYP450 CYP2J2 cDNA was a gift from Dr. Rheem Totah (University of Washington, Seattle, WA). CYP2J2 and CYP450 reductase were expressed in *Escherichia coli* and purified as previously described (Hanna et al., 1998; Smith et al., 2008). Human intestinal microsomes were purchased from BD Biosciences (Woburn, MA).

Preparation of Microsomes from Rat Livers. The rat livers were a gift from Dr. Carrie Ferrario (University of Michigan, Ann Arbor, MI). The diet resistant (DR) and diet-induced obese (DIO) rats from which these livers were collected were originally purchased from Taconic (Germantown, NY). The preparation of microsomes was performed as described previously (Lin et al., 1998). Briefly, rat livers were chopped and subsequently homogenized using a Tissue Tearor (Biospec Product Inc.) in homogenization buffer (100 mM potassium phosphate buffer, pH 7.4, 1 mM EDTA, and 150 mM KCl). The homogenate was centrifuged at 10,000 *g* for 30 min and the supernatant was filtered through gauze to remove the fat. The supernatant was then ultracentrifuged at 100,000 *g* for 75 min. The resulting pellet was resuspended using a glass pestle in a Dounce homogenizer in pyrophosphate buffer (100 mM tetrasodium pyrophosphate, pH 7.4, and 1 mM EDTA) to remove hemoglobin. The homogenate was centrifuged again at 100,000 *g* for 75 min and the resulting pellet was resuspended in suspension buffer (100 mM potassium phosphate buffer, pH 7.4, 1 mM EDTA, and 20% glycerol). Bovine serum albumin was used as the standard for the BCA Protein Assay (Pierce, Rockford, IL) which was used to determine the protein concentration of the

microsomes and the reduced CO difference spectrum was used to determine the P450 concentration (Omura and Sato, 1964). Briefly, microsomes (50 µL) were suspended in 0.1 M phosphate buffer, pH 7.4, containing 20% glycerol to a total volume of 0.5 mL in a 1 cm^2 cell. The microsomes were reduced by the addition of a few milligrams of sodium dithionite and an absorbance baseline was measure using a Shimadzu UV-Vis recording spectrophotometer UV-2501PC. The solution was bubbled with CO for 30 s and the absorbance measured again. The Beer-Lambert Law (A = εbc) was used to calculate the concentration "c", where "A" is the difference in absorbance between baseline and the peak that absorbed at 450 nm, and "b" and "ε" are known constants 1 cm and 90 $mM^{-1}cm^{-1}$, respectively.

AEA Metabolism Assays. CYP2J2 was reconstituted with reductase (1:2 ratio) in lipid (L-α-dilauroyl-phosphocholine) on ice for 60 min as described previously (Snider et al., 2007; von Weymarn et al., 2004). The metabolism of anandamide was determined using incubation mixtures (0.5 mL) containing 100 mM potassium phosphate buffer (pH 7.4), catalase, anandamide (1.25-50 µM), and reconstituted CYP2J2 (50 pmols). For microsomal studies, 200 µg aliquots of microsomal protein were combined with 100 mM potassium phosphate buffer, pH 7.4, 3.3 mM $MgCl_2$, and anandamide in the presence or absence of the P450 inhibitors, danazol (100 nM) for CYP2J2, ketoconazole (1 µM) for CYP3A4 and sulfaphenazole for CYP2C9 (10 µM), in a final volume of 0.25 mL. Reactions were initiated by the addition of 1 mM (recombinant) or 1.3 mM (microsomes) NADPH and allowed to continue with shaking for 25-30 min at 37°C. Control reactions were performed in the absence of NADPH. The reactions were terminated by the addition of 1-2 ml of cold ethyl acetate. After the addition of the internal standard, anandamide-d_8,

the samples were vortexed for 2 min and centrifuged at full speed using a desktop centrifuge for 5 min. The organic layer was collected and dried down under a constant stream of nitrogen gas. The dried samples were resuspended in 100 μL of methanol and 10 μL aliquots were subjected to electrospray ionization-liquid chromatography/mass spectrometry (ESI-LC/MS) analysis. The standard curves for the various metabolites that were used for the quantification and determination of the K_M and k_{cat} values were generated by subjecting various known amounts of authentic standards to the same sample workup and ESI-LC/MS analysis.

ESI-LC/MS Analysis. Samples (10 μL) were injected onto a Hypersil ODS column (5 μm, 4.6 × 100 mm; Thermo Fisher Scientific, Waltham, MA) that had been equilibrated with 25% solvent A (0.1% acetic acid in water) and 75% solvent B (0.1% acetic acid in methanol). The metabolites were resolved using the following gradient: 0 to 5 min, 75% B; 5 to 20 min, 75 to 100% B; 20 to 25 min, 100% B; 25 to 26 min, 100 to 75% B; and 26 to 30 min, 75% B. The flow rate was 0.3 ml/min. The column effluent was directed into the LCQ mass analyzer (Thermo Fisher Scientific). The ESI conditions were as follows: sheath gas, 90 arbitrary units; auxiliary gas, 30 arbitrary units; capillary temperature, 200°C; and spray voltage, 4.5 V. Data were acquired in positive ion mode for anandamide and its metabolites using the Xcalibur software package (Thermo Fisher Scientific) with one full scan from 300 to 500 mass/charge ratio (m/z) followed by one data-dependent scan of the most intense ion.

Data Analysis. Nonlinear regression analyses of the data were performed using GraphPad Prism 6 (GraphPad Software Inc., San Diego, CA; http://www.graphpad.com).

Results

Metabolism of Anandamide by Human Recombinant CYP2J2. Arachidonic acid (AA) is metabolized by recombinant CYP2J2 to form four regioisomeric EETs (Wu et al., 1996). As shown in Figure 2.1, AEA is very similar to AA in structure. AA is required for the biosynthesis of AEA. The AEA precursor, *N*-arachidonyl-phosphatidylethanolamine (NAPE), is formed when the calcium-dependent enzyme, *N*-acyltransferase, catalyzes the transfer of AA from the sn-1 position of a glycerophospholipid to the amino group of phosphatidylethanolamine (Snider et al., 2010; Wang and Ueda, 2009). The precursor can then be converted to AEA via several pathways that have been reviewed in the literature (Hansen et al., 2000; Jin et al., 2009; Schmid et al., 1990; Snider et al., 2010), but the most direct pathway is catalyzed by a NAPE-specific phospholipase D (Okamoto et al., 2009). Due to the similarities between the structures of AEA and AA, and the fact that AEA is a substrate for several other CYP450s including CYP2D6, CYP3A4, and CYP2B6 (Omura and Sato, 1964; Snider et al., 2007; Snider et al., 2008; Sridar et al., 2011), we investigated the possibility that anandamide could also be a substrate for CYP2J2.

Figure 2.2 shows the extracted ion chromatograms for the metabolism of anandamide by purified human CYP2J2. Figure 2.2 (Top) is the extracted ion chromatogram at *m/z* 348 and it shows the positive ion formed by anandamide in the mass spectrometer which eluted at 23.6 min under the LC/MS conditions described in *Materials and Methods*. The bottom chromatogram shows the five mono-oxygenated products with *m/z* values of 364 that eluted at 15.2, 18.1, 19.1, 19.6, and 20.5 min (Fig.

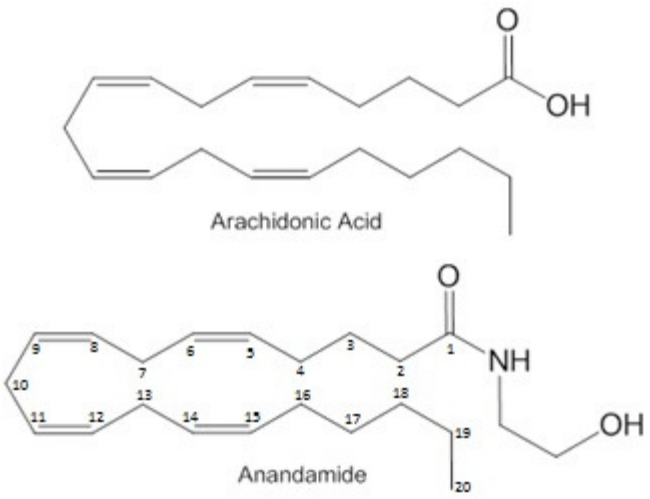

Figure 2.1. Structures of arachidonic acid and anandamide. Arachidonic acid and anandamide are identical in structure with the exception that arachidonic acid has a hydroxyl group on carbon one while anandamide has an ethanolamine group on carbon one.

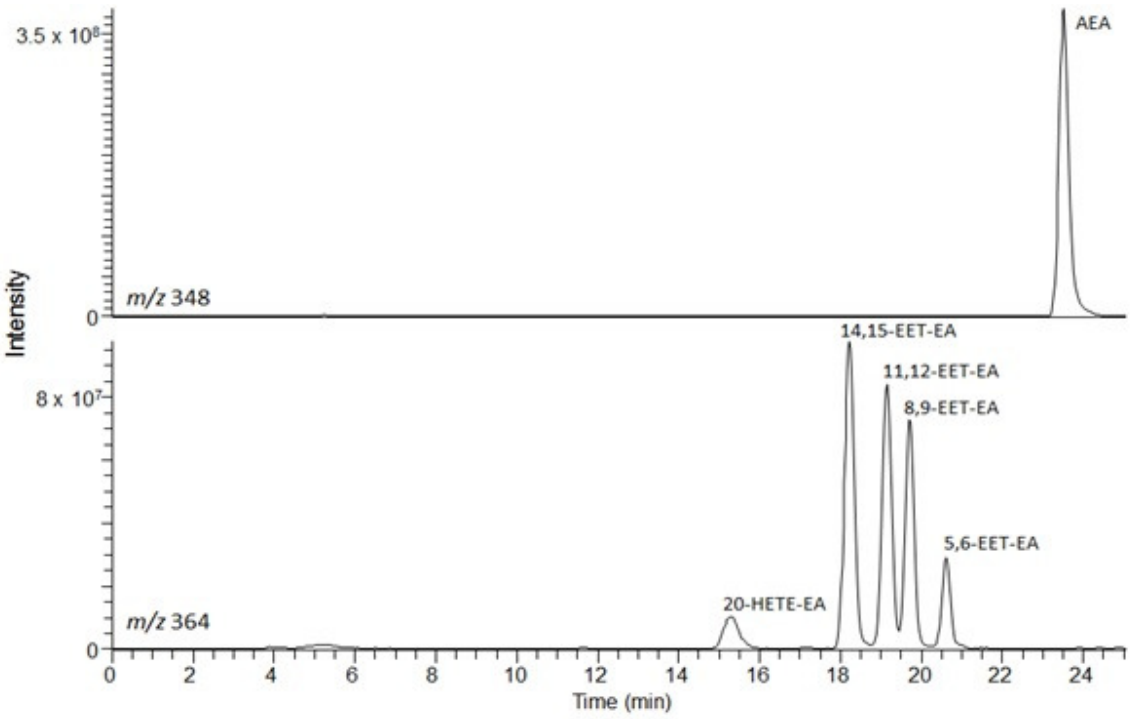

Figure 2.2. AEA metabolism by CYP2J2. Purified CYP2J2 was reconstituted with reductase (1:2 ratio) in 10 μg of lipid (L-α-dilauroyl-phosphocholine) on ice for 30 min. The reconstituted enzyme (15 μL) was added to the incubation mixture (0.5 mL) containing 100 mM potassium phosphate buffer (pH 7.4), anandamide (10 μM), and catalase. Reactions were initiated by the addition of 1 mM of NADPH and allowed to continue with shaking for 30 min at 37°C. The reactions were terminated, metabolites extracted, and products analyzed by ESI-LC/MS as described in *Materials and Methods*. The extracted ion chromatogram observed at *m/z* 348, shows the parent ion, anandamide, eluting at 23 min (Top). The extracted ion chromatogram observed at *m/z* 364, shows the monooxygenated product peaks which elute at approximately 15.3, 18.2, 19.1, 19.7, and 20.6 min for 20-HETE-EA, 14,15-, 11,12-, 8,9-, and 5,6-EET-EA, respectively (Bottom). Product identity was verified by comparing the retention times and fragmentation patterns of the products formed with their respective commercial standards.

2.2). Based on their retention times and fragmentation patterns when compared with authentic standards (data not shown), the metabolites were identified as 20-HETE-EA, 14,15-, 11,12-, 8,9-, and 5,6-EET-EAs, respectively. Four di-oxygenated products were observed in the extracted ion chromatogram at *m*/*z* 380 (Figure 2.3) which eluted at approximately 8, 11, 13, 14, and 16 min; however, these products could not be unequivocally identified due the lack of commercially available di-oxygenated AEA metabolites.

Kinetic Studies on the Metabolism of Anandamide by Human Recombinant CYP2J2. The reaction conditions used to determine the kinetic constants, K_M and k_{cat}, for the hydroxylation and epoxygenation of anandamide by purified CYP2J2 were shown to be linear with respect to protein concentration (up to 25 pmols) and time of incubation (up to 25 min) (data not shown). As shown in Figure 2.4, the metabolism of anandamide exhibited typical Michaelis-Menten kinetics for the formation of 20-HETE-EA and 5,6-, 8,9-, 11,12-, and 14,15- EET-EAs. The observed K_M values calculated from the data in Figure 2.4 using GraphPad Prism 6 software were 10, 468, 104, 101, and 103 μM and the k_{cat} values were 0.2, 23.3, 3.6, 4.1, and 6.9 pmol/min/pmol of CYP450, respectively. The efficiency of the enzyme for the formation of all five metabolites, as measured by the k_{cat}/K_M values, was relatively the same for all products formed with values of 0.02, 0.05, 0.03, 0.04, and 0.07 for the 5,6-, 8,9-, 11,12-, 14,15-EET-EAs, and 20-HETE-EA, respectively.

AEA Metabolism by Human Intestinal Microsomes. Because the intestine is one of the peripheral organs involved in energy balance, we investigated the ability of

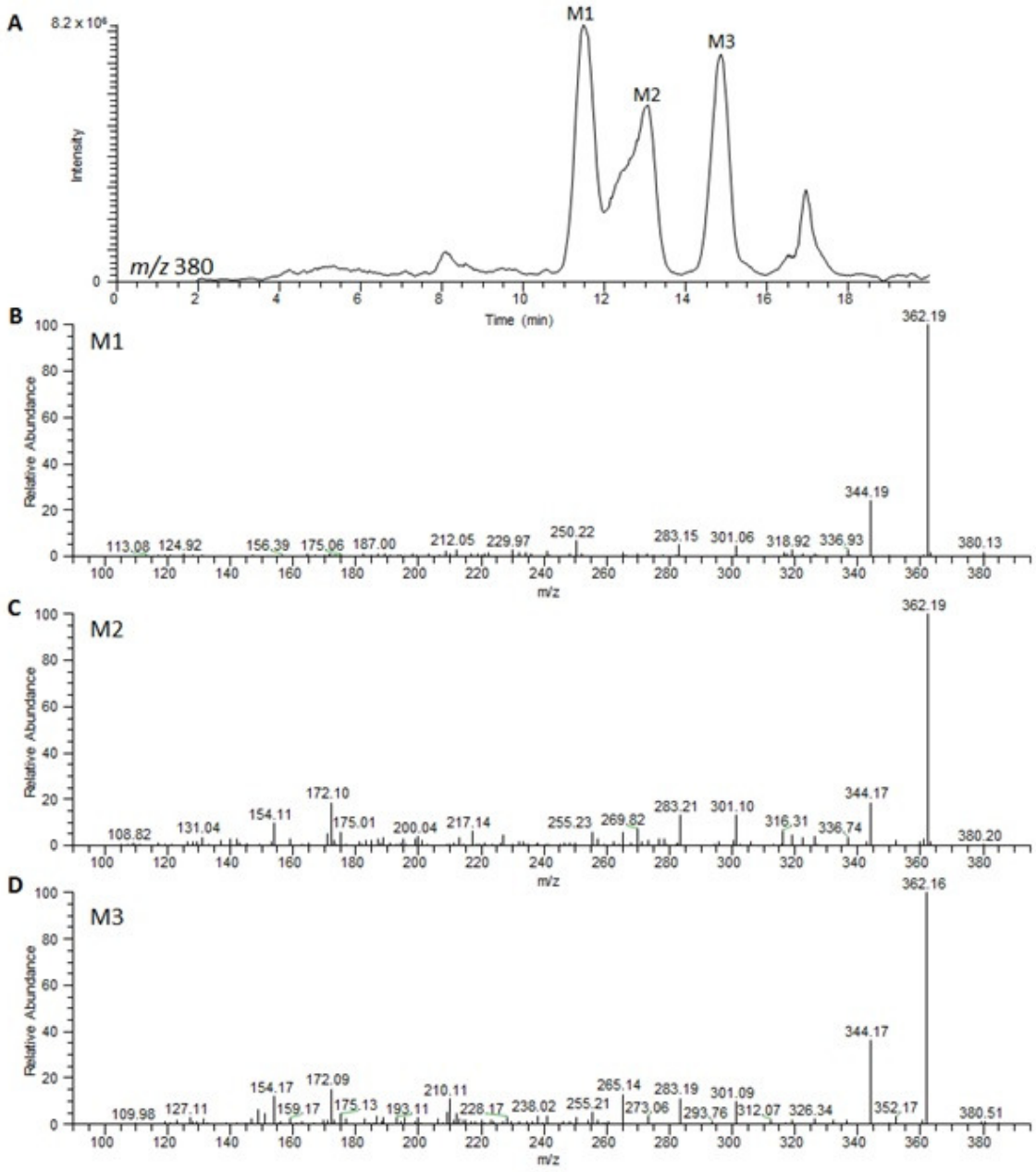

Figure 2.3. Formation of di-oxygenated metabolites of AEA by CYP2J2. Recombinant CYP2J2 was reconstituted with reductase (1:2 ratio) in lipid (L-α-dilauroyl-phosphocholine) on ice for 30 min. The enzyme source (15 µL) was added to the incubation mixture (0.5 mL) containing 100 mM potassium phosphate buffer (pH 7.4), anandamide (50 µM), and catalase. Reactions were initiated by the addition of 1 mM of NADPH and allowed to continue for 30 min at 37°C. The metabolites were extracted and analyzed as described previously in *Materials and Methods.* The extracted ion chromatogram observed at *m/z* 380, shows that at least three di-oxygenated products are formed (A). The fragmentation patterns for the three unidentified metabolites M1 (B), M2 (C), and M3 (D) are shown.

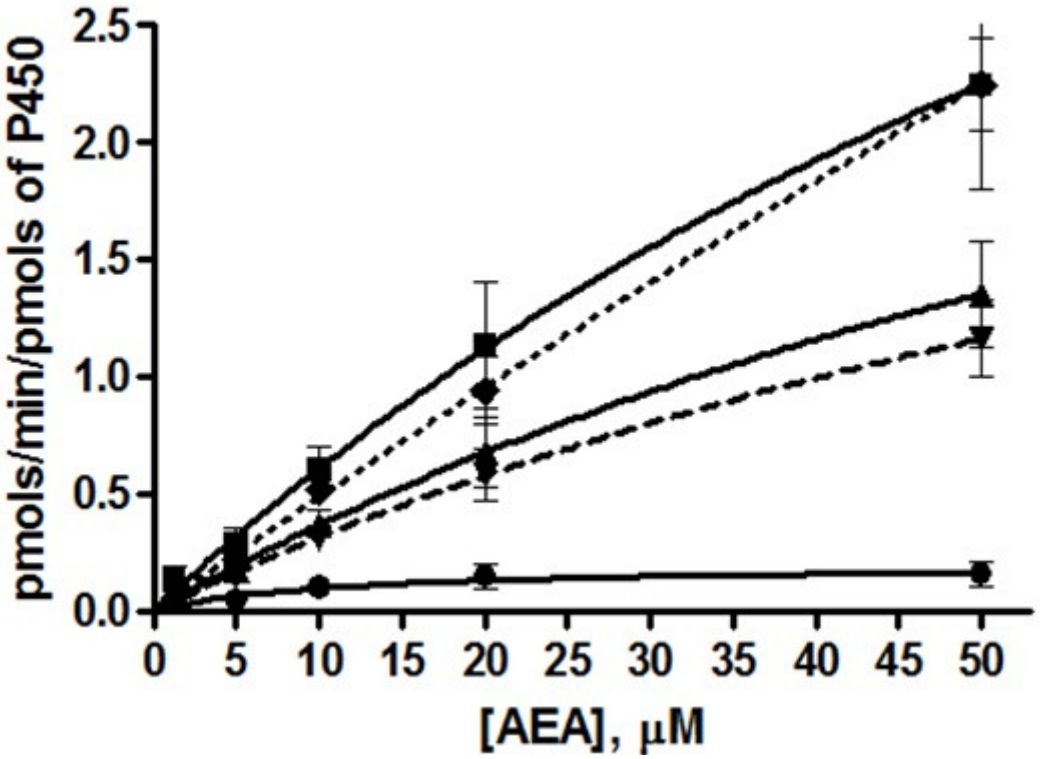

Figure 2.4. Kinetic analysis of anandamide metabolism by purified CYP2J2. Varying concentrations of anandamide (1.25-50 μM) were metabolized by reconstituted CYP2J2 (25 pmol) for 25 min at 37°C. The symbols for the metabolites are: 14,15-EET-EA (■), 11,12-EET-EA (▲), 8,9-EET-EA (▼), 5,6-EET-EA (♦), and 20-HETE-EA (●). Standard curves were generated for each metabolite to determine the amount of product formed. Experiments were done in duplicate and repeated four times (n = 8). Error bars represent SEM values.

human intestinal microsomes (HIM) to metabolize AEA. Incubations containing 200 µg of HIM were used to metabolize AEA for 30 min at 37°C as described in *Materials and Methods*. Figure 2.5 shows all the metabolites formed from AEA metabolism by HIM. Figure 2.5 (Top) shows the extracted ion chromatogram at *m/z* 364 for the metabolites from this reaction with peaks eluting at 15.9, 18.4, 19.2, 19.8, and 20.7 min, which correspond to 20-HETE-EA, 14,15-, 11,12-, 8,9-, and 5,6-EET-EAs, respectively. Although no standard is commercially available for positive identification of this product, the product eluting at 17.3 min is thought to be 19-HETE-EA (Pratt-Hyatt et al., 2010; Snider et al., 2007; Snider et al., 2009). The peaks eluting at 11.6, 13.4, and 15.6 min observed at *m/z* 382 correspond to the diols formed when the epoxides (*m/z* 364) are hydrolyzed (Figure 2.5 (Bottom)). Evidence to support this can be seen with the increase of epoxide formation and the decrease in diol formation in the presence of AUDA (10 µM), a soluble epoxide hydrolase inhibitor (dashed line) (Morisseau and Hammock, 2013).

Figure 2.6 shows the kinetic curves for the products formed by the metabolism of AEA by intestinal microsomes. Two different kinetic models were utilized to determine the K_m and V_{max} for 20-HETE-EA, 5,6-, 8,9-, and 11,12-EET-EAs. The levels of 14,15- formation under these conditions were too low to calculate accurate values for the kinetic constants. Likewise, the kinetic information for 19-HETE-EA could not be calculated because there is no standard available for this metabolite. Double reciprocal plots were used to determine the kinetic constants for the EET-EAs and the formation of 20-HETE-EA followed Michaelis-Menten kinetics. The K_m values for 20-HETE-EA, 5,6-, 8,9-, and 11,12-EET-EAs were 141, 312, 495, and 1700 µM, respectively. The V_{max} values

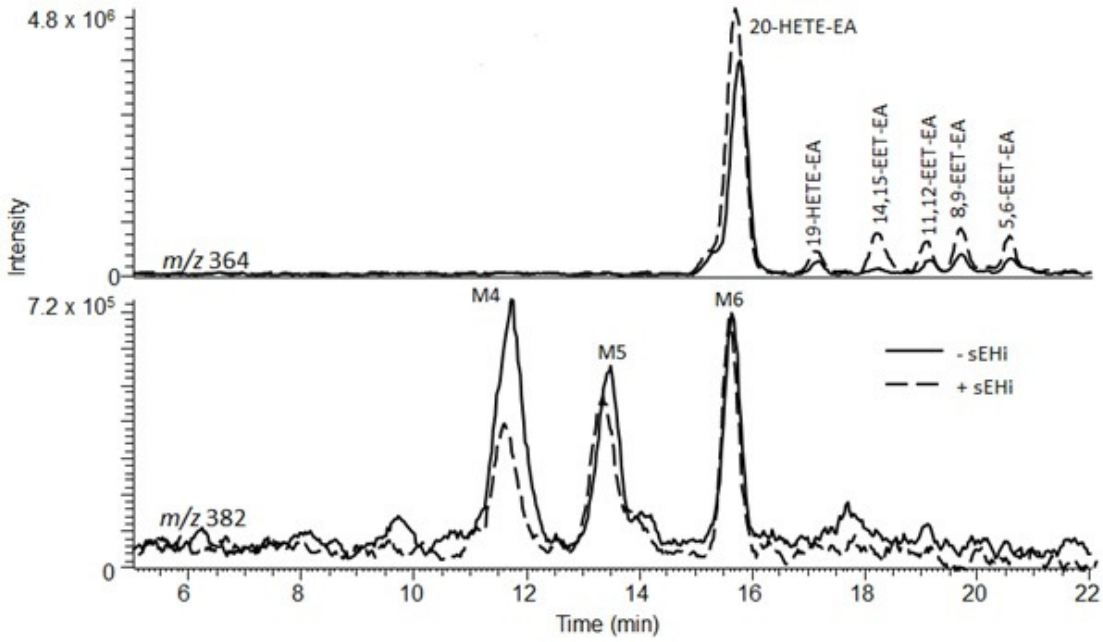

Figure 2.5. AEA metabolism by HIM in the presence and absence of AUDA. Human intestinal microsomes (200 µg) were incubated with anandamide (25 µM) for 30 min at 37°C and the metabolites were extracted and analyzed as described in *Materials and Methods*. The extracted ion chromatograms for the mono-oxygenated products (*m/z* 364, Top) and the diols formed by the hydrolysis of the epoxides (*m/z* 382, Bottom) are shown. The dashed lines represent the chromatogram observed in the presence of 10 µM of AUDA, a soluble epoxide hydrolase inhibitor (sEHI), and the solid lines represent the products formed in the absence of the sEHI.

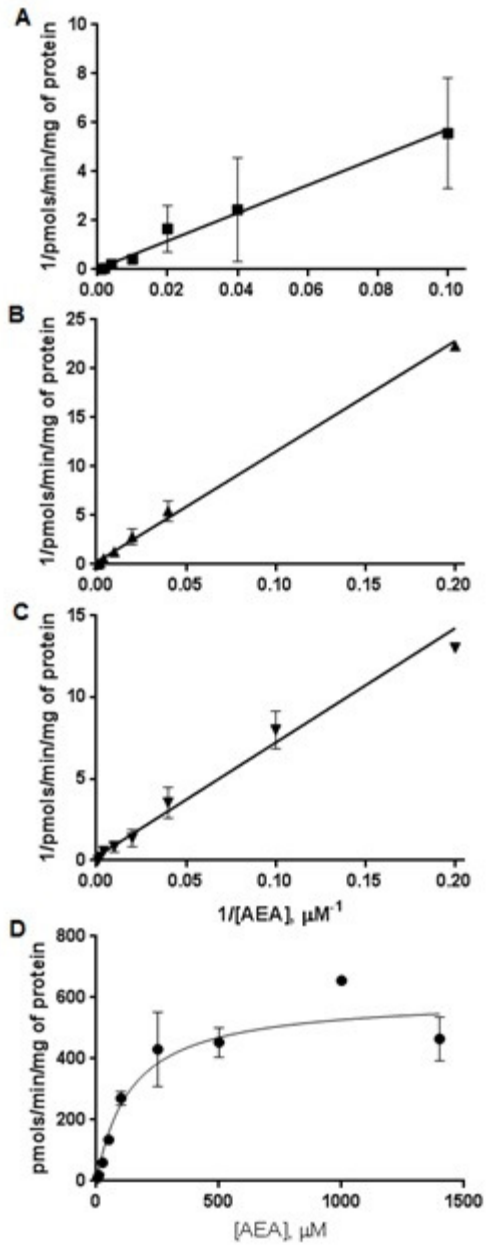

Figure 2.6. Kinetics for the metabolism of AEA by HIM. Human intestinal protein (0.8 mg/mL) was reacted with AEA (5-1400 μM) in 0.1 M potassium phosphate buffer containing $MgCl_2$. The reaction was initiated with NADPH (1.3 mM) and incubated at 37°C for 30 min with agitation. The reaction was quenched with 1 mL of ice cold ethyl acetate and the metabolites were extracted and prepared for analysis as described in *Materials and Methods.* The double reciprocal plot was used to determine the kinetic parameters for 11,12-EET-EA (■) (A), 8,9-EET-EA (▲) (B), and 5,6-EET-EA (▼) (C). A Michaelis-Menten kinetic plot was used to determine the kinetic parameters for 20-HETE-EA (●) (D). The data were plotted using the GraphPad Prism 6 software and each point represents the mean ± SEM (n = 6).

calculated were 602, 4.4, 4.3, and 30 pmols/min/mg of protein for 20-HETE-EA, 5,6-, 8,9-, and 11,12-EET-EAs, respectively.

Contribution of Individual P450s to the Metabolism of AEA by HIM. Several cytochrome P450s are expressed in the intestines at detectable levels including CYP3A4, CYP2C9, and CYP2J2 (Paine et al., 2006). Selective chemical inhibitors for CYP3A4 (ketoconazole), CYP2C9 (sulphaphenazole), or CYP2J2 (danazol) (Lee et al., 2012) were used to determine the relative contribution of each P450 to AEA metabolism in the intestine. In the absence of AUDA, no detectable amount of 14,15-EET-EA was formed at the concentration of AEA used for this experiment; however, 11,12-, 8,9-, and 5,6-EET-EAs were formed in addition to 19- and 20-HETE-EA. The bar graph in Figure 2.7 displays the changes in the formation of various mono-oxygenated products in the presence of the selective P450 inhibitors, while Table 2.1 shows the numerical values. Based on the decrease in product formation after inhibition of selected P450 activity as compared to control, only CYP2C9 and CYP3A4 appear to contribute significantly to the formation of 11,12-EET-EA and 20-HETE-EA, respectively (Figure 2.7 and Table 2.1).

Changes in the Metabolism of AEA in Obese Rats. To determine if there is a difference in AEA metabolism as a result of obesity, liver microsomes were made from diet-induced obese (DIO) rats and diet-resistant (DR) rats as described in *Materials and Methods*. In addition, we studied the difference in AEA metabolism in rats fed a normal diet (ND) and rats fed a junk food diet (JFD). Interestingly, rat liver microsomes (RLM) do not form the traditional P450-mediated EET-EAs and HETE-EAs from AEA seen with human liver microsomes. The candidates selected for monitoring had to fit the following criteria: (1) their formation is dependent on the presence of NADPH,

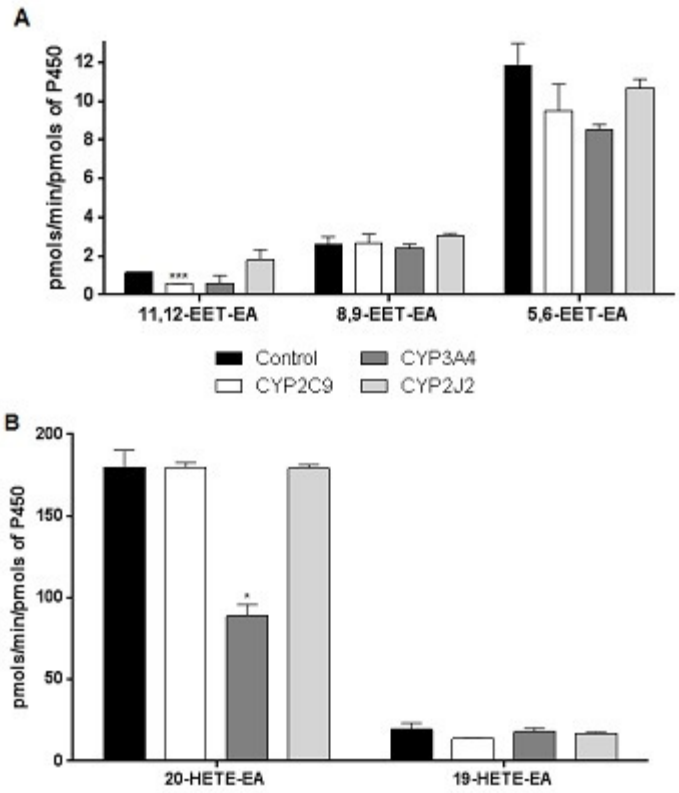

Figure 2.7. Contributions of individual P450s to AEA metabolism by HIM. The HIM (200 µg) were incubated with anandamide (100 µM) for 30 min at 37°C in the presence of vehicle, the selective CYP3A4 inhibitor ketoconazole (1 µM), the selective CYP2C9 inhibitor sulfaphenazole (10 µM), or the selective CYPJ2 inhibitor danazol (100 nM). The reactions were quenched with ice cold ethyl acetate and the metabolites were extracted and analyzed as described in *Materials and Methods*. (A) Epoxide formation in pmols/min/pmols of P450, (B) hydroxylated products formed in pmols/min/pmols of P450. Statistical significance determined by GraphPad Prism 6 Program using the Holm-Sidak method, *, $P < 0.05$; ***, $P < 0.001$. Each bar represents the mean ± SEM for one experiment completed in duplicate.

	Control	CYP2C9	CYP3A4	CYP2J2
11,12-EET-EA	1.2 ± 0.006	0.6 ± 0.01	0.6 ± 0.4	1.8 ± 0.5
8,9-EET-EA	2.6 ± 0.4	2.7 ± 0.5	2.4 ± 0.2	3.1 ± 0.1
5,6-EET-EA	11.9 ± 1.1	9.5 ± 1.4	8.5 ± 0.2	10.7 ± 0.4
20-HETE-EA	179.8 ± 10.4	179.4 ± 3.2	89.1 ± 6.7	179.3 ± 2.2
19-HETE-EA	19.4 ± 3.9	13.9 ± 0.3	17.9 ± 2.3	16.8 ± 1.0

Table 2.1. Numerical values for product formation by P450s in the presence of specific inhibitors. The control column shows the amount of each product formed in the presence of vehicle. The CYP2C9, CYP3A4, and CYP2J2 columns show the amount of product formed in the presence of the selective inhibitors sulfaphenazole (10 μM), ketoconazole (1 μM), and danazol (100 nM), respectively. The compounds and concentrations used were previously shown to be effective at inhibiting the respective P450 (Hashizume et al., 2002; Lee et al., 2012). The values are taken directly from the bar graphs in Figure 2.7 and represent the mean ± SEM in pmols/min/mg of protein.

(2) the presence of selective inhibitors for COX and LOX did not inhibit formation, and (3) the presence of an inhibitor of the NADPH-cytochrome P450 reductase decreases its formation. Figure 2.8 shows a bar graph for the three P450-mediated products, M7, M8, and M9, that were selected to be monitored to compare differences in P450 activity in obese vs. lean animals and animals on a normal diet vs. a junk food diet. Two of the metabolites are observed at *m/z* 356 and elute at 16.6 (M7) and 17.5 min (M8). The third product is observed at *m/z* 380 and elutes at 22 min (M9).

The rats used for this experiment were 65 days old upon arrival and both DR and DIO rats were fed a ND. At 120 days of age, some DR rats were fed a JFD while another group of DR rats continued on the ND. Likewise, some DIO rats continued on a ND while others started the JFD. Rats continued on the ND or the JFD for an additional 40 days until they were sacrificed and the livers were harvested. All rats had free access to either the ND, standard lab chow (Purina Lab Diet 5001: 4.5% fat, 23% protein, 6.2% sugar; 4 kcal/g), or the JFD, a mashed mixture of 40 g of potato chips, 130 g of peanut butter, 40 g of chocolate chip cookies, 130 g of Nesquik powdered chocolate flavoring, and 200 g of standard lab chow (19.6% fat, 14% protein, 25.7% sugar; 4.5 kcal/g). The average weight of the rat model on the different diets is as follows: DIO rats fed JFD > DIO rats fed ND > DR rats fed JFD > DR rats fed ND. In addition to the differences in weight, DIO rats fed the JFD also exhibited glucose intolerance and relative insulin resistance (Levin et al., 1997).

Rat liver microsomes derived from DR rats fed a ND, DR rats fed a JFD, and DIO rats fed a ND were incubated with AEA (100 µM) for 30 min at 37°C. Figure 2.9A shows

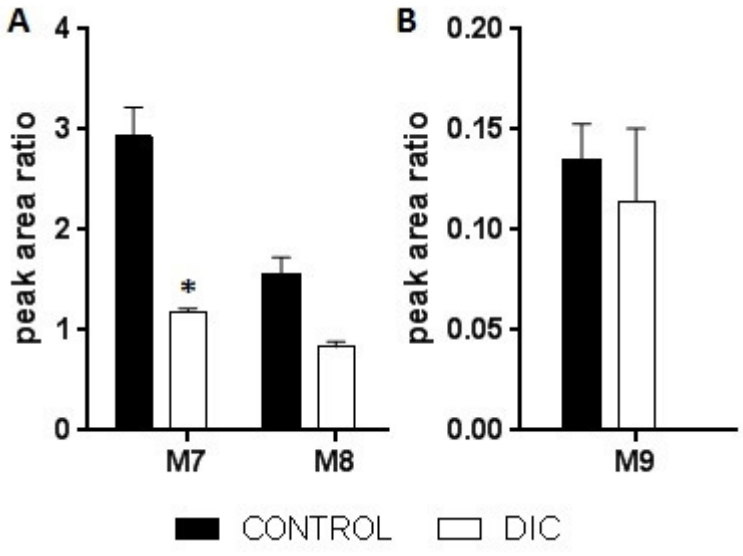

Figure 2.8. Determination of P450-mediated metabolites formed by rat liver microsomes. Anandamide (100 µM) was incubated with RLM (200 µg) in the presence of vehicle or 10 µM of indomethacin, a COX inhibitor (data not shown), nordihydroguaiaretic acid, a LOX inhibitor (data not shown), 1-aminobenzotriazole, a P450 inhibitor (data not shown), or diphenyliodonium chloride (DIC), a P450 reductase inhibitor. The reactions were incubated for 30 min at 37°C and the products were extracted and analyzed by ESI-LC/MS as described in *Materials and Methods* for products observed at (A) *m/z* 356 and (B) *m/z* 380. The bar graph represents the peak area ratio (product peak area: AEA-d_8 peak area) for the amount of product formed as the mean ± SEM from two separate experiments.*, $P < 0.05$.

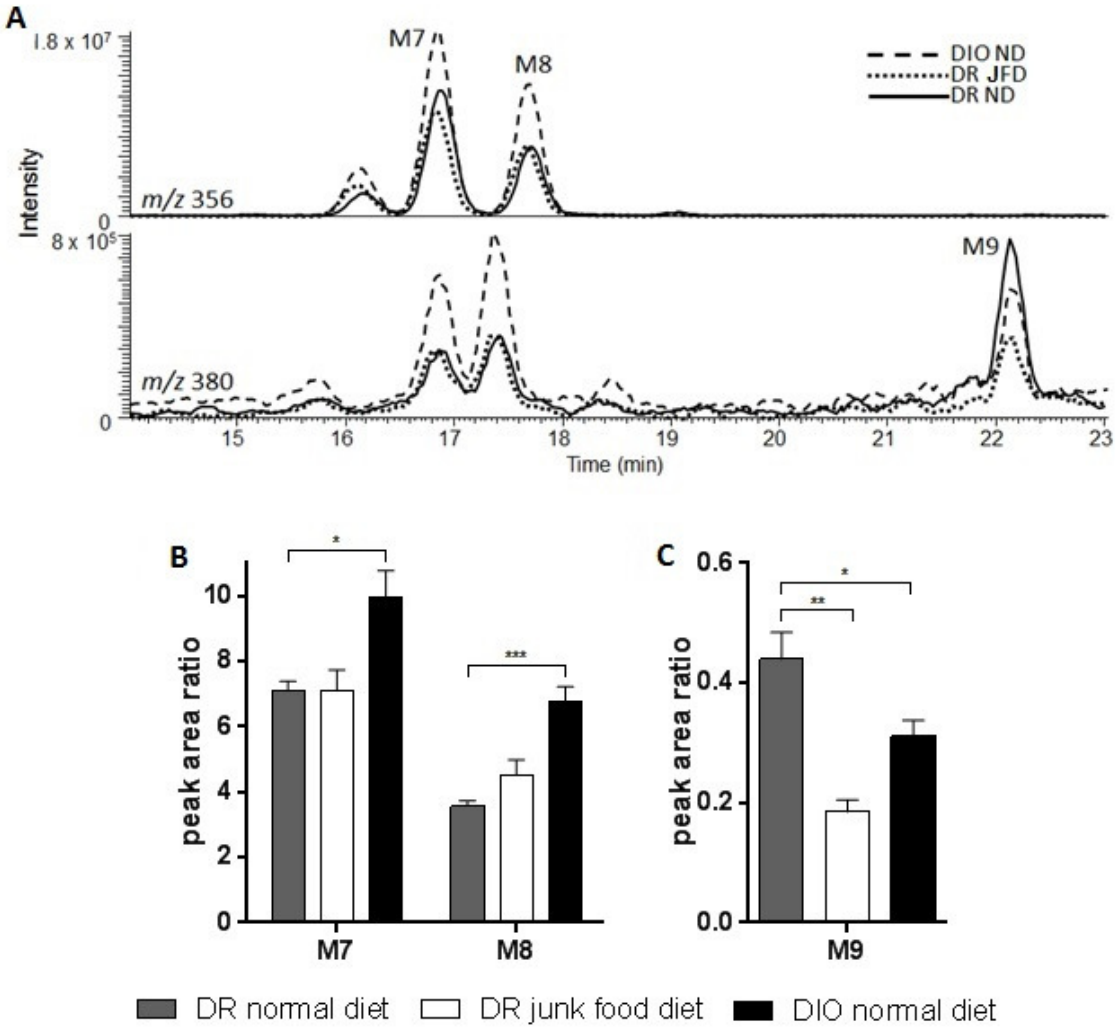

Figure 2.9. Effect of obesity and diet on P450-catalyzed metabolism of AEA by RLM. Liver microsomes were prepared from Levin rats selectively bred to be susceptible or resistant to diet induced obesity on junk food (JFD) and/or normal diet (ND). Rat liver microsomal protein (200 µg) was incubated with AEA (100 µM) for 30 min at 37°C and product formation was determined as previously described. (A) The extracted ion chromatogram of M7 (*m/z* 356), M8 (*m/z* 356), and M9 (*m/z* 380), representative of the microsomes made from DR rat on a normal diet (solid line), DR rat on a junk food diet (dotted line), or DIO rat on a normal diet (dashed line). The corresponding bar graph shows the relative amounts of the monitored P450 products as measured by the peak area ratio at *m/z* 356 (B) and *m/z* 380 (C). The amount of product formed is the mean ± SEM from two separate experiments performed in duplicate. Statistical significance was determined using the Holm-Sidak method in the GraphPad Prism 6 Program, *, $P < 0.05$; **, $P < 0.01$; ***, $P < 0.001$.

the extracted ion chromatograms for each of the samples monitoring the three aforementioned P450-mediated products at *m/z* 356 and 380. Figure 2.9B shows bar graphs quantifying the information. For products M7 and M8, there was a significant increase in product formation by liver microsomes from the DIO rats on a ND when compared to the DR rat on either the ND or JFD. On the other hand, there was a significant decrease in the formation of M9 by the livers of DR rats fed a JFD and DIO rats fed a ND when compared to DR rats fed a ND.

Discussion

Normally, AEA is hydrolyzed by FAAH to give arachidonic acid and ethanolamine; however, AEA can also be oxidized by COX-2, LOX, and CYP450 enzymes. COX-2 catalyzes the oxidation of AEA to prostaglandin ethanolamides or prostamides (Kozak et al., 2002; Ritter et al., 2012; Yang et al., 2005; Yu et al., 1997). Prostamide $F_{2\alpha}$ and its analog bimatoprost act at the prostamide receptor to increase hair growth, reduce fat disposition, and mediate nociception (Woodward et al., 2013). Lipoxygenase converts AEA into several hydroxyanandamides (Hampson et al., 1995). 12-Hydroxyanandamide, a brain metabolite, has an affinity for the for the CB_1 receptor in the nanomolar range and can inhibit forskolin-stimulated cAMP production suggesting a possible physiological role as well (Hampson et al., 1995). Likewise, cytochrome P450s can epoxygenate AEA to give the 5,6-, 8,9-, 11,12-, and 14,15-EET-EAs and hydroxylate it to give 20- and 19-HETE-EA (Snider et al., 2007; Snider et al., 2008; Sridar et al., 2011; Stark et al., 2008).

To date, the CYP450s known to metabolize AEA are found primarily in the liver, kidney, and brain (Snider et al., 2007; Snider et al., 2008; Sridar et al., 2011). CYP2J2 is the most abundantly expressed CYP450 in the cardiovascular system (Wu et al., 1996), but it is also known to participate in the intestinal metabolism of a couple of non-sedating antihistamines (Hashizume et al., 2002; Matsumoto et al., 2002). CYP2J2 metabolizes AA, which is structurally similar to AEA, to give four EETs which have a plethora of biological actions in the body. Because CYP2J2 plays an important role in the metabolism of AA, it is possible that CYP2J2 might play an important role in the metabolism of AEA as well. This study was performed to investigate CYP2J2 metabolism of AEA and its involvement in the intestinal metabolism of AEA. Moreover, we also investigated the effects of obesity and a junk food diet on AEA metabolism in the rat liver.

We are the first to report that human recombinant CYP2J2 metabolizes AEA to give five mono-oxygenated products: the 5,6-, 8,9-, 11,12-, 14,15-EET-EAs and 20-HETE-EA. This metabolite profile is similar to that reported by other labs for the metabolism of AA by recombinant CYP2J2 that yielded the four epoxides, 14,15-, 11,12-, 8,9-, and 5,6-EETs, in addition to the several HETEs (King et al., 2002; Wu et al., 1996). Although CYP2J2 is thought to function primarily as an epoxygenase, it does hydroxylate some substrates including AA, terfenadine, and ebastine (Hashizume et al., 2002; King et al., 2002; Lafite et al., 2006; Wu et al., 1996). Our studies determined the kinetic constants, K_M and k_{cat}, for each of the five metabolites formed. A caveat for the kinetic parameters reported for the EET-EAs is that the formation of these products never

reached saturation even up to 1 mM of AEA (data not shown). As a result, the calculated kinetic constants are extrapolated and can only serve as estimated values.

Although the EET-EAs had different values for their kinetic parameters, similar deviations in these kinetic values have been seen for the metabolism of AEA by other CYP450s and for the different regioisomers formed during CYP450-mediated metabolism of AA (Daikh et al., 1994; Kiss et al., 2000; Pratt-Hyatt et al., 2010; Snider et al., 2008; Sridar et al., 2011). Although the metabolism of AEA by CYP2J2 is not as efficient, estimated by calculating k_{cat}/K_M, as that observed for some of the other P450s such as CYP2D6 or CYP2B6, these kinetic parameters are comparable to those reported for CYP3A4 (Pratt-Hyatt et al., 2010; Snider et al., 2008; Sridar et al., 2011). In the presence of 50 µM AEA, the total catalytic turnover rate for recombinant CYP2J2 was calculated to be about 7 nmol of total product formed/nmol of CYP2J2/min. For comparison, in the presence of 100 µM AA, two separate labs have determined the turnover to be 0.065 and 0.165 nmol of total product formed/nmol of CYP2J2/min (King et al., 2002; Wu et al., 1996). Although plasma levels of AA are significantly higher than AEA (3-4 mM vs. 300-400 nM), the actual concentrations of AEA in subcellular compartments, such as the plasma membrane, are most likely significantly higher (Brash, 2001; Fernandez-Rodriquez et al., 2004; Shinde et al., 2012). This suggests that AEA may be a substrate for CYP2J2 *in vivo*.

Several di-oxygenated products were observed at *m/z* 380 in the extracted ion chromatograms of the metabolites formed by recombinant CYP2J2 (Figure 2.3). These were minor products compared to the EET-EAs. Because di-oxygenated AEA metabolite standards are not commercially available, we were unable to conclusively identify the

products formed. CYP2D6 is known to di-oxygenate AEA to form several hydroxyepoxyeicosatrienoic acid ethanolamides (HEET-EAs) (Snider et al., 2008). It is possible that these CYP2J2-catalyzed products observed at *m/z* 380 are structurally similar.

The ECS activity in the intestine plays a crucial role in energy balance; therefore, it is important to know the identities and relative amounts of the AEA metabolites formed in the intestine. The metabolite profile for HIM is similar to that of HLM with the formation of 20- and 19-HETE-EAs and 11,12-, 8,9-, and 5,6-EET-EAs (Snider et al., 2007). However, the formation of the 14,15-EET-EA was only observed using concentrations of AEA above 100 µM or in the presence of a soluble epoxide hydrolase inhibitor. The efficiencies or V_{max}/K_m values for the formation of 20-HETE-EA, 5,6-, 8,9-, and 11,12-EET-EAs were 4, 0.01, 0.009, and 0.02 µL/min/mg of protein. Because the presence of AUDA increased the formation of the EET-EAs, this suggests the presence of epoxide hydrolase (EH) in HIM preparations. Although it is expected that microsomes may contain microsomal EH, AUDA is a soluble EH inhibitor and should not inhibit microsomal EH activity (Morisseau and Hammock, 2013). It is likely that the inhibition of EET-EAs formation in the presence of AUDA is a substrate competition effect and not inhibition of microsomal EH activity; however, it is not impossible for some soluble EH activity to be present. Because the EET-EAs are constantly being hydrolyzed by EHs, the kinetic constants calculated for HIM may not be entirely reliable. The 20-HETE-EA metabolite is the major product of P450-catalyzed AEA metabolism in HLM and HIM (Snider et al., 2007). In relation to the epoxides, the 8,9-EET-EA was the preferred product formed by HLM, but the 5,6-EET-EA seems to be the preferred

product formed by HIM although the efficiency for its formation is the same as 11,12-EET-EA. Although CYP2J2 is present in the intestine, it does not appear to be a significant contributor to AEA metabolism in the intestine in comparison with other P450s. On the other hand, CYP3A4 and CYP2C9 are responsible for about 50% of the 20-HETE-EA and 11,12-EET-EA produced in the intestine, respectively. Other P450s such as CYP2C19 and CYP2D6, both of which are known to be expressed at appreciable levels in the intestine, probably contribute significantly to AEA metabolism in the intestine as well (Paine et al., 2006; Snider et al., 2008). A caveat to this study is that no test was completed to determine the presence of the P450s; however, the product description provided by BD Biosciences reported activity for CYP3A4, CYP2C9, and CYP2J2.

Plasma AEA levels are positively associated with body mass index. As a result, obese individuals exhibit higher concentrations of AEA when compared to lean controls (Engeli et al., 2005; Quercioli et al., 2011). An important aspect of obesity is the chronic low level inflammation (Kim et al., 2013).The affinity of AEA for the CB1R is four times that of its affinity for the CB2 receptor (Felder et al., 1995). CB1 receptor activation is believed to be pro-inflammatory, while CB2 receptor activation is thought to be anti-inflammatory (Han et al., 2009; Rajesh et al., 2008). Thus, the AEA tone may contribute to the chronic inflammation associated with obesity. The CB2R is also important in intestinal motility, especially during inflammation. Immune cells in the mucosal regions of the gastrointestinal tract express CB2 receptors which downregulate leukocyte infiltration and inflammation via inhibition of adhesion and migration, apoptosis of activated immune cells, and cytokine and chemokine production (Cabral and Staab, 2005;

Klein, 2005; Lunn et al., 2006). The migration of dendritic cells to various inflammatory sites is necessary to initiate immune responses and activation of the CB2 receptor can inhibit this process. Activation of the CB2 receptor causes a decrease in cAMP levels, and as a result, ERK activation decreases causing a decrease in the expression of matrix metalloproteinase (MMP-9) which facilitates the migration of inflammatory cells (Adhikary et al., 2012). As a result, CB2 receptor activation may be an endogenous mechanism to combat inflammation (Wright et al., 2008).

Previous studies from our lab have suggested a physiological importance for the 5,6-EET-EA metabolite of AEA since it has a nanomolar affinity for the CB2 receptor and it can decrease intracellular cAMP accumulation in Chinese hamster ovary cells expressing the CB2 receptor (Snider et al., 2009). Moreover, this metabolite is more biologically stable than the parent AEA with an estimated half-life of 32 min (Snider et al., 2009). This half-life is four times longer than the half-life reported for the structurally similar 5,6-EET metabolite formed by the metabolism of AA (Fulton et al., 1998). Since the 5,6-EET-EA is the major AEA metabolite formed in the intestine, it may play an important anti-inflammatory role in the intestine.

Microsomes prepared from the livers of rats selectively bred to be susceptible or resistant to diet-induced obesity were used to determine if obesity and/or diet had any effect on AEA metabolism in the liver. The RLM did not form the expected metabolites of AEA, the EET-EAs and the HETE-EAs. This may be because rat and human P450s are not identical and the liver P450 isomer content may differ as well. One group investigated AEA metabolism by mouse brain and liver microsomes (Broheim et al., 1995). The liver formed at least 20 different metabolites, but none of those metabolites

were positively identified. Conversely, the mouse brain formed only two metabolites with a positive ion mass of 365. So, it is not unlikely that RLM would form different metabolites than HLM. Because RLM did not form the epoxides and hydroxides of AEA formed by human P450s, three other P450-mediated metabolites were identified and observed for changes in their formation with regard to weight and diet.

Using the P450 reductase inhibitor DIC, three alternative P450-catalyzed metabolites were identified having *m/z* values at 356 and 380. All P450s require reductase as an electron donor in order for metabolism to occur. Although DIC did not eliminate all product formation, this can be explained by the use of only one concentration of DIC. It is possible that if higher concentrations were used, there would be a complete inhibition of product formation. Even though the identities of M7(*m/z* 356), M8 (*m/z* 356), and M9 (*m/*z 380) were not determined, previous studies suggest that AEA metabolites that ionize at *m/z* 380 are secondary EET-EA products that are dioxygenated (Snider et al., 2008). For the M7 and M8 products, obesity seems to be the more important determinant when investigating AEA metabolism than diet. Conversely, for the M9 metabolite, the junk food diet seems to have more effect on its formation than obesity.

Increased anandamide levels in overweight people exhibit a correspondence with decreased FAAH activity which increases the likelihood of anandamide being metabolized via alternative pathways such as by cyclooxygenases, lipoxygenases, and P450s (Engeli et al., 2005; Ligresti et al., 2013). However, the expression levels of these enzymes are sometimes altered due to inflammation and obesity. Evidence suggests that COX and LOX mRNA levels and activities are increased during obesity (Ahren et al.,

2000; Xu et al., 2005). Since COX metabolizes AA to proinflammatory prostaglandins and thromboxanes (PGE_2 and TXA_2)) which induce the production of inflammatory cytokines, such as IL-1β, IL-6, and TNF-α from macrophages, the increase in COX activity may promote the inflammatory state observed in obesity (Tilley et al., 2001). Likewise, research suggests that LOX activity may be pro-inflammatory as well (Li et al., 2013; Neels, 2013).

Conversely, several P450s exhibit decreased expression in animal models of obesity and inflammation (Morgan, 1997; Renton, 2001; Wamberg et al., 2013; Zhao et al., 2006). Studies utilizing animal models of obesity suggest a decrease in P450 epoxygenase activity with a concomitant increase in epoxide hydrolase activity, but no effect on P450 ω-hydrolase activity (Laffer et al., 2004; Theken et al., 2012a; Zhao et al., 2005). Moreover, obese individuals have been reported to have a decrease in CYP2J2 expression in subcutaneous adipose tissue and significantly lower plasma EET levels when compared to control subjects (Theken et al., 2012b; Wamberg et al., 2013). Because P450s produce pro-inflammatory ω-hydroxylated fatty acids and anti-inflammatory epoxygenated fatty acids, the decrease in the anti-inflammatory mediators may contribute to the inflammation observed in obesity. The impact of a junk food diet rich in ω-6 fatty acids on epoxide formation is evident by the altered formation of M9. Since RLM did not form the EET-EAs or the HETE-EAs, they are probably not the best model to study obesity. However, the important point is that in obesity AEA is increased, but P450 activity is likely decreased. This would likely cause a decrease in the anti-inflammatory epoxygenated fatty acids, such as the EET-EAs, and subsequently increase inflammation.

References

Adhikary, S., Kocieda, V.P., Yen, J.H., Tuma, R.F., and Ganea, D. (2012). Signaling through cannabinoid receptor 2 suppresses murine dendritic cell migration by inhibiting matrix metalloproteinase 9 expression. Blood *120*, 3741-3749.

Ahima, R.S. (2008). Revisiting leptin's role in obesity and weight loss. J Clin Invest *118*, 2380-2383.

Ahren, B., Magrum, L.J., Havel, P.J., Greene, S.F., Phinney, S.D., Johnson, P.R., and Stern, J.S. (2000). Augmented insulinotropic action of arachidonic acid through the lipoxygenase pathway in the obese Zucker rat. Obes Res *8*, 475-480.

Alberich Jorda, M., Rayman, N., Tas, M., Verbakel, S.E., Battista, N., van Lom, K., Lowenberg, B., Maccarrone, M., and Delwel, R. (2004). The peripheral cannabinoid receptor Cb2, frequently expressed on AML blasts, either induces a neutrophilic differentiation block or confers abnormal migration properties in a ligand-dependent manner. Blood *104*, 526-534.

Alpini, G., and Demorrow, S. (2009). Changes in the endocannabinoid system may give insight into new and effective treatments for cancer. Vitam Horm *81*, 469-485.

Alvheim, A.R., Malde, M.K., Osei-Hyiaman, D., Lin, Y.H., Pawlosky, R.J., Madsen, L., Kristiansen, K., Froyland, L., and Hibbeln, J.R. (2012). Dietary linoleic acid elevates endogenous 2-AG and anandamide and induces obesity. Obesity (Silver Spring) *20*, 1984-1994.

Alvheim, A.R., Torstensen, B.E., Lin, Y.H., Lillefosse, H.H., Lock, E.J., Madsen, L., Hibbeln, J.R., and Malde, M.K. (2013). Dietary linoleic acid elevates endogenous 2-arachidonoylglycerol and anandamide in Atlantic salmon (Salmo salar L.) and mice, and induces weight gain and inflammation in mice. Br J Nutr *109*, 1508-1517.

Annuzzi, G., Piscitelli, F., Di Marino, L., Patti, L., Giacco, R., Costabile, G., Bozzetto, L., Riccardi, G., Verde, R., Petrosino, S., Rivellese, A.A., and Di Marzo, V. (2010). Differential alterations of the concentrations of endocannabinoids and related lipids in the subcutaneous adipose tissue of obese diabetic patients. Lipids Health Dis *9*, 43.

Ashton, J.C., and Smith, P.F. (2007). Cannabinoids and cardiovascular disease: the outlook for clinical treatments. Curr Vasc Pharmacol *5*, 175-185.

Bifulco, M., Laezza, C., Gazzerro, P., and Pentimalli, F. (2007). Endocannabinoids as emerging suppressors of angiogenesis and tumor invasion (review). Oncol Rep *17*, 813-816.

Bornheim, L.M., Kim, K.Y., Chen, B., and Correia, M.A. (1995) Microsomal cytochrome P450-mediated liver and brain anandamide metabolism. Biochem Pharmacol *50*, 677-686.

Brash, A.R. (2001). Arachidonic acid as a bioactive molecule. J Clin Invest *107*, 1339-1345.

Cabral, G.A., and Staab, A. (2005). Effects on the immune system. Handb Exp Pharmacol, 385-423.

Cota, D., Marsicano, G., Lutz, B., Vicennati, V., Stalla, G.K., Pasquali, R., and Pagotto, U. (2003a). Endogenous cannabinoid system as a modulator of food intake. Int J Obes Relat Metab Disord *27*, 289-301.

Cota, D., Marsicano, G., Tschop, M., Grubler, Y., Flachskamm, C., Schubert, M., Auer, D., Yassouridis, A., Thone-Reineke, C., Ortmann, S., Tomassoni, F., Cervino, C., Nisoli, E.,
Linthorst, A.C., Pasquali, R., Lutz, B., Stalla, G.K., and Pagotto, U. (2003b). The endogenous cannabinoid system affects energy balance via central orexigenic drive and peripheral lipogenesis. J Clin Invest *112*, 423-431.

Cote, M., Matias, I., Lemieux, I., Petrosino, S., Almeras, N., Despres, J.P., and Di Marzo, V. (2007). Circulating endocannabinoid levels, abdominal adiposity and related cardiometabolic risk factors in obese men. Int J Obes (Lond) *31*, 692-699.

Daikh, B.E., Lasker, J.M., Raucy, J.L., and Koop, D.R. (1994). Regio- and stereoselective epoxidation of arachidonic acid by human cytochromes P450 2C8 and 2C9. J Pharmacol Exp Ther *271*, 1427-1433.

Di Carlo, G., and Izzo, A.A. (2003). Cannabinoids for gastrointestinal diseases: potential therapeutic applications. Expert Opin Investig Drugs *12*, 39-49.

Di Marzo, V. (2008). Targeting the endocannabinoid system: to enhance or reduce? Nat Rev Drug Discov *7*, 438-455.

Di Marzo, V., Bifulco, M., and De Petrocellis, L. (2004). The endocannabinoid system and its therapeutic exploitation. Nat Rev Drug Discov *3*, 771-784.

Di Marzo, V., Goparaju, S.K., Wang, L., Liu, J., Batkai, S., Jarai, Z., Fezza, F., Miura, G.I., Palmiter, R.D., Sugiura, T., and Kunos, G. (2001). Leptin-regulated endocannabinoids are involved in maintaining food intake. Nature *410*, 822-825.

Dutheil, F., Dauchy, S., Diry, M., Sazdovitch, V., Cloarec, O., Mellottee, L., Bieche, I., Ingelman-Sundberg, M., Flinois, J.P., de Waziers, I., Beaune, P., Declèves, X., Duyckaerts,
C., and Loriot, M,A. (2009). Xenobiotic-metabolizing enzymes and transporters in the normal human brain: regional and cellular mapping as a basis for putative roles in cerebral function. Drug Metab Dispos *37*, 1528-1538.

Eckardt, K., Sell, H., Taube, A., Koenen, M., Platzbecker, B., Cramer, A., Horrighs, A., Lehtonen, M., Tennagels, N., and Eckel, J. (2009). Cannabinoid type 1 receptors in

human skeletal muscle cells participate in the negative crosstalk between fat and muscle. Diabetologia *52*, 664-674.

Enayetallah, A.E., French, R.A., Thibodeau, M.S., and Grant, D.F. (2004). Distribution of soluble epoxide hydrolase and of cytochrome P450 2C8, 2C9, and 2J2 in human tissues. J Histochem Cytochem *52*, 447-454.

Engeli, S., Bohnke, J., Feldpausch, M., Gorzelniak, K., Janke, J., Batkai, S., Pacher, P., Harvey-White, J., Luft, F.C., Sharma, A.M., and Jordan, J. (2005). Activation of the peripheral endocannabinoid system in human obesity. Diabetes *54*, 2838-2843.

Felder, C.C., Joyce, K.E., Briley, E.M., Mansouri, J., Mackie, K., Blond, O., Lai, Y., Ma, A.L., and Mitchell, R.L. (1995). Comparison of the pharmacology and signal transduction of the human cannabinoid CB1 and CB2 receptors. Mol Pharmacol *48*, 443-450.

Fernandez-Rodriguez, C.M., Romero, J., Petros, T.J., Bradshaw, H., Gasalla, J.M., Gutierrez, M.L., Lledo, J.L., Santander, C., Fernandez, T.P., Tomas, E., Cacho, G., and Walker, J.M. (2004). Circulating endogenous cannabinoid anandamide and portal, systemic and renal hemodynamics in cirrhosis. Liver Int *24*, 477-483.

Fulton, D., Falck, J.R., McGiff, J.C., Carroll, M.A., and Quilley, J. (1998). A method for the determination of 5,6-EET using the lactone as an intermediate in the formation of the diol. J Lipid Res *39*, 1713-1721.

Hampson, A.J., Hill, W.A., Zan-Phillips, M., Makriyannis, A., Leung, E., Eglen, R.M., and Bornheim, L.M. (1995). Anandamide hydroxylation by brain lipoxygenase:metabolite structures and potencies at the cannabinoid receptor. Biochim Biophys Acta *1259*, 173-179.

Han, K.H., Lim, S., Ryu, J., Lee, C.W., Kim, Y., Kang, J.H., Kang, S.S., Ahn, Y.K., Park, C.S., and Kim, J.J. (2009). CB1 and CB2 cannabinoid receptors differentially regulate the production of reactive oxygen species by macrophages. Cardiovasc Res *84*, 378-386.

Hanna, I.H., Teiber, J.F., Kokones, K.L., and Hollenberg, P.F. (1998). Role of the alanine at position 363 of cytochrome P450 2B2 in influencing the NADPH- and hydroperoxide-supported activities. Arch Biochem Biophys *350*, 324-332.

Hansen, H.S., Moesgaard, B., Hansen, H.H., and Petersen, G. (2000). N-Acylethanolamines and precursor phospholipids - relation to cell injury. Chem Phys Lipids *108*, 135-150.

Hashizume, T., Imaoka, S., Mise, M., Terauchi, Y., Fujii, T., Miyazaki, H., Kamataki, T., and Funae, Y. (2002). Involvement of CYP2J2 and CYP4F12 in the metabolism of ebastine in human intestinal microsomes. J Pharmacol Exp Ther *300*, 298-304.

Jin, X.H., Uyama, T., Wang, J., Okamoto, Y., Tonai, T., and Ueda, N. (2009). cDNA cloning and characterization of human and mouse Ca(2+)-independent phosphatidylethanolamine N-acyltransferases. Biochim Biophys Acta *1791*, 32-38.

Kim, J., Li, Y., and Watkins, B.A. (2013). Fat to treat fat: emerging relationship between dietary PUFA, endocannabinoids, and obesity. Prostaglandins Other Lipid Mediat *104-105*, 32-41.

King, L.M., Ma, J., Srettabunjong, S., Graves, J., Bradbury, J.A., Li, L., Spiecker, M., Liao, J.K., Mohrenweiser, H., and Zeldin, D.C. (2002). Cloning of CYP2J2 gene and identification of functional polymorphisms. Mol Pharmacol *61*, 840-852.

Kiss, L., Schutte, H., Mayer, K., Grimm, H., Padberg, W., Seeger, W., and Grimminger, F. (2000). Synthesis of arachidonic acid-derived lipoxygenase and cytochrome P450 products in the intact human lung vasculature. Am J Respir Crit Care Med *161*, 1917-1923.

Klein, T.W. (2005). Cannabinoid-based drugs as anti-inflammatory therapeutics. Nat Rev Immunol *5*, 400-411.

Kozak, K.R., Crews, B.C., Morrow, J.D., Wang, L.H., Ma, Y.H., Weinander, R., Jakobsson, P.J., and Marnett, L.J. (2002). Metabolism of the endocannabinoids, 2-arachidonylglycerol and anandamide, into prostaglandin, thromboxane, and prostacyclin glycerol esters and ethanolamides. J Biol Chem *277*, 44877-44885.

Kulkarni-Narla, A., and Brown, D.R. (2000). Localization of CB1-cannabinoid receptor immunoreactivity in the porcine enteric nervous system. Cell Tissue Res *302*, 73-80.

Kulkarni-Narla, A., and Brown, D.R. (2001). Opioid, cannabinoid and vanilloid receptor localization on porcine cultured myenteric neurons. Neurosci Lett *308*, 153-156.

Laffer, C.L., Laniado-Schwartzman, M., Nasjletti, A., and Elijovich, F. (2004). 20-HETE and circulating insulin in essential hypertension with obesity. Hypertension *43*, 388-392.

Lafite, P., Dijols, S., Buisson, D., Macherey, A.C., Zeldin, D.C., Dansette, P.M., and Mansuy, D. (2006). Design and synthesis of selective, high-affinity inhibitors of human cytochrome P450 2J2. Bioorg Med Chem Lett *16*, 2777-2780.

Lambert, D.M. (2007). Allergic contact dermatitis and the endocannabinoid system: from mechanisms to skin care. ChemMedChem *2*, 1701-1702.

Lee, C.A., Jones, J.P., 3rd, Katayama, J., Kaspera, R., Jiang, Y., Freiwald, S., Smith, E., Walker, G.S., and Totah, R.A. (2012). Identifying a selective substrate and inhibitor pair for the evaluation of CYP2J2 activity. Drug Metab Dispos *40*, 943-951.

Levin, B.E., Dunn-Meynell, A.A., Balkan, B., and Keesey, R.E. (1997) Selective breeding for diet-induced obesity and resistance in Sprague-Dawley rats. Am J Physiol *273*, R725-R730.

Li, J., Rao, J., Liu, Y., Cao, Y., Zhang, Y., Zhang, Q., and Zhu, D. (2013). 15-Lipoxygenase promotes chronic hypoxia-induced pulmonary artery inflammation via positive interaction with nuclear factor-kappaB. Arterioscler Thromb Vasc Biol *33*, 971-979.

Ligresti, A., Martos, J., Wang, J., Guida, F., Allara, M., Palmieri, V., Luongo, L., Woodward, D., and Di Marzo, V. (2013). Prostamide F receptor antagonists with inhibitory activity at FAAH: a way to prevent the confounding effects of pro-inflammatory mediators formed following selective FAAH inhibition? Br J Pharmacol.

Lin, H.L., Roberts, E.S., and Hollenberg, P.F. (1998). Heterologous expression of rat P450 2E1 in a mammalian cell line: in situ metabolism and cytotoxicity of N-nitrosodimethylamine. Carcinogenesis *19*, 321-329.

Lunn, C.A., Reich, E.P., and Bober, L. (2006). Targeting the CB2 receptor for immune modulation. Expert Opin Ther Targets *10*, 653-663.

Ma, J., Qu, W., Scarborough, P.E., Tomer, K.B., Moomaw, C.R., Maronpot, R., Davis, L.S., Breyer, M.D., and Zeldin, D.C. (1999). Molecular cloning, enzymatic characterization, developmental expression, and cellular localization of a mouse cytochrome P450 highly expressed in kidney. J Biol Chem *274*, 17777-17788.

Mascolo, N., Izzo, A.A., Ligresti, A., Costagliola, A., Pinto, L., Cascio, M.G., Maffia, P., Cecio, A., Capasso, F., and Di Marzo, V. (2002). The endocannabinoid system and the molecular basis of paralytic ileus in mice. FASEB J *16*, 1973-1975.

Matias, I., Bisogno, T., and Di Marzo, V. (2006a). Endogenous cannabinoids in the brain and peripheral tissues: regulation of their levels and control of food intake. Int J Obes (Lond) *30 Suppl 1*, S7-S12.

Matias, I., Gonthier, M.P., Orlando, P., Martiadis, V., De Petrocellis, L., Cervino, C., Petrosino, S., Hoareau, L., Festy, F., Pasquali, R., Roche, R., Maj, M., Pagotto, U., Monteleone, P., and Di Marzo, V. (2006b). Regulation, function, and dysregulation of endocannabinoids in models of adipose and beta-pancreatic cells and in obesity and hyperglycemia. J Clin Endocrinol Metab *91*, 3171-3180.

Matias, I., Petrosino, S., Racioppi, A., Capasso, R., Izzo, A.A., and Di Marzo, V. (2008). Dysregulation of peripheral endocannabinoid levels in hyperglycemia and obesity: Effect of high fat diets. Mol Cell Endocrinol *286*, S66-78.

Matsumoto, S., Hirama, T., Matsubara, T., Nagata, K., and Yamazoe, Y. (2002). Involvement of CYP2J2 on the intestinal first-pass metabolism of antihistamine drug, astemizole. Drug Metab Dispos *30*, 1240-1245.

Morgan, E.T. (1997). Regulation of cytochromes P450 during inflammation and infection. Drug Metab Rev *29*, 1129-1188.

Morisseau, C., and Hammock, B.D. (2013). Impact of soluble epoxide hydrolase and epoxyeicosanoids on human health. Annu Rev Pharmacol Toxicol *53*, 37-58.

Nagai, N., Sakane, N., and Moritani, T. (2005). Metabolic responses to high-fat or low-fat meals and association with sympathetic nervous system activity in healthy young men. J Nutr Sci Vitaminol (Tokyo) *51*, 355-360.

Naughton, S.S., Mathai, M.L., Hryciw, D.H., and McAinch, A.J. (2013). Fatty Acid modulation of the endocannabinoid system and the effect on food intake and metabolism. Int J Endocrinol *2013*, 361895.

Neels, J.G. (2013). A role for 5-lipoxygenase products in obesity-associated inflammation and insulin resistance. Adipocyte *2*, 262-265.

Nesto, R.E. and Mackie, K. (2008) Endocannabinoid system and its implications for obesity and cardiovascular risk. Eur Heart J *10*, B34-B41.

Nishimura, M., Yaguti, H., Yoshitsugu, H., Naito, S., and Satoh, T. (2003). Tissue distribution of mRNA expression of human cytochrome P450 isoforms assessed by high-sensitivity real-time reverse transcription PCR. Yakugaku Zasshi *123*, 369-375.

Okamoto, Y., Tsuboi, K., and Ueda, N. (2009). Enzymatic formation of anandamide. Vitam Horm *81*, 1-24.

Omura, T., and Sato, R. (1964). The Carbon Monoxide-Binding Pigment of Liver Microsomes. I. Evidence for Its Hemoprotein Nature. J Biol Chem *239*, 2370-2378.

Paine, M.F., Hart, H.L., Ludington, S.S., Haining, R.L., Rettie, A.E., and Zeldin, D.C. (2006). The human intestinal cytochrome P450 "pie". Drug Metab Dispos *34*, 880-886.

Pertwee, R.G. (1999). Evidence for the presence of CB1 cannabinoid receptors on peripheral neurones and for the existence of neuronal non-CB1 cannabinoid receptors. Life Sci *65*, 597-605.

Pinto, L., Izzo, A.A., Cascio, M.G., Bisogno, T., Hospodar-Scott, K., Brown, D.R., Mascolo, N., Di Marzo, V., and Capasso, F. (2002). Endocannabinoids as physiological regulators of colonic propulsion in mice. Gastroenterology *123*, 227-234.

Pratt-Hyatt, M., Zhang, H., Snider, N.T., and Hollenberg, P.F. (2010). Effects of a commonly occurring genetic polymorphism of human CYP3A4 (I118V) on the metabolism of anandamide. Drug Metab Dispos *38*, 2075-2082.

Quercioli, A., Pataky, Z., Vincenti, G., Makoundou, V., Di Marzo, V., Montecucco, F., Carballo, S., Thomas, A., Staub, C., Steffens, S., Seimbille, Y., Golay, A., Ratib, O., Harsch, E., Mach, F., and Schindler, T.H. (2011). Elevated endocannabinoid plasma levels are associated with coronary circulatory dysfunction in obesity. Eur Heart J *32*, 1369-1378.

Rajesh, M., Mukhopadhyay, P., Hasko, G., Huffman, J.W., Mackie, K., and Pacher, P. (2008). CB2 cannabinoid receptor agonists attenuate TNF-alpha-induced human vascular smooth muscle cell proliferation and migration. Br J Pharmacol *153*, 347-357.

Renton, K.W. (2001). Alteration of drug biotransformation and elimination during infection and inflammation. Pharmacol Ther *92*, 147-163.

Ritter, J.K., Li, C., Xia, M., Poklis, J.L., Lichtman, A.H., Abdullah, R.A., Dewey, W.L., and Li, P.L. (2012). Production and actions of the anandamide metabolite prostamide E2 in the renal medulla. J Pharmacol Exp Ther *342*, 770-779.

Schlicker, E., and Kathmann, M. (2001). Modulation of transmitter release via presynaptic cannabinoid receptors. Trends Pharmacol Sci *22*, 565-572.

Schmid, H.H., Schmid, P.C., and Natarajan, V. (1990). N-acylated glycerophospholipids and their derivatives. Prog Lipid Res *29*, 1-43.

Shinde, D.D., Kim, K.B., Oh, K.S., Abdalla, N., Liu, K.H., Bae, S.K., Shon, J.H., Kim, H.S., Kim, D.H., and Shin, J.G. (2012). LC-MS/MS for the simultaneous analysis of arachidonic acid and 32 related metabolites in human plasma: Basal plasma concentrations and aspirin-induced changes of eicosanoids. J Chromatogr B Analyt Technol Biomed Life Sci *911*, 113-121.

Smith, H.E., Jones, J.P., 3rd, Kalhorn, T.F., Farin, F.M., Stapleton, P.L., Davis, C.L., Perkins, J.D., Blough, D.K., Hebert, M.F., Thummel, K.E., and Totah, R.A. (2008). Role of cytochrome P450 2C8 and 2J2 genotypes in calcineurin inhibitor-induced chronic kidney disease. Pharmacogenet Genomics *18*, 943-953.

Snider, N.T., Kornilov, A.M., Kent, U.M., and Hollenberg, P.F. (2007). Anandamide metabolism by human liver and kidney microsomal cytochrome p450 enzymes to form hydroxyeicosatetraenoic and epoxyeicosatrienoic acid ethanolamides. J Pharmacol Exp Ther *321*, 590-597.

Snider, N.T., Nast, J.A., Tesmer, L.A., and Hollenberg, P.F. (2009). A cytochrome P450-derived epoxygenated metabolite of anandamide is a potent cannabinoid receptor 2-selective agonist. Mol Pharmacol *75*, 965-972.

Snider, N.T., Sikora, M.J., Sridar, C., Feuerstein, T.J., Rae, J.M., and Hollenberg, P.F. (2008). The endocannabinoid anandamide is a substrate for the human polymorphic cytochrome P450 2D6. J Pharmacol Exp Ther *327*, 538-545.

Snider, N.T., Walker, V.J., and Hollenberg, P.F. (2010). Oxidation of the endogenous cannabinoid arachidonoyl ethanolamide by the cytochrome P450 monooxygenases: physiological and pharmacological implications. Pharmacol Rev *62*, 136-154.

Sridar, C., Snider, N.T., and Hollenberg, P.F. (2011). Anandamide oxidation by wild-type and polymorphically expressed CYP2B6 and CYP2D6. Drug Metab Dispos *39*, 782-788.

Stark, K., Dostalek, M., and Guengerich, F.P. (2008). Expression and purification of orphan cytochrome P450 4X1 and oxidation of anandamide. FEBS J *275*, 3706-3717.

Storr, M.A., and Sharkey, K.A. (2007). The endocannabinoid system and gut-brain signalling. Curr Opin Pharmacol *7*, 575-582.

Theken, K.N., Deng, Y., Schuck, R.N., Oni-Orisan, A., Miller, T.M., Kannon, M.A., Poloyac, S.M., and Lee, C.R. (2012a). Enalapril reverses high-fat diet-induced alterations in cytochrome P450-mediated eicosanoid metabolism. Am J Physiol Endocrinol Metab *302*, E500-509.

Theken, K.N., Schuck, R.N., Edin, M.L., Tran, B., Ellis, K., Bass, A., Lih, F.B., Tomer, K.B., Poloyac, S.M., Wu, M.C., Hinderliter, A.L., Zeldin, D.C., Stouffer, G.A., and Lee, C.R. (2012b). Evaluation of cytochrome P450-derived eicosanoids in humans with stable atherosclerotic cardiovascular disease. Atherosclerosis *222*, 530-536.

Tilley, S.L., Coffman, T.M., and Koller, B.H. (2001). Mixed messages: modulation of inflammation and immune responses by prostaglandins and thromboxanes. J Clin Invest *108*, 15-23.

Ueda, N., Yamamoto, K., Yamamoto, S., Tokunaga, T., Shirakawa, E., Shinkai, H., Ogawa, M., Sato, T., Kudo, I., Inoue, K., Takizawa, H., Nagano, T., Hirobe, M., Matsuki, N., and Saito, H. (1995). Lipoxygenase-catalyzed oxygenation of arachidonylethanolamide, a cannabinoid receptor agonist. Biochim Biophys Acta *1254*, 127-134.

von Weymarn, L.B., Blobaum, A.L., and Hollenberg, P.F. (2004). The mechanism-based inactivation of p450 2B4 by tert-butyl 1-methyl-2-propynyl ether: structural determination of the adducts to the p450 heme. Arch Biochem Biophys *425*, 95-105.

Wamberg, L., Christiansen, T., Paulsen, S.K., Fisker, S., Rask, P., Rejnmark, L., Richelsen, B., and Pedersen, S.B. (2013). Expression of vitamin D-metabolizing enzymes in human adipose tissue-the effect of obesity and diet-induced weight loss. Int J Obes (Lond) *37*, 651-657.

Wang, J., and Ueda, N. (2009). Biology of endocannabinoid synthesis system. Prostaglandins Other Lipid Mediat *89*, 112-119.

Woodward, D.F., Wang, J.W., and Poloso, N.J. (2013). Recent progress in prostaglandin F2alpha ethanolamide (prostamide F2alpha) research and therapeutics. Pharmacol Rev *65*, 1135-1147.

Wright, K.L., Duncan, M., and Sharkey, K.A. (2008). Cannabinoid CB2 receptors in the gastrointestinal tract: a regulatory system in states of inflammation. Br J Pharmacol *153*, 263-270.

Wu, S., Moomaw, C.R., Tomer, K.B., Falck, J.R., and Zeldin, D.C. (1996). Molecular cloning and expression of CYP2J2, a human cytochrome P450 arachidonic acid epoxygenase highly expressed in heart. J Biol Chem *271*, 3460-3468.

Xu, Z.G., Lanting, L., Vaziri, N.D., Li, Z., Sepassi, L., Rodriguez-Iturbe, B., and Natarajan, R. (2005). Upregulation of angiotensin II type 1 receptor, inflammatory mediators, and enzymes of arachidonate metabolism in obese Zucker rat kidney: reversal by angiotensin II type 1 receptor blockade. Circulation *111*, 1962-1969.

Yang, W., Ni, J., Woodward, D.F., Tang-Liu, D.D., and Ling, K.H. (2005). Enzymatic formation of prostamide F2alpha from anandamide involves a newly identified intermediate metabolite, prostamide H2. J Lipid Res *46*, 2745-2751.

Yu, M., Ives, D., and Ramesha, C.S. (1997). Synthesis of prostaglandin E2 ethanolamide from anandamide by cyclooxygenase-2. J Biol Chem *272*, 21181-21186.

Zeldin, D.C., Foley, J., Boyle, J.E., Moomaw, C.R., Tomer, K.B., Parker, C., Steenbergen, C., and Wu, S. (1997). Predominant expression of an arachidonate epoxygenase in islets of Langerhans cells in human and rat pancreas. Endocrinology *138*, 1338-1346.

Zeldin, D.C., Foley, J., Ma, J., Boyle, J.E., Pascual, J.M., Moomaw, C.R., Tomer, K.B., Steenbergen, C., and Wu, S. (1996). CYP2J subfamily P450s in the lung: expression, localization, and potential functional significance. Mol Pharmacol *50*, 1111-1117.

Zhao, X., Dey, A., Romanko, O.P., Stepp, D.W., Wang, M.H., Zhou, Y., Jin, L., Pollock, J.S., Webb, R.C., and Imig, J.D. (2005). Decreased epoxygenase and increased epoxide hydrolase expression in the mesenteric artery of obese Zucker rats. Am J Physiol Regul Integr Comp Physiol *288*, R188-196.

Zhao, X., Quigley, J.E., Yuan, J., Wang, M.H., Zhou, Y., and Imig, J.D. (2006). PPAR-alpha activator fenofibrate increases renal CYP-derived eicosanoid synthesis and improves endothelial dilator function in obese Zucker rats. Am J Physiol Heart Circ Physiol *290*, H2187-2195.

CHAPTER III

Inhibition of the Hydrolysis of Epoxyeicostrienoic Acid Ethanolamides Using the Soluble Epoxide Hydrolase Inhibitors AUDA, APAU, and TPPU

Abstract

The endocannabinoid anandamide is metabolized by several P450s to give four epoxyeicosatrienoic acid ethanolamides (EET-EAs). The biological functions of these metabolites have yet to be determined. Much progress has been made in understanding the purpose of the structurally related metabolites of arachidonic acid, the epoxyeicosatrienoic acids (EETs), as a result of the development of soluble epoxide hydrolase inhibitors (sEHIs). Soluble epoxide hydrolase (sEH) is the main enzyme responsible for the hydrolysis of the epoxide-containing EETs to the less chemically reactive dihydroxyeicosatrienoic acids (DHETs). Since it is likely that sEH is also responsible for the hydrolysis of EET-EAs to DHET-EAs, it is possible that the same sEHIs can be used to inhibit the hydrolysis of the EET-EAs. As a result, the sEHIs AUDA, APAU, and TPPU were investigated for their ability to inhibit the hydrolysis of the EET-EAs by sEH. The 5,6-, 8,9-, 11,12-, and 14,15-EET-EAs are formed as a result of human liver S9 metabolism of AEA. Preliminary kinetic assays determined that for 19- and 20-HETE-EAs, the K_m values were 199 and 63 μM, respectively, and the V_{max} values were determined to be 137 and 503 pmols/min/mg of protein, respectively. Since the kinetic assays for the formation of the epoxides were performed in the absence of sEHIs,

the rates of formation of the EET-EAs could not be accurately measured since the epoxides were also being hydrolyzed rapidly. As a result, the kinetic parameters could not be determined. Subsequent studies demonstrated that AUDA had an EC_{50} value of 5.6 μM for inhibiting the hydrolysis of 14,15-EET-EA and APAU exhibited EC_{50} values of 4.7 and 10.4 μM for inhibiting the hydrolysis of 11,12- and 14,15-EET-EAs, respectively. TPPU did not significantly inhibit the hydrolysis of any of the EET-EAs. Future studies leading to the design of more specific and potent inhibitors of the epoxide hydrolases responsible for EET-EA hydrolysis may be of great value in elucidating the biological roles of the EET-EAs.

Introduction

The endogenous cannabinoid arachidonoyl ethanolamine or anandamide (AEA) is oxidized by cytochrome P450s (P450s) to give several different metabolites, including the four regioisomeric epoxides 5,6-, 8,9-, 11,12-, and 14,15-epoxyeicosatrienoic acid ethanolamides (EET-EAs) (Snider et al., 2007; Snider et al., 2008; Snider et al., 2010; Sridar et al., 2011; Stark et al., 2008). Data suggest that these epoxides are readily hydrolyzed by epoxide hydrolases (EHs) to give the 1,2-diols thereby forming the corresponding dihydroxyeicosatrienoic acid ethanolamides (DHET-EAs) (Morisseau and Hammock, 2005; Snider et al., 2007). As a result of the transitory nature of the epoxides, it may be difficult to ascertain their biological functions in the body experimentally.

Humans have several EHs which are members of the α/β-hydrolase fold family and utilize a two-step mechanism to open epoxides and add a water molecule (Morisseau and Hammock, 2005). *EPHX1* and *EPHX2* are the genes that encode for the two most

notable EH family members, microsomal epoxide hydrolase (mEH) and soluble epoxide hydrolase (sEH), respectively (Decker et al., 2009; Morisseau and Hammock, 2005). The names of the enzymes correspond to their cellular localization. While mEH is found in the smooth endoplasmic reticulum or microsomes, sEH is found in the cytosol and peroxisomes (Enayetallah et al., 2006; Hosagrahara et al., 2004). Although mEH is primarily known for its ability to catalyze the hydrolysis of epoxides of xenobiotics and toxins, it can also hydrolyze fatty acid epoxides such as the EETs; however, sEH is far more efficient at catalyzing the hydrolysis of fatty acid epoxides (Marowsky et al., 2009; Morisseau et al., 2010; Oesch, 1973). Because of this, it is likely that sEH may be the primary enzyme responsible for the hydrolysis of the EET-EAs *in vivo*.

The EET-EAs are structurally similar to the P450-catalyzed arachidonic acid (AA) epoxide metabolites, the epoxyeicosatrienoic acids (EETs). These compounds only differ by the functional group attached to the α-carbon. While EETs have a hydroxyl group attached to the first carbon, EET-EAs have an ethanolamine group attached to the corresponding carbon. Experiments utilizing sEH isolated from rabbits determined that the EETs are subject to hydrolysis by sEH, but this enzyme prefers the epoxide to be 14-16 carbons away from the carboxylic acid (Morisseau and Hammock, 2005; Zeldin et al., 1993). As a result, the 14,15-EET isomer is the preferred substrate, whereas the 5,6-EET is an unlikely substrate (Zeldin et al., 1993). Although the EETs are quite labile *in vivo* due to their sEH-mediated hydrolysis to DHETs, a wealth of information is known about their biological functions and this can be attributed to commercially available standards, reliable quantification methods, and perhaps more importantly, the development of soluble epoxide hydrolase inhibitors (sEHI) (Morisseau and Hammock, 2005, 2013).

Here we describe the first investigation of the abilities of three potent sEHIs for EET hydrolysis to prevent the conversion of the EET-EAs to DHET-EAs in human liver S9 fractions.

Methods and Materials

Materials. Anandamide, anandamide-d_8, 5,6-EET-EA, 8,9-EET-EA, 11,12-EET-EA, 14,15-EET-EA, and 20-HETE-EA were purchased from Cayman Chemical (Ann Arbor, MI). 1-(1-acetypiperidin-4-yl)-3-adamantanylurea (APAU), 12-(3-admantan-1-yl-ureido) dodecanoic acid (AUDA), and 1-trifluoromethoxyphenyl-3-(1-propionylpiperidin-4-yl) urea (TPPU) were gifts from Dr. Bruce Hammock (University of California-Davis, Davis, CA). Pooled human liver S9 fractions were purchased from BioreclamationIVT (Baltimore, MD). All other reagents were of the highest quality and were obtained from commercial sources.

Anandamide Metabolism Assays. The metabolism of anandamide was determined using incubation mixtures (0.25 mL) containing human liver S9 fractions (0.8 mg/mL), 100 mM potassium phosphate buffer (pH 7.4), 3.3 mM $MgCl_2$, and anandamide. Varying amounts of APAU, AUDA, and TPPU were added to the reactions as indicated in the figure legends. Reactions were initiated by the addition of 1.3 mM NADPH and allowed to continue for 20-30 min at 37°C. Control reactions were performed in the absence of NADPH. The reactions were terminated by the addition of 1 ml of cold ethyl acetate. After the addition of the internal standard, anandamide-d_8, the samples were vortexed for 2 min and centrifuged at full speed using a desktop centrifuge for 5 min. This extraction procedure was performed a total of two times. The organic layers were

dried down under a constant stream of nitrogen gas. The dried samples were resuspended in 100 μL of methanol and 10 μL aliquots were subjected to electrospray ionization-liquid chromatography/mass spectrometry (ESI-LC/MS) analysis. The standard curves for the various metabolites that were used for the quantification and determination of the K_M and V_{maz} values were generated by subjecting various known amounts of authentic standards to ESI-LC/MS analysis.

ESI-LC/MS Analysis. Samples (10 μL) were injected onto a Hypersil ODS column (5 μm, 4.6 × 100 mm; Thermo Fisher Scientific, Waltham, MA) that was equilibrated with 25% solvent A (0.1% acetic acid in water) and 75% solvent B (0.1% acetic acid in methanol). The metabolites were resolved using the following gradient: 0 to 5 min, 75% B; 5 to 20 min, 75 to 100% B; 20 to 25 min, 100% B; 25 to 26 min, 100 to 75% B; and 26 to 30 min, 75% B. The flow rate was 0.3 ml/min. The column effluent was directed into the LCQ mass analyzer (Thermo Fisher Scientific). The ESI conditions were as follows: sheath gas, 90 arbitrary units; auxiliary gas, 30 arbitrary units; capillary temperature, 200°C; and spray voltage, 4.5 V. Data were acquired in positive ion mode for anandamide and its metabolites using the Xcalibur software package (Thermo Fisher Scientific) with one full scan from 300 to 500 mass/charge ratio (*m*/*z*) followed by one data-dependent scan of the most intense ion.

Data Analysis. Nonlinear regression analyses of the data were performed using GraphPad Prism 6 (GraphPad Software Inc., San Diego, CA; http://www.graphpad.com).

Results

Human Liver S9 Metabolism of Anandamide. Before we could determine the efficacy of the selected sEHIs for inhibiting the hydrolysis of the EET-EAs, we had to investigate the metabolism of AEA by human liver S9 fractions. S9 fraction preparation was first described by Garner and coworkers (Garner et al., 1972). Basically, the tissue, liver in this situation, is homogenized and centrifuged for 10 min at 9000 *g*. The supernatant is the S9 fraction. The total ion chromatogram (TIC) and extracted ion chromatograms for the metabolites formed having *m/z* values of 364 and 382 can be seen in Figure 3.1. Six mono-oxygenated metabolites were detected. Two of the metabolites were hydroxylated, 19- and 20-HETE-EA, and four were epoxygenated, 5,6-, 8,9-, 11,12-, and 14,15-EET-EA. These were identified from their retention times and MS/MS spectra by comparison with authentic standards, except for 19-HETE-EA, for which an authentic standard is not yet available. In order to determine the kinetic data, we used assay conditions where product formation was linear with respect to the protein concentration and the selected incubation time. The kinetic data for substrate concentration vs. product formation were plotted for 14,15-, 11,12-, 8,9-, and 5,6-EET-EA, see Figure 3.2. Because we were unable to reach saturation at the concentrations of AEA used, the kinetic parameters for these metabolites could not be determined. The formation of 19- and 20-HETE-EAs by human liver S9 exhibited simple Michaelis-Menten kinetics and nonlinear regression was used to calculate the apparent K_m and V_{max} values. The K_m values calculated for the formation of 19- and 20-HETE-EA were 199 and 63 μM, respectively, and the V_{max} values were 137 and 503 pmol/min/mg of protein, respectively, for 19- and 20-HETE-EA formation (Figure 3.2).

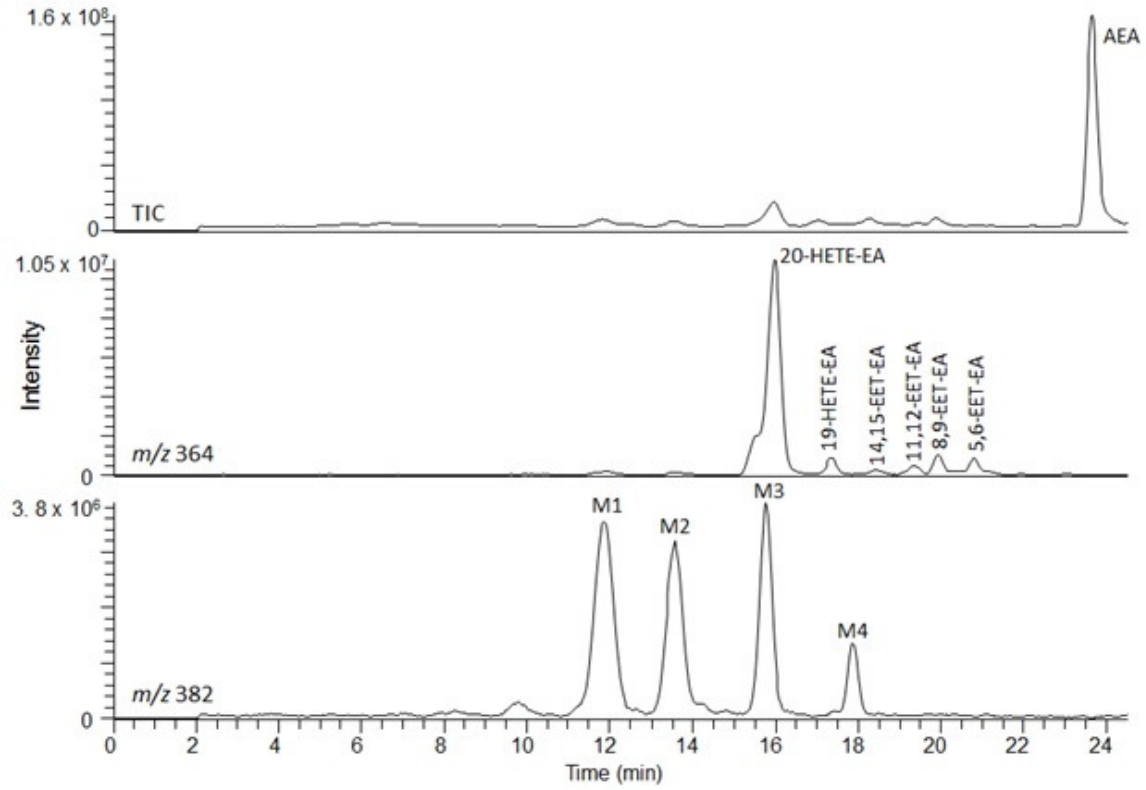

Figure 3.1. AEA metabolism by human liver S9. Liver S9 protein (0.8 mg/mL) was incubated with AEA (100 µM) in 100 mM potassium phosphate buffer, pH 7.4, containing 3.3 mM $MgCl_2$. The reaction was started by the addition of 1.3 mM of NADPH and the samples were incubated at 37°C with shaking. The reaction was stopped with ice cold ethyl acetate after 20 min. The metabolites were extracted from the reaction mixture as described in *Materials and Methods*. The TIC shows all the ions detected by the LC/MS (Top). The ions observed at *m/z* 364 represent the mono-oxygenated metabolites, the HETE-EAs and the EET-EAs (Middle).The peaks observed at *m/z* 382 are the DHET-EAs that result from the hydrolysis of the EET-EAs by epoxide hydrolase (Bottom).

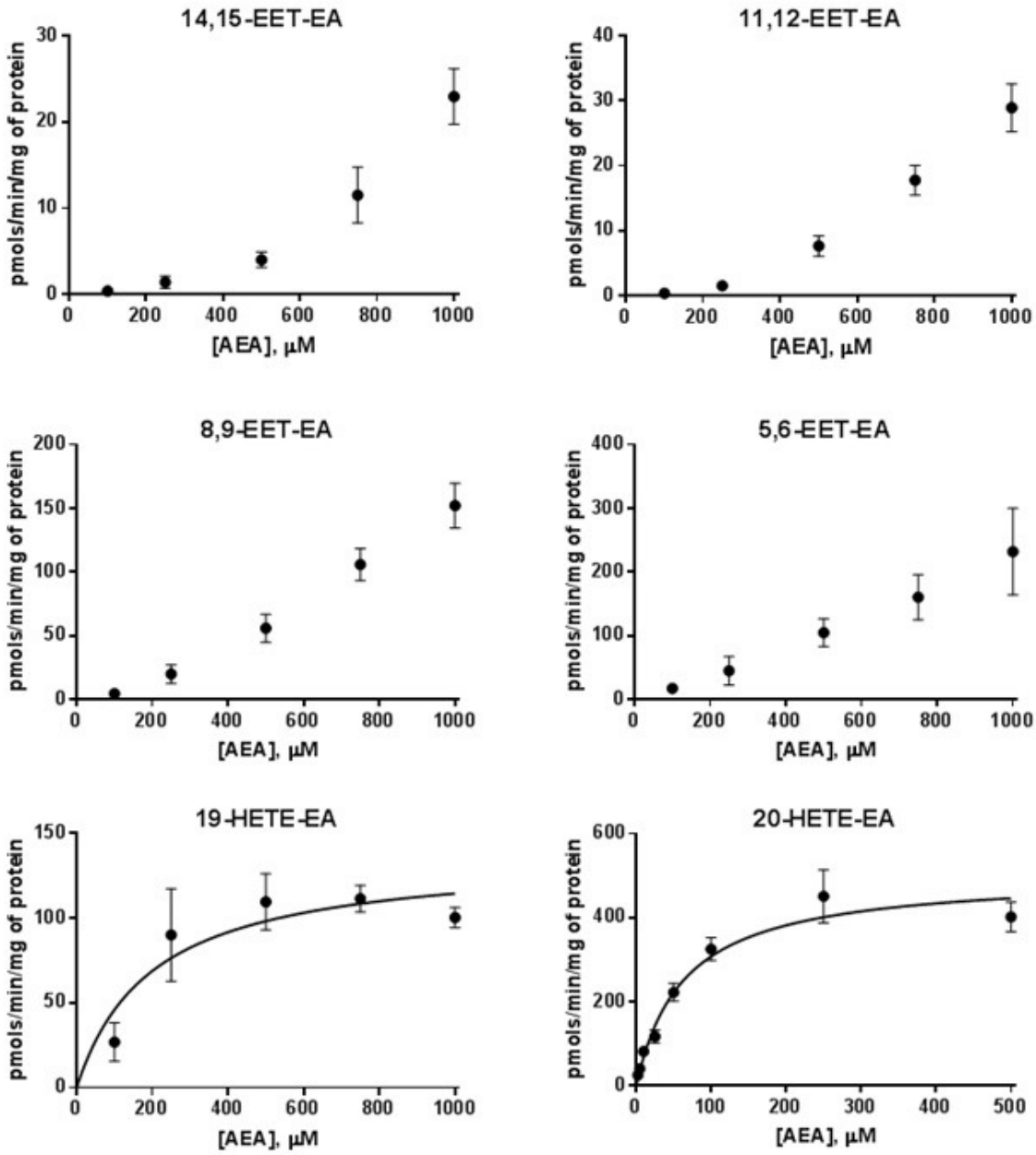

Figure 3.2. Kinetic data for the metabolism of AEA by human liver S9. Reaction mixtures containing human liver S9 (200 µg) and AEA (2.5-1000 µM) were incubated for 10 and 20 (20-HETE-EA only) min in 0.1 M phosphate buffer, pH 7.4, at 37°C with shaking. The reactions were quenched and the samples were extracted as described in *Materials and Methods*. The amount of metabolites formed was calculated based on a standard curve obtained for each metabolite. Since an authentic standard for 19-HETE-EA is not available, its formation is based on the standard curve for 20-HETE-EA. The rate data were fitted to the Michaelis-Menten enzyme kinetic model using the Graphpad Prism 6 software.

The Effect of AUDA on EET-EA Levels Measured in Liver S9 Incubations. AUDA is a potent sEHI that is commonly used to inhibit sEH-mediated hydrolysis of EETs in several *in vitro* and *in vivo* models (Inceoglu et al., 2006; Olearczyk et al., 2006; Xu et al., 2006). Due to the structural similarities between the EETs and the EET-EAs, we tested AUDA for its ability to inhibit the hydrolysis of the EET-EAs. Figure 3.3 shows the extracted ion chromatograms at *m/z* 364 and 382 from which the relative levels of EET-EAs and DHET-EAs present can be determined, respectively. For the epoxide metabolites, increasing the concentration of AUDA generally caused the expected increase in the area of the respective peaks. Similarly, the peaks representative of the DHET-EAs decreased in area as the amount of AUDA added to the incubations increased. Because we were unable to accurately quantify the amount of DHET-EAs formed, we were unable to determine if the increase in EET-EA formation was indirectly proportional to the decrease in DHET-EA formation. Interestingly, at the highest concentration of AUDA tested (100 μM), the peak areas decreased for all of the epoxides except for the 14,15-EET-EA. Since AUDA also caused a significant decrease in the amount of 20-HETE-EA formed, this decrease in product formation may be due to inhibition of P450-catalyzed metabolism of AEA to form the epoxides.

Determination of the EC_{50} Values for AUDA, APAU, and TPPU. Because AUDA was able to increase the total amounts of the EET-EAs measured following liver S9 metabolism, we also investigated the effects on the two other sEHIs, APAU and TPPU on epoxide levels formed by human liver S9 using a similar approach. From these assays, the EC_{50} values for the inhibition of the hydrolysis of each of the AEA epoxide

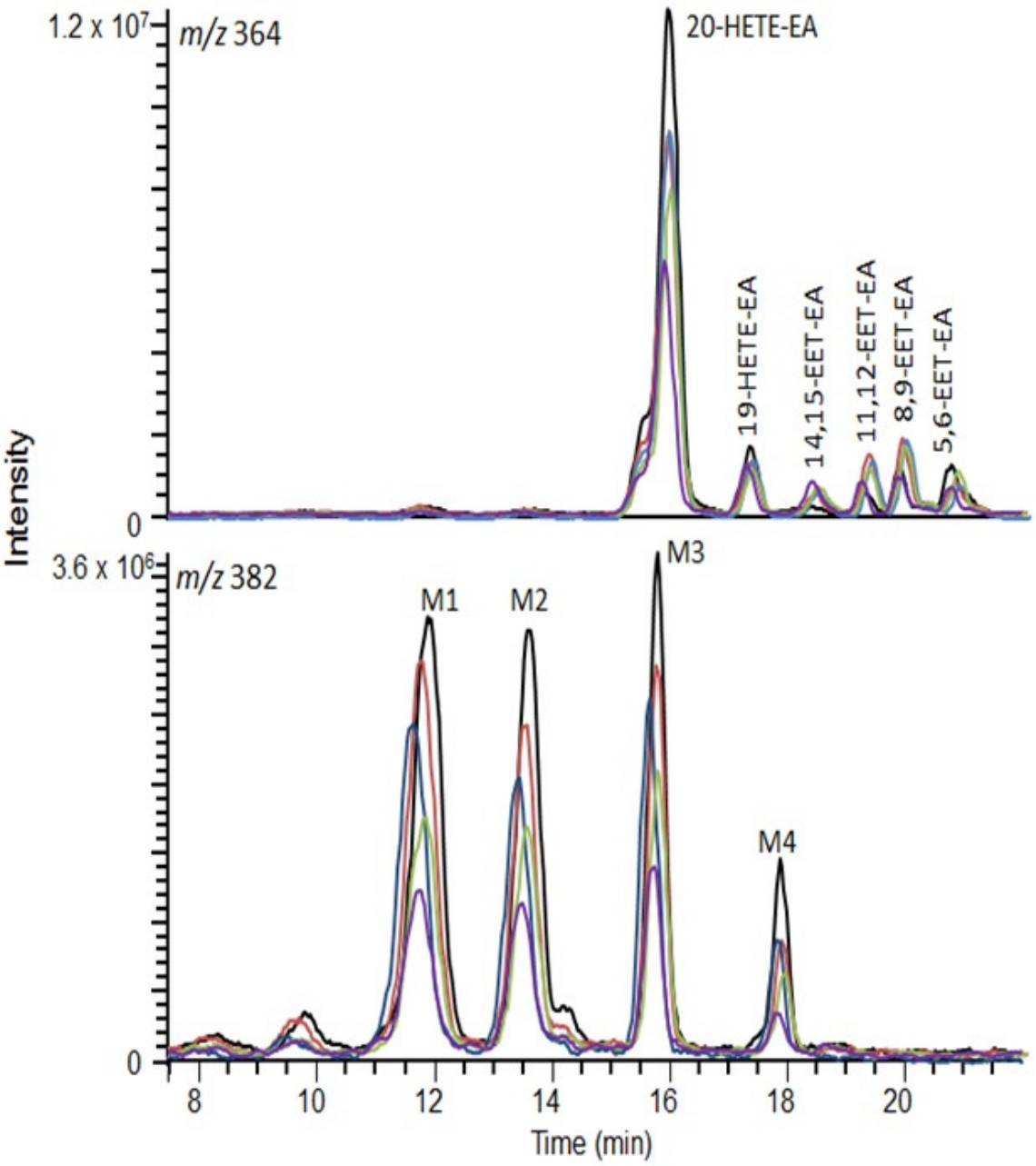

Figure 3.3. Formation of EET-EAs and DHET-EAs by human liver S9 in the presence of AUDA. Human liver S9 protein (0.8 mg/mL) was incubated with AEA (100 µM) and varying concentrations of AUDA in 0.1 M phosphate buffer containing $MgCl_2$ for 30 min at 37°C with shaking. The reaction was stopped and the metabolites extracted as previously described in *Materials and Methods*. The color traces represent the following concentrations of AUDA added: vehicle only (black), 0.1 µM (red), 1 µM (blue), 10 µM (green), and 100 µM (purple).

metabolites were investigated for AUDA, APAU, and TPPU, all of which are potent inhibitors of sEH and thus EET hydrolysis. All of the sEHIs used exhibited IC_{50} values at nanomolar levels for the inhibition of sEH activity (Jones et al., 2006; Morisseau et al., 2002; Rose et al., 2010). A wide range of concentrations was initially tried for each of the sEHIs to determine the correct range of inhibitor concentration to perform the EC_{50} evaluations for the inhibition of EET-EA hydrolysis.

AUDA slightly increased 11,12-EET-EA levels, had no effect of 8,9-EET-EA levels, and decreased 5,6-EET-EA levels in a dose dependent manner (Figure 3.4A and B). AUDA significantly increased the formation of 14,15-EET-EA and its EC_{50} value was calculated as 5.6 ± 0.002 μM (Figure 3.4C). Although the presence of APAU significantly increased the formation of all four of the EET-EAs as compared to control (Figure 3.5A and B), EC_{50} values could only be calculated for 11,12- and 14,15-EET-EAs which were 4.7 ± 0.002 μM and 10.4 ± 0.003 μM, respectively (Figure 3.5C and D). Figure 3.6 shows the amount of product formed in response to increasing concentrations of TPPU. Although the addition of TPPU did significantly increase formation of 14,15- and 11,12-EET-EAs, this did not occur in a dose dependent manner. In addition, TPPU had no effect on the formation of 8,9- and 5,6-EET-EAs. As a result, no EC_{50} values could be obtained from the TPPU data.

Discussion

Anandamide is an endogenous cannabinoid that elicits several beneficial effects in the body mediated by cannabinoid receptor dependent and independent pathways

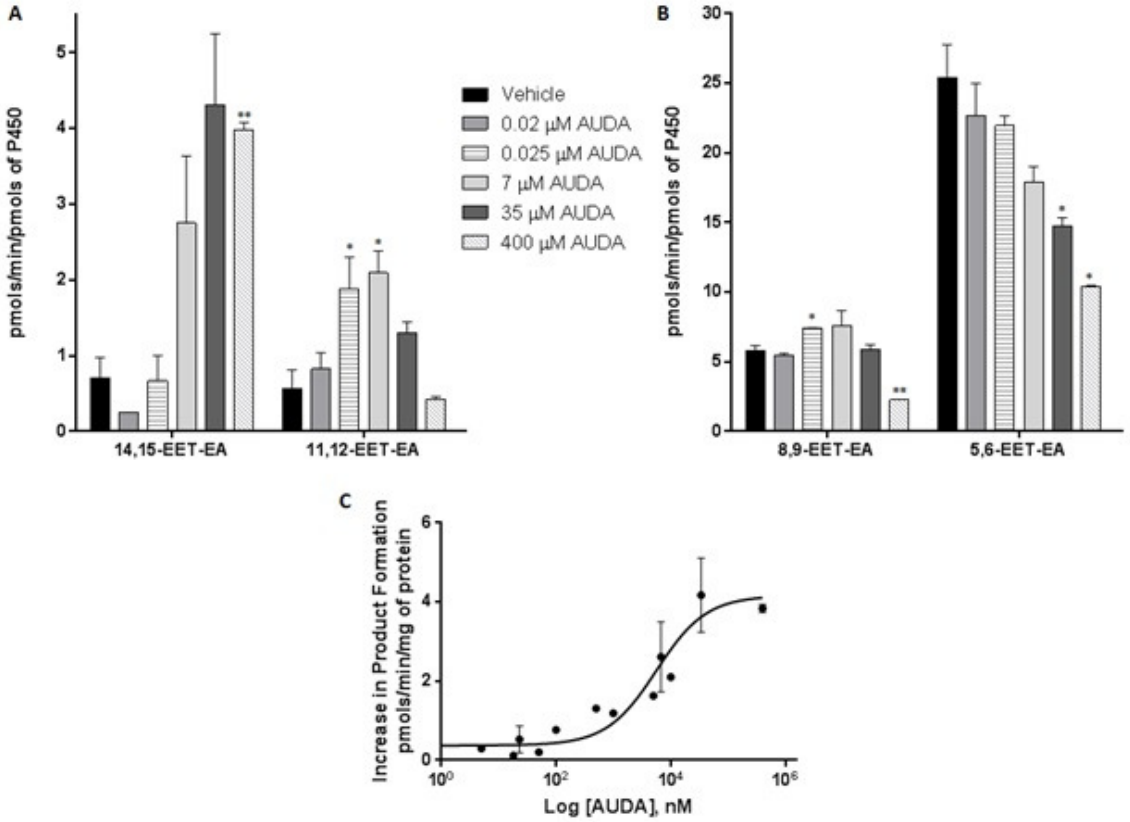

Figure 3.4. EC_{50} determination for AUDA. Human liver S9 (200 µg) was incubated with AUDA (0.1 nM-400 µM) in the reaction buffer as described in *Materials and Methods*. NADPH (1.3 mM) was added to start the reactions which were incubated for 30 min 37°C. The reactions were stopped with 1mL of ethyl acetate and extracted twice. Sample preparation was performed as described in *Materials and Methods*. The bars in (A) and (B) represent the mean ± SEM from one experiment performed in duplicate. Statistical significance was determined using the Holm-Sidak method in the Graphpad Prism 6 program. The points plotted in (C) for 14,15-EET-EA were obtained by subtracting the control amount from the total amount measured. Data points without error bars represent individual measurements. Data points with error bars represent the mean ± SEM for one experiment performed in duplicate. *, $P < 0.05$; **, $P < 0.01$.

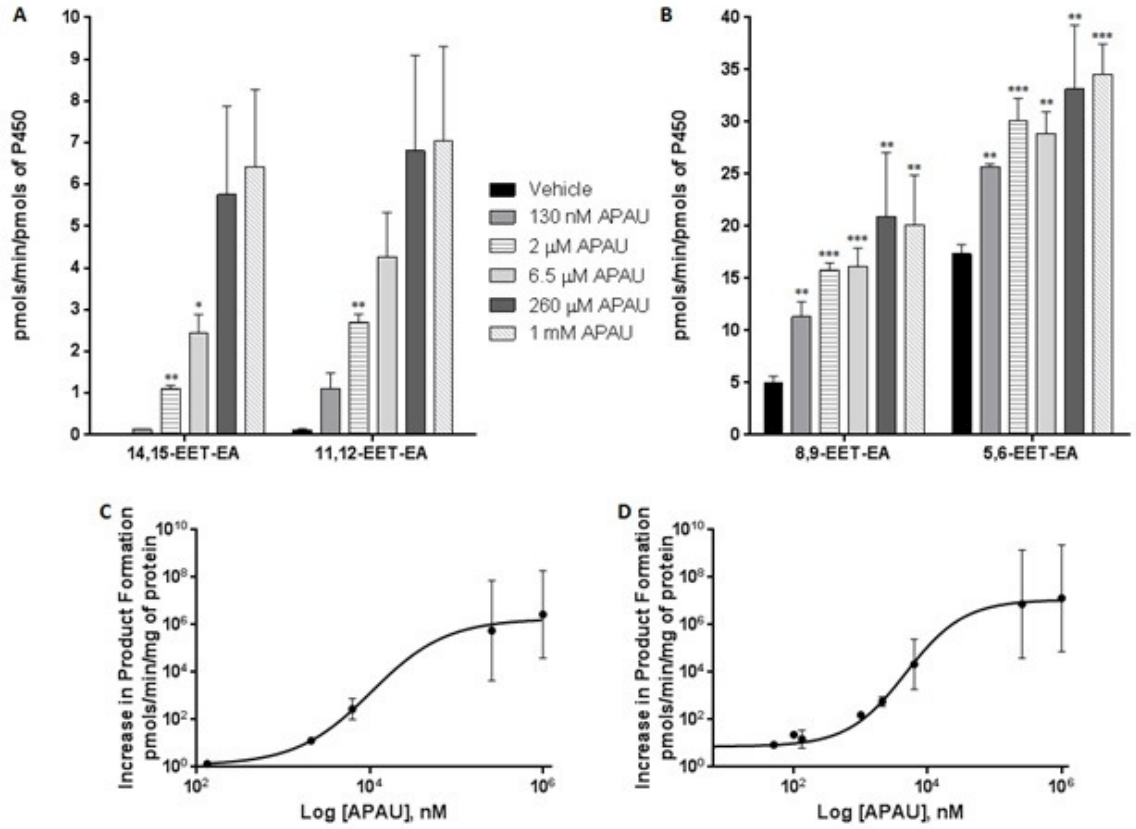

Figure 3.5. EC_{50} determination for APAU. Human liver S9 (0.8 mg/mL) was incubated with APAU (1 nM-1 mM) in the reaction buffer as described in *Materials and Methods*. NADPH (1.3 mM) was added to initiate the reactions which were continued for 30 min 37°C. The reactions were stopped and samples extracted as previously described in *Materials and Methods*. The bars in (A) and (B) represent the mean ± SEM from one experiment performed in duplicate. Statistical significance was determined using the Holm-Sidak method in the Graphpad Prism 6 program. The points plotted in (C) for 14,15-EET-EA and (D) for 11,12-EET-EA represent the increase in product formation above control levels. Data points represent the mean ± SEM for one experiment performed in duplicate. *, $P < 0.05$; **, $P < 0.01$; ***, $P < 0.001$.

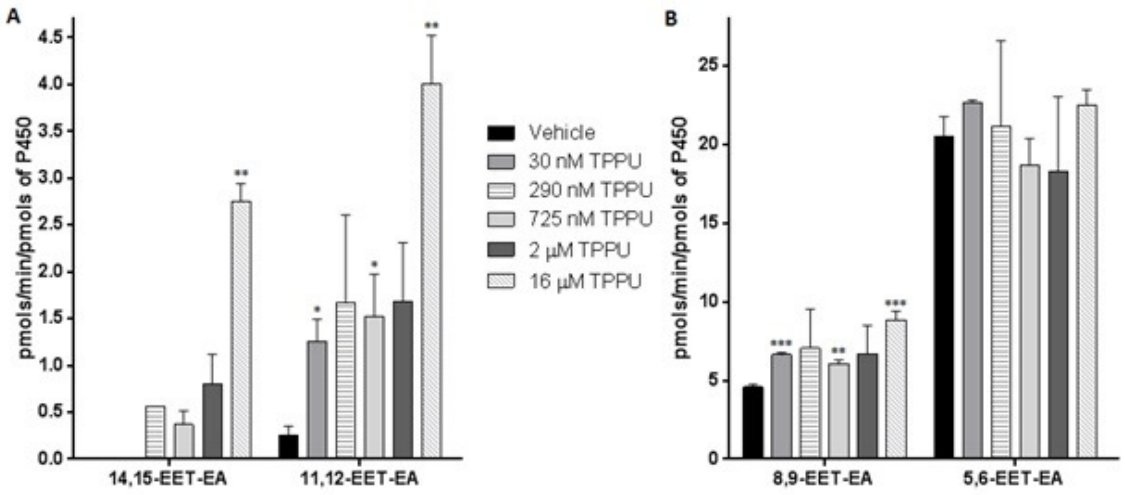

Figure 3.6. Effect of TPPU on EET-EA levels. Human liver S9 fraction (200 µg) was incubated with TPPU (1 nM-250 µM) in 100 mM potassium phosphate buffer, pH 7.4. The reactions were initiated by the addition of NADPH (1.3 mM) and samples were incubated for 30 min 37°C with shaking. The reactions were quenched with 1mL of ethyl acetate and extracted twice. Sample preparation was performed as described in *Materials and Methods*. Although there were several treatment groups that varied significantly from control, these variations did not occur in a dose dependent manner and therefore the EC_{50} values could not be calculated. The bars represent the mean ± SEM from one experiment performed in duplicate. Statistical significance was determined using the Holm-Sidak method in GraphPad Prism 6 program. *, $P < 0.05$; **, $P < 0.01$; ***, $P < 0.001$.

(Snider et al., 2010). Several P450s are known to metabolize AEA to give the 19- and 20-HETE-EAs and the 5,6-, 8,9-, 11,12- and 14,15-EET-EAs (Pratt-Hyatt et al., 2010; Snider et al., 2007; Snider et al., 2008; Sridar et al., 2011; Stark et al., 2008). The structure of AEA is closely related to that of AA. AA is metabolized by P450s to give several HETEs and 5,6-, 8,9-, 11,12- and 14,15-EET (Roman, 2002) . Soluble epoxide hydrolase inhibitors have been used to inhibit EET hydrolysis and study their biological functions *in vivo* (Morisseau and Hammock, 2013). As a result, we investigated the ability of three potent sEHIs to inhibit the hydrolysis of the EET-EAs in an effort to determine their usefulness in studying the biological of the EET-EAs *in vivo*. We chose to use the human liver S9 preparation as an enzyme source because it should exhibit higher sEH activity than microsomal preparations which should not include the cytosolic fraction.

We first investigated the metabolism of AEA by human liver S9 fractions. Figure 3.1 showed the LC/MS chromatogram of the products formed. The metabolites were the same as those known to be formed by human liver microsomes (HLM) (Snider et al., 2007); however, the product profile was slightly different. With HLM, 8,9-EET-EA was the major product observed; however, with human liver S9, the 5,6-EET-EA was determined to be the major product (Snider et al., 2007). Whether this difference is due to the differences in the pools of the livers used for the preparation of the S9 and the microsomes or an intrinsic difference between S9 and microsomal metabolism is not clear. The S9 fraction contains microsomal and cytosolic proteins. Investigations completed by Slaughter and coworkers determined that microsomal incubations and cytosolic incubation were able to oxidize and reduce the COX-2 inhibitor rofecoxib,

respectively (Slaughter et al., 2003). Therefore, the presence of the cytosol in the enzyme source from this work as compared to previous studies may account for the observed differences. Moreover, the presence of multiple isoforms of epoxide hydrolases, such as microsomal, soluble, and potentially others, makes it difficult to definitively determine the kinetic parameters of these labile compounds suggesting that microsomes are a better enzyme source to study kinetics; however, the reaction conditions reported here are probably more similar to *in vivo* conditions than the microsomal studies with regard to enzymatic activity.

It is possible that both mEH and sEH are present in the human liver S9 fraction. This may explain why at the concentrations of AEA used, we were unable reach saturation for the formation of the EET-EAs and determine K_m and V_{max} values. The K_m we reported for liver S9 formation of 20-HETE-EA is about 25 times higher than the K_m reported in HLM (Snider et al., 2007). On the other hand, our reported V_{max} value was two times greater than that reported for HLM (Snider et al., 2007). The kinetics for 19-HETE-EA were not reported in the previous study, so there is no comparison to be made; however, the liver S9 is more efficient at 20-HETE-EA formation than 19-HETE-EA formation based on V_{max}/K_m values of 8 and 0.7 pmols/min/mg of protein, respectively.

Only the IC_{50} values for sEH activity as measured using the radioactive substrate [^{3}H]-tDPPO or the fluorescent substrate α-cyanocarbonate have been reported in the literature for the three sEHIs studied (Jones et al., 2006; Morisseau et al., 2002; Rose et al., 2010). However, one lab has reported an EC_{50} value for AUDA of 2 μM for inhibition of 14,15-EET-induced vasorelaxation of precontracted bovine coronary arteries (Falck et al., 2009). This value is comparable to the EC_{50} value of 5 μM reported here for

AUDA inhibition of 14,15-EET-EA hydrolysis. We observed that AUDA inhibited the hydrolysis of the 14,15- and 11,12-EET-EAs at low micromolar levels leading to increased levels of epoxides, but decreases in the yields of the epoxides were observed at higher levels for 5,6-, 8,9-, and 11,12-EET-EAs. Increasing the AUDA concentration caused a continuous decrease in 5,6-EET-EA formation at all concentrations used. AUDA also inhibited 20-HETE-EA formation in a dose-dependent manner, but had little to no effect on the formation of 19-HETE-EA (Figure 3.3). AUDA is rapidly metabolized *in vivo*, and its adamantine group is sensitive to P450-catalyzed oxidation (Morisseau and Hammock, 2013). Thus, the decreases in the EET-EA levels and 20-HETE-EA formation at higher concentrations of AUDA may be due to competitive inhibition of the P450s responsible for their formation by AUDA. It is unlikely that either APAU or TPPU are inhibitors of P450 activity since their presence did not significantly affect 20-HETE-EA formation (data not shown).

APAU caused an increase in the levels of all of the EET-EAs, but EC_{50} values could only be calculated for the 14,15- and 11,12-EET-EAs. TPPU caused significant increases in the epoxide levels at the highest concentration tested for 11,12- and 14,15-EET-EA, but the inhibition data were not consistent enough to calculate an EC_{50} value. TPPU had a relatively minor effect on 8,9-EET-EA levels and no effect on 5,6-EET-EA hydrolysis. The various degrees of inhibition exhibited by the sEHIs for the hydrolysis of each of the EET-EAs suggest that the substrate preference of sEH for these metabolites may be similar to that for the EETs with 14,15-EET-EA being the preferred substrate, followed by 11,12-, 8,9-, and with 5,6-EET-EA being the least preferred.

In conclusion, humans have several different EHs (Decker et al., 2009; Morisseau and Hammock, 2013), and it is likely that at least two of the major forms, mEH and sEH, are present in the liver S9 fraction used as an enzyme source for these studies. It is known that potent inhibitors of sEH such as AUDA, APAU, and TPPU do not inhibit mEH activity and vice versa, inhibitors of mEH do not inhibit sEH (Morisseau et al., 2008; Shen and Hammock, 2012). The presence of at least two isoforms of EHs in the S9 fraction and the use of inhibitors specific for only one isoform may be responsible for the differences observed in the inhibition, or lack thereof for the four different EET-EAs. There may be differences in selectivity for each of the EET-EAs when observing mEH activity vs. sEH activity. Future studies investigating the specific EHs (soluble or microsomal) responsible for the hydrolysis of each of the EET-EAs and the development of compounds more specific and potent for the inhibition of the EHs responsible for the hydrolysis of the EET-EAs will be required in order to have a better chance of elucidating the effects of EET-EAs *in vivo*.

References

Decker, M., Arand, M., and Cronin, A. (2009). Mammalian epoxide hydrolases in xenobiotic metabolism and signalling. Arch Toxicol *83*, 297-318.

Diani-Moore, S., Ma, Y., Gross, S.S., and Rifkind, A.B. (2013). Increases in Levels of Epoxyeicosatrienoic and Dihydroxyeicosatrienoic Acids (EETs and DHETs) in Liver and Heart In Vivo by 2,3,7,8-tetrachlorodibenzo-p-dioxin (TCDD) and in Hepatic EET:DHET Ratios by Cotreatment with TCDD and the Soluble Epoxide Hydrolase Inhibitor AUDA. Drug Metab Dispos.

Enayetallah, A.E., French, R.A., Barber, M., and Grant, D.F. (2006). Cell-specific subcellular localization of soluble epoxide hydrolase in human tissues. J Histochem Cytochem *54*, 329-335.

Falck, J.R., Kodela, R., Manne, R., Atcha, K.R., Puli, N., Dubasi, N., Manthati, V.L., Capdevila, J.H., Yi, X.Y., Goldman, D.H., Morisseau, C., Hammock, B.D., and Campbell, W.B. (2009). 14,15-Epoxyeicosa-5,8,11-trienoic acid (14,15-EET) surrogates containing epoxide bioisosteres: influence upon vascular relaxation and soluble epoxide hydrolase inhibition. J Med Chem *52*, 5069-5075.

Garner, R.C., Miller, E.C., and Miller, J.A. (1972). Liver microsomal metabolism of aflatoxin B 1 to a reactive derivative toxic to Salmonella typhimurium TA 1530. Cancer Res *32*, 2058-2066.

Hosagrahara, V.P., Rettie, A.E., Hassett, C., and Omiecinski, C.J. (2004). Functional analysis of human microsomal epoxide hydrolase genetic variants. Chem Biol Interact *150*, 149-159.

Imig, J.D. (2000). Epoxygenase metabolites. Epithelial and vascular actions. Mol Biotechnol *16*, 233-251.

Inceoglu, B., Jinks, S.L., Schmelzer, K.R., Waite, T., Kim, I.H., and Hammock, B.D. (2006). Inhibition of soluble epoxide hydrolase reduces LPS-induced thermal hyperalgesia and mechanical allodynia in a rat model of inflammatory pain. Life Sci *79*, 2311-2319.

Jiang, J.G., Chen, C.L., Card, J.W., Yang, S., Chen, J.X., Fu, X.N., Ning, Y.G., Xiao, X., Zeldin, D.C., and Wang, D.W. (2005). Cytochrome P450 2J2 promotes the neoplastic phenotype of carcinoma cells and is up-regulated in human tumors. Cancer Res *65*, 4707-4715.

Jones, P.D., Tsai, H.J., Do, Z.N., Morisseau, C., and Hammock, B.D. (2006). Synthesis and SAR of conformationally restricted inhibitors of soluble epoxide hydrolase. Bioorg Med Chem Lett *16*, 5212-5216.

Kroetz, D.L., and Zeldin, D.C. (2002). Cytochrome P450 pathways of arachidonic acid metabolism. Curr Opin Lipidol *13*, 273-283.

Marowsky, A., Burgener, J., Falck, J.R., Fritschy, J.M., and Arand, M. (2009). Distribution of soluble and microsomal epoxide hydrolase in the mouse brain and its contribution to cerebral epoxyeicosatrienoic acid metabolism. Neuroscience *163*, 646-661.

Morisseau, C., Goodrow, M.H., Newman, J.W., Wheelock, C.E., Dowdy, D.L., and Hammock, B.D. (2002). Structural refinement of inhibitors of urea-based soluble epoxide hydrolases. Biochem Pharmacol *63*, 1599-1608.

Morisseau, C., and Hammock, B.D. (2005). Epoxide hydrolases: mechanisms, inhibitor designs, and biological roles. Annu Rev Pharmacol Toxicol *45*, 311-333.

Morisseau, C., and Hammock, B.D. (2013). Impact of soluble epoxide hydrolase and epoxyeicosanoids on human health. Annu Rev Pharmacol Toxicol *53*, 37-58.

Morisseau, C., Inceoglu, B., Schmelzer, K., Tsai, H.J., Jinks, S.L., Hegedus, C.M., and Hammock, B.D. (2010). Naturally occurring monoepoxides of eicosapentaenoic acid and docosahexaenoic acid are bioactive antihyperalgesic lipids. J Lipid Res *51*, 3481-3490.

Morisseau, C., Newman, J.W., Wheelock, C.E., Hill Iii, T., Morin, D., Buckpitt, A.R., and Hammock, B.D. (2008). Development of metabolically stable inhibitors of Mammalian microsomal epoxide hydrolase. Chem Res Toxicol *21*, 951-957.

Oesch, F. (1973). Mammalian epoxide hydrases: inducible enzymes catalysing the inactivation of carcinogenic and cytotoxic metabolites derived from aromatic and olefinic compounds. Xenobiotica *3*, 305-340.

Olearczyk, J.J., Field, M.B., Kim, I.H., Morisseau, C., Hammock, B.D., and Imig, J.D. (2006). Substituted adamantyl-urea inhibitors of the soluble epoxide hydrolase dilate mesenteric resistance vessels. J Pharmacol Exp Ther *318*, 1307-1314.

Pratt-Hyatt, M., Zhang, H., Snider, N.T., and Hollenberg, P.F. (2010). Effects of a commonly occurring genetic polymorphism of human CYP3A4 (I118V) on the metabolism of anandamide. Drug Metab Dispos *38*, 2075-2082.

Roman, R.J. (2002). P-450 metabolites of arachidonic acid in the control of cardiovascular function. Physiol Rev *82*, 131-185.

Rose, T.E., Morisseau, C., Liu, J.Y., Inceoglu, B., Jones, P.D., Sanborn, J.R., and Hammock, B.D. (2010). 1-Aryl-3-(1-acylpiperidin-4-yl)urea inhibitors of human and murine soluble epoxide hydrolase: structure-activity relationships, pharmacokinetics, and reduction of inflammatory pain. J Med Chem *53*, 7067-7075.

Shen, H.C., and Hammock, B.D. (2012). Discovery of inhibitors of soluble epoxide hydrolase: a target with multiple potential therapeutic indications. J Med Chem *55*, 1789-1808.

Slaughter, D., Takenaga, N., Lu, P., Assang, C., Walsh, D.J., Arison, B.H., Cui, D., Halpin, R.A., Geer, L.A., Vyas, K.P., and Baillie, T.A. (2003). Metabolism of rofecoxib in vitro using human liver subcellular fractions. Drug Metab Dispos *31*, 1398-1408.

Snider, N.T., Kornilov, A.M., Kent, U.M., and Hollenberg, P.F. (2007). Anandamide metabolism by human liver and kidney microsomal cytochrome p450 enzymes to form hydroxyeicosatetraenoic and epoxyeicosatrienoic acid ethanolamides. J Pharmacol Exp Ther *321*, 590-597.

Snider, N.T., Sikora, M.J., Sridar, C., Feuerstein, T.J., Rae, J.M., and Hollenberg, P.F. (2008). The endocannabinoid anandamide is a substrate for the human polymorphic cytochrome P450 2D6. J Pharmacol Exp Ther *327*, 538-545.

Snider, N.T., Walker, V.J., and Hollenberg, P.F. (2010). Oxidation of the endogenous cannabinoid arachidonoyl ethanolamide by the cytochrome P450 monooxygenases: physiological and pharmacological implications. Pharmacol Rev *62*, 136-154.

Sridar, C., Snider, N.T., and Hollenberg, P.F. (2011). Anandamide oxidation by wild-type and polymorphically expressed CYP2B6 and CYP2D6. Drug Metab Dispos *39*, 782-788.

Stark, K., Dostalek, M., and Guengerich, F.P. (2008). Expression and purification of orphan cytochrome P450 4X1 and oxidation of anandamide. FEBS J *275*, 3706-3717.

Xu, D., Li, N., He, Y., Timofeyev, V., Lu, L., Tsai, H.J., Kim, I.H., Tuteja, D., Mateo, R.K., Singapuri, A.*, et al.* (2006). Prevention and reversal of cardiac hypertrophy by soluble epoxide hydrolase inhibitors. Proc Natl Acad Sci U S A *103*, 18733-18738.

Zeldin, D.C., Kobayashi, J., Falck, J.R., Winder, B.S., Hammock, B.D., Snapper, J.R., and Capdevila, J.H. (1993). Regio- and enantiofacial selectivity of epoxyeicosatrienoic acid hydration by cytosolic epoxide hydrolase. J Biol Chem *268*, 6402-6407.

CHAPTER IV

Metabolism of the Synthetic Cannabinoid JWH-018 and Its Effect on Heart Rate and Blood Pressure in Rats

Abstract

The marijuana substitute, "Spice" or "K2", is a significant drug of abuse in the United States and abroad. The side effects observed from using this product range from mild to deadly. JWH-018 is one of the main synthetic cannabinoids (SCs) that acts as the active ingredient in Spice products. It is important to understand the metabolism of this drug in the body to determine if the parent and/or an active metabolite cause the observed toxicities. This information may aid in the discovery of a treatment for toxicity due to this and similar compounds. Although several cytochrome P450s have been investigated for their ability to metabolize JWH-018, CYP2J2, a P450 primarily expressed in the heart which is a critical target organ for JWH-018 toxicity, has not been studied in detail. In the reconstituted system, CYP2J2 metabolizes JWH-018 mostly to give the JWH-018 ω-1-OH metabolite with an observed K_M of 10 μM and a k_{cat} value of 0.2 pmol/min/pmol of P450. These kinetic parameters are comparable to those for CYP2C9, which is believed to contribute significantly to JWH-018 metabolism in the liver; however, CYP2J2 is not as efficient as CYP2C9 at the metabolism of JWH-018. In addition, the metabolism of JWH-018 was studied in human intestinal and liver microsomes and in an animal model. Although several different metabolites were formed, the major product was a reduced

dihydroxydiol metabolite which could not be identified unequivocally. This product was formed by all of the human and rat organ tissues examined. Animal studies suggest that JWH-018 does not affect heart rate, but it does cause a significant increase in blood pressure. Future studies are needed to determine the efficacy of the major metabolic products of JWH-018 *in vivo*, especially the dihydroxydiol product, since several JWH-018 metabolites are known to retain biological activity.

Introduction

Cannabis or marijuana has been used medically and recreationally for thousands of years (Mechoulam and Hanus, 2000; Robson, 2005). Generally, SCs are based on the structure of the major psychoactive compound in marijuana, Δ^9-tetrahydrocannabinol (Δ^9-THC). The therapeutic potential of cannabinoid-based compounds did not become evident until after the cloning of the two cannabinoid receptors (Matsuda et al., 1990; Munro et al., 1993). Both receptors are primarily associated with G-proteins of the $G\alpha_i$ and $G\alpha_o$ families, and as a result, their activation leads to inhibition of cAMP accumulation in cells (Howlett, 2005; Pertwee, 2005); however, coupling of the receptors to other G-proteins has been reported as well (Glass and Felder, 1997; Lauckner et al., 2005). Cannabinoid 1 receptors (CB1Rs) are abundantly expressed in the brain, but are also present in peripheral tissues such as the heart and lungs at much lower levels (Galiegue et al., 1995). The cannabinoid 2 receptor (CB2R) is mostly expressed in the immune system (Galiegue et al., 1995). In order to study the cannabinoid system, Dr. John W. Huffman created the JWH family of SCs. One of these compounds, JWH-018

(see Figure 4.1), is found in almost all of the K2 products currently available (Atwood et al., 2010; Huffman et al., 1994; Wiley et al., 1998).

Since 2004, K2 products have been marketed legally as natural herbal incense at convenience stores, gas stations, and via the Internet. As a result, many users believe that the products are "safe" because of easy availability and lack of government regulation (Every-Palmer, 2011). However, in 2011, the Drug Enforcement Administration placed five SCs, including JWH-018, into Schedule I of the Controlled Substances Act (Pant et al., 2012). K2 products usually contain non-psychoactive plant matter which has been altered by the addition of various SCs (Atwood et al., 2010; Hudson et al., 2010; Uchiyama et al., 2010; Zuba et al., 2011). These products are believed to be popular, especially among teenagers and young adults, due to their potent psychoactivity, availability, and lack of detection in commonly used drug tests (Every-Palmer, 2011).

Unlike SC-containing products such as K2, marijuana contains over 60 cannabinoids that modulate the effects of Δ^9-THC (Pertwee, 2008). The synthetic cannabinoids present in K2 products have a higher affinity and greater efficacy at CB1Rs than Δ^9-THC, which increases the chance of toxicity (Gunderson et al., 2012). Moreover, metabolites of synthetic cannabinoids are known to bind to and activate the CB1R, more so than Δ^9-THC, which makes toxicity more likely after K2 usage (Brents et al., 2011; Chimalakonda et al., 2012). Moreover, studies utilizing monkeys revealed that SCs such as JWH-018 have a short duration of action which may lead to more frequent usage (Ginsburg et al., 2012). The relatively short duration time for their effects combined with increased potency at CB1Rs could lead to a greater risk for dependence (Ginsburg et al., 2012). Due to its five carbon side chain, JWH-018 is also an optimum ligand for the

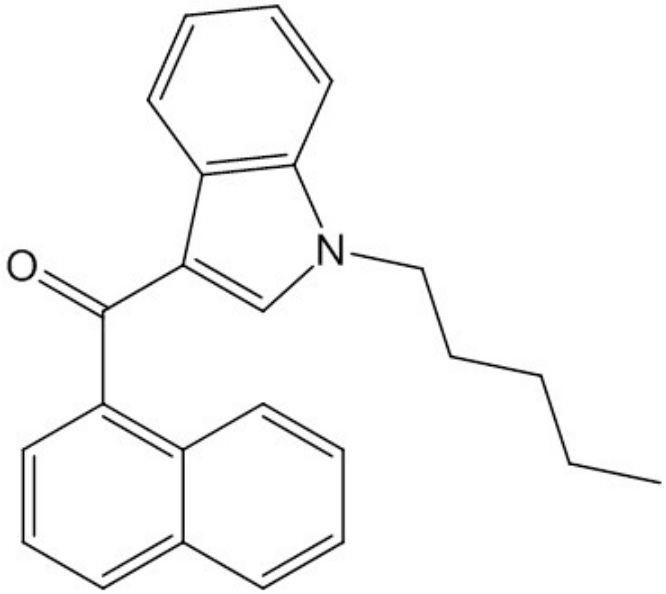

Figure 4.1. Structure of JWH-018.

CB2R with a K_i of 2.9 nM which is comparable to its affinity at the CB1R (Aung et al., 2000). Since little is known about the pharmacology and toxicity of JWH-018 and its metabolites in humans, research is needed to investigate the metabolism of JWH-018 and the effects of it and its pharmacologically active metabolites in the body.

JWH-018 undergoes extensive cytochrome P450-mediated phase I metabolism and redistribution into body fat (Poklis et al., 2012). Cytochrome P450s or CYPs are a superfamily of mono-oxygenases involved in the metabolism of a wide variety of endogenous and exogenous compounds (Ortiz de Montellano, 2005). Oxidized CYP metabolites can be subsequently glucuronidated by UDP-glucuronosyltransferases (Seely et al., 2012), as a result, the majority of JWH-018 metabolites are excreted as glucuronides in human urine (Chimalakonda et al., 2011a; Chimalakonda et al., 2011b), including the three major metabolites of JWH-018: the ω-OH, ω-1-OH, and ω-COOH (Chimalakonda et al., 2011b; ElSohly et al., 2011; Lapoint et al., 2011; Moran et al., 2011).

Using human liver microsomes, Chimalakonda and coworkers determined that CYP2C9 is responsible for the formation of the ω-OH and ω-1-OH metabolites of JWH-018, whereas CYP1A2 is responsible for the formation of the carboxylated metabolite (Chimalakonda et al., 2012). CYP2J2 is a P450 epoxygenase mainly expressed in the cardiovascular system, but it is also expressed in the intestines, lung, kidney, liver, brain, salivary ducts, stomach, and vascular smooth muscle cells (Enayetallah et al., 2004). Due to the cardiovascular side effects observed after exposure to JWH-018 in K2 products, the ability of the major cardiovascular P450, CYP2J2, to metabolize JWH-018 was investigated. Moreover, *in vitro* and *in vivo* animal studies utilizing rats were completed

to observe the metabolism of JWH-018 and its effects on heart rate and blood pressure. JWH-018 is normally administered via inhalation so that the lungs and heart are the first two organs to be exposed to the compound; however, there are some reports describing JWH-018 ingestion. In this situation, JWH-018 undergoes first pass metabolism by the intestine and liver. JWH-018 can be metabolized in the intestine and the metabolites and the remaining JWH-018 are absorbed into the portal vein and travel to the liver where additional metabolism occurs. After the remaining JWH-018 and its metabolites leave the liver, these compounds enter systemic circulation and can potentially cause several physiological effects, including those related to the cardiovascular system. As a result, the metabolism of JWH-018 by human intestine and liver microsomes was also investigated to determine the metabolite profiles.

Materials and Methods

Materials. AM251, ω-OH and ω-1-OH JWH-018 were purchased from Cayman Chemical (Ann Arbor, MI). JWH-018 was purchased from Ark Pharm, Inc. (Libertyville, IL). Rat hearts and livers were gifts from the lab of Dr. Margaret Gnegy (University of Michigan, Ann Arbor, MI). All other reagents were of the highest quality and were obtained from commercial sources.

Enzymes. The human CYP450 CYP2J2 cDNA was a gift from Dr. Rheem Totah (University of Washington, Seattle, WA). CYP2J2 and CYP450 reductase were expressed in *Escherichia coli* and purified as previously described (Hanna et al., 1998; Smith et al., 2008). Human intestine (Lot #s: 3077535; 05866) and liver (Lot #: 88114) microsomes were purchased from BD Biosciences (Woburn, MA).

Preparation of Microsomes from Rat Hearts and Livers. The preparation of microsomes was performed as described previously (Lin et al., 1998). Briefly, the hearts or livers of three Sprague Dawley rats were pooled, chopped, and subsequently homogenized using a Tissue Tearor (Biospec Product Inc.) in homogenization buffer (100 mM potassium phosphate buffer, pH 7.4, 1 mM EDTA, and 150 mM KCl). The homogenate was centrifuged at 10,000 *g* for 30 min and the supernatant was filtered through gauze to remove the fat. The supernatant was ultracentrifuged at 100,000 *g* for 75 min. The resulting pellet was resuspended using a glass pestle in a Dounce homogenizer in pyrophosphate buffer (100 mM tetrasodium pyrophosphate, pH 7.4 and 1 mM EDTA) to remove hemoglobin. The homogenate was centrifuged again at 100,000 *g* for 75 min and the resulting pellet was resuspended in suspension buffer (100 mM potassium phosphate buffer, pH 7.4, 1 mM EDTA, and 20% glycerol). Bovine serum albumin was used as the standard for the BCA Protein Assay (Pierce, Rockford, IL) which was used to determine the protein concentrations of the microsomes.

JWH-018 Metabolism Assays. *Recombinant Protein.* CYP2J2 was reconstituted with reductase (1:2) and L-α-dilauroyl-phosphocholine (DLPC) lipid on ice for 60 min as described previously (Snider et al., 2007; von Weymarn et al., 2004). The metabolism of JWH-018 was determined using incubation mixtures (0.25 mL) containing 100 mM potassium phosphate buffer (pH 7.4), catalase (22 μg), JWH-018 (5-50 μM), and reconstituted CYP2J2. The reactions were initiated by the addition of 1.2 mM of NADPH and allowed to continue for 15 min at 37°C.

Microsomal JWH-018 Metabolism Studies. Human intestinal microsomes (HIM), human liver microsomes (HLM), rat heart microsomes (RHM), or rat liver microsomes

(RLM) (0.8 mg/mL) were combined with 100 mM potassium phosphate buffer, pH 7.4, 3.3 mM $MgCl_2$ and 100 µM JWH-018 in a final volume of 250 µL. The reactions were initiated by the addition of 1.3 mM NADPH and allowed to continue for 20 (RLM), 30 (HIM and HLM), and 45 (RHM) min. Control reactions were performed in the absence of NADPH. Product formation was linear with respect to time and protein concentration under these conditions.

All reactions were terminated by the addition of 1 ml of ice cold ethyl acetate. After the addition of the internal standard, JWH-018-d_9, the samples were vortexed briefly and centrifuged at full speed using a desktop Eppendorf centrifuge for 15 min. The organic layer was dried down under a constant stream of nitrogen gas. The dried samples were resuspended in 100 µL of 50% acetonitrile and subjected to electrospray ionization-liquid chromatography/mass spectrometry (ESI-LC/MS) analysis. The standard curves for the metabolites used for the quantification and the determination of the K_M and k_{cat} values were determined by injecting various known amounts of authentic standards into the ESI-LC/MS for analysis.

ESI-LC/MS Analysis. Samples (10 µL) were injected onto a ZORBAX Eclipse XDB-C18 column (3.5 µm, 3 × 150 mm; Agilent Technologies, Santa Clara, CA) that was equilibrated with 50% solvent A (0.1% formic acid in water) and 50% solvent B (0.1% formic acid in acetonitrile). The metabolites were resolved using the following gradient: 0 to 20 min, 50% B; 20 to 21 min, 50 to 95% B; 21 to 35 min, 95% B. The flow rate was 0.3 ml/min. The column effluent was directed into the LCQ mass analyzer (Thermo Fisher Scientific). The ESI conditions were as follows: sheath gas, 90 arbitrary units; auxiliary gas, 30 arbitrary units; capillary temperature, 250°C; and spray voltage,

4.5 V. Data were acquired in positive ion mode for JWH-018 and its metabolites using the Xcalibur software package (Thermo Fisher Scientific) with one full scan from 300 to 500 mass/charge ratio (*m*/*z*) followed by one data-dependent scan of the most intense ion.

Animal Studies. *Animals.* Sprague-Dawley rats purchased from Harlan, Inc. (Indianapolis, IN) were housed in groups with a continuous availability of food and water. Housing and experimental rooms functioned on a 12 hr light/dark cycle at 21°C. The protocols used were approved by the University of Michigan University Committee on the Use and Care of Animals and satisfied the guidelines set forth by the NIH Guide for the Use of Laboratory Animals.

Surgical Procedures. The rats were fitted with telemetric transmitters (TA11PA-C40 or TL11M2-C50-PXT, Data Sciences International, Transoma Medical Inc., St. Paul, MN) using the anesthetics ketamine (90 mg/kg, i.p.) and xylazine (10 mg/kg, i.p.) in order to measure heart rate (HR) and mean arterial pressure (MAP) as previously described (Jutkiewicz et al., 2013). Briefly, the monitoring system consisted of implanted battery-operated transmitters, Physiotel receivers, the DSI Data Exchange Matrix, and the Dataquest A.R.T. system. The data collected by the receiver were stored on a computer. The transmitter was placed in a subcutaneous pocket between the skin and muscle on the abdominal side. A suture secured the subcutaneous catheter that extended from the base of the transmitter into the femoral artery 2-3 cm. The rats were allowed to recover at least seven days prior to experimentation.

Experimental Design. The caged rats were placed on top of the receivers and baseline data were recorded for at least one hour prior to the experiment to allow heart rate and mean arterial pressure to return to resting levels. To control for the responses to

the intraperitoneal (i.p.) injections and handling procedures used for these experiments, all rats were given a saline injection at least 30 min prior to the start of the experiment. All doses were administered i.p. in a volume of 1 mL/kg.

Data Analysis. The heart rate and blood pressure data were calculated using the Dataquest A.R.T. Gold Analysis 3.01 software. This program averaged the heart rate (HR) and mean arterial pressure (MAP) values for every 10 s. Those values were subsequently averaged for every minute. Individual rat data were then calculated as the percent change from resting HR or MAP. Nonlinear regression, two-way ANOVA, and unpaired *t* test with Welch's correction of the data were performed using GraphPad Prism 6 (GraphPad Software Inc., San Diego, CA; http://www.graphpad.com).

Results

Metabolism of JWH-018 by Human Recombinant CYP2J2. JWH-018 undergoes an extensive cytochrome P450-mediated phase I metabolism and redistribution into body fat (Poklis et al., 2012). Utilizing recombinant human proteins and human liver microsomes, Chimalakonda and others determined that CYP2C9 is primarily responsible for the formation of the ω-OH JWH-018 and ω-1-OH JWH-018 metabolite whereas, CYP1A2 is responsible for the formation of the carboxylated metabolite (Chimalakonda et al., 2012). CYP2J2 is a P450 epoxygenase mainly expressed in the cardiovascular system, but it is also expressed in the intestines, lung, kidney, liver, brain, salivary ducts, stomach, and vascular smooth muscle cells (Enayetallah et al., 2004). Due to the very significant cardiovascular side effects observed after exposure to JWH-018 in various K2

products, we investigated the ability of the major cardiovascular P450, CYP2J2, to metabolize JWH-018.

Figure 4.2 shows the ESI-LC/MS chromatogram for the metabolism of JWH-018 by purified human CYP2J2. The extracted ion chromatogram at *m/z* 358 at the bottom of the figure shows the two mono-oxygenated metabolites formed during JWH-018 metabolism by CYP2J2. Although several different mass-to-charge ratios were monitored including *m/z* 358, 374, and 390, only the two mono-oxygenated products were observed. At *m/z* 358, the N-(5-hydroxypentyl) (ω-OH) and the N-(4-hydroxypentyl) (ω-1-OH) metabolites of JWH-018 eluted after approximately 23 and 24 min, respectively. These were the only products observed for CYP2J2-catalyzed oxidation of JWH-018. The identities of the products were confirmed based on retention times and fragmentation patterns of commercially available standards (data not shown). Of the two products formed, the JWH-018 ω-1-OH metabolite was the major product formed.

Kinetic Studies on the Metabolism of JWH-018 by Human Recombinant CYP2J2. Although the metabolism of JWH-018 was previously shown by the lab of Dr. Jeffrey Moran (poster), this is the first investigation regarding the kinetics of this reaction. To determine the ability of CYP2J2 to metabolize JWH-018, the kinetic parameters, K_M and k_{cat}, were determined for the two hydroxylated products. The CYP2J2-catalyzed formation of the ω-OH and ω-1-OH products was linear with both the protein concentration and time used to determine the kinetic constants (data not shown). As shown in Figure 4.3, the formation of the JWH-018 ω-OH and ω-1-OH metabolites exhibited typical Michaelis-Menten kinetics with observed K_M values of 11 and 10 μM and k_{cat} values of 0.03 and 0.2 pmol/min/pmol of P450, respectively. The efficiency of

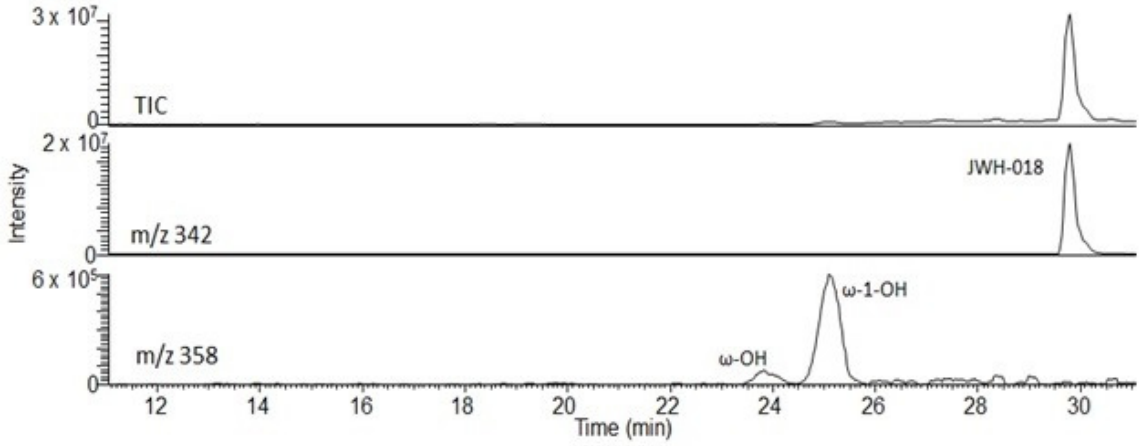

Figure 4.2. JWH-018 metabolism by recombinant CYP2J2. Purified CYP2J2 was reconstituted with reductase (1:2 ratio) in lipid (L-α-dilauroyl-phosphocholine) on ice for at least 60 min. This enzyme source (9 µL) was added to the incubation mixture (0.25 mL) containing 100 mM potassium phosphate buffer (pH 7.4), JWH-018 (50 µM), and catalase. Reactions were initiated by the addition of 1.2 mM NADPH and allowed to continue for 15 min at 37°C. The total ion chromatogram (TIC) shows the all the ions captured by the LC/MS (Top). The middle chromatogram shows the positive ion formed by the parent compound, JWH-018, at *m/z* 342 which eluted after 29.8 min. The extracted ion chromatogram observed at *m/z* 358, shows the monooxygenated product peaks which elute at approximately 23.2 and 24.4 min for JWH-018 ω-OH and JWH-018 ω-1-OH, respectively. The product identities were verified by comparing the retention times and fragmentation patterns of the products formed with their respective commercial standards.

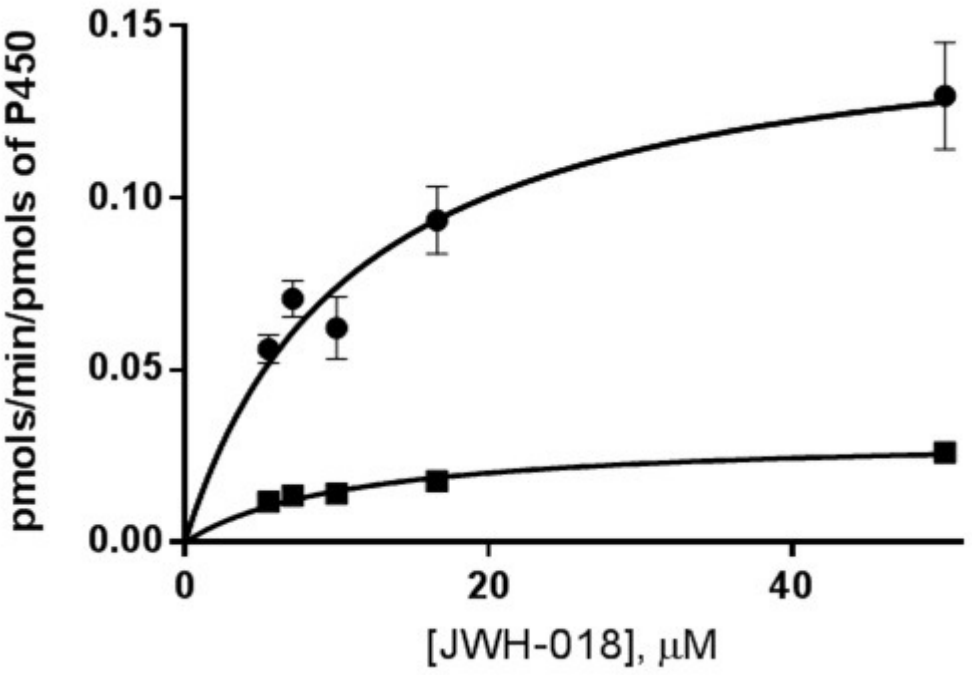

Figure 4.3. Kinetics for JWH-018 metabolism by purified CYP2J2. Several concentrations of JWH-018 (5-50 μM) were metabolized by purified CYP2J2 for 15 min at 37°C, as described in *Materials and Methods.* To determine the amount of product formed, a standard curve was constructed for the metabolites using commercially available standards. The two mono-oxygenated products formed were ω-1-OH (●) and ω-OH JWH-018 (■). The data are the average of three separate experiments performed in triplicate. Error bars represent SEM values.

CYP2J2 to convert JWH-018 to the ω-OH and ω-1-OH metabolites is 0.003 and 0.02 $\mu M^{-1}min^{-1}$, respectively.

The Effect of JWH-018 on Heart Rate and Blood Pressure in Rats. When the heart rate (HR) and mean arterial pressure (MAP) returned to resting levels after a control saline injection, the rats were injected with either vehicle (1:1:3-ethanol:alkamuls-EL620:sterile water) or the CB1R antagonist AM251 (10 mg/kg) as a pretreatment. After 30 min, the rats in those two groups were then injected with the vehicle or JWH-018 (3 mg/kg). The HRs and MAPs of these rats were monitored for three hours after the treatment dose. Figure 4.4 shows the data collected by telemetry in five minute intervals for the HR (Figure 4.4A) and the MAP (Figure 4.4B). Although JWH-018 seemed to have little to no effect on HR, it did cause a significant increase in the MAP. Pretreatment with AM251, the CB1R antagonist, partially blocked the increase in blood pressure caused by administration of JWH-018. However, about 20 min into the 30 min pretreatment, the HRs and MAPs of the rats returned to resting levels for the vehicle injected rats, but the HRs and MAPs for the rats pretreated with AM251 never decreased and were significantly different from vehicle-treated rats (data not shown). Inhibition of presynaptic CB1R in the cardiovascular system cause the release of neurotransmitters which subsequently increase heart rate and blood pressure.

Substrate Competition Between JWH-018 and Arachidonic Acid. CYP2J2 metabolizes arachidonic acid (AA) to yield four epoxides that have been shown to participate in the regulation of cardiovascular homeostasis (Roman, 2002). Since JWH-018 is also a substrate for CYP2J2, it is possible that JWH-018 interferes with AA metabolism contributing to the observed effects in the cardiovascular system. Figure 4.5

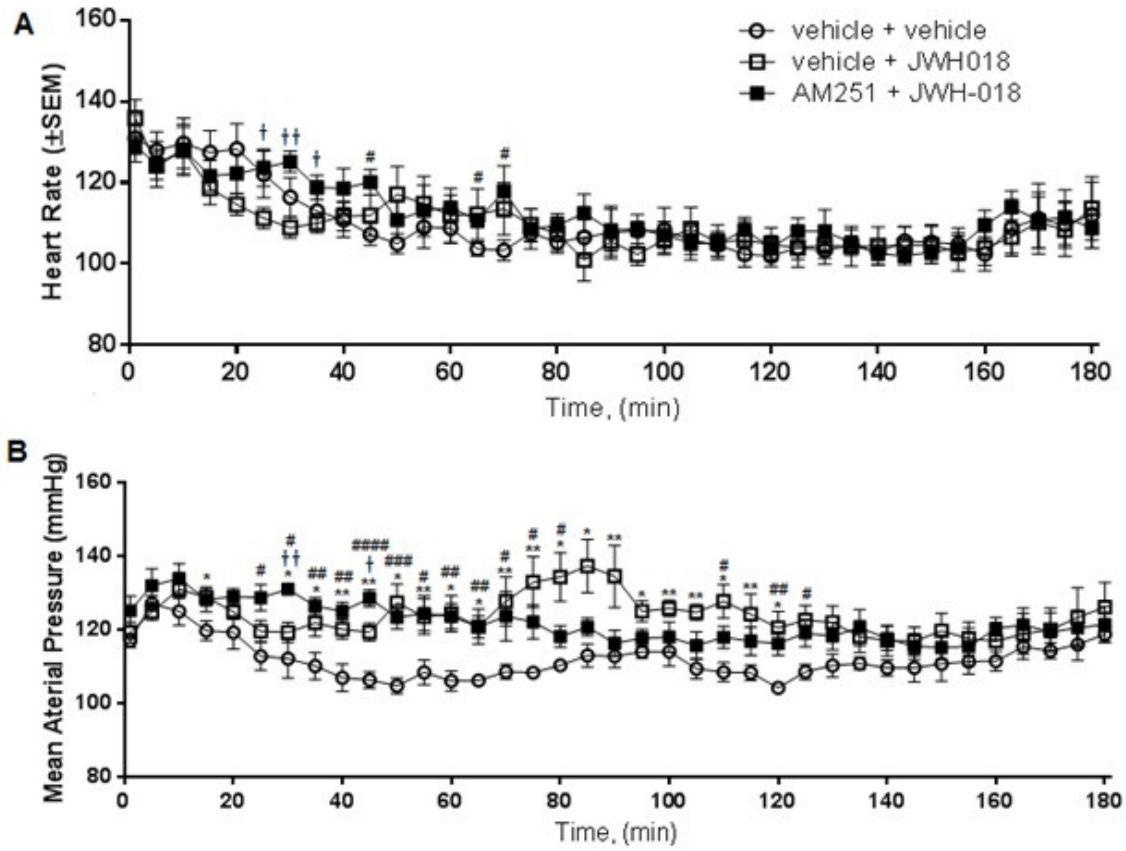

Figure 4.4. The effect of JWH-018 on heart rate and blood pressure in rats. Sprague-Dawley rats were given an intraperitoneal (i.p.) pretreatment injection of either vehicle or the CB1R antagonist, AM251 (10 mg/kg). After 30 min, the rats were administered an i.p. injection of vehicle (vehicle + vehicle, ○, n= 6); or 3 mg/kg dose of JWH-018 (vehicle + JWH-018, □, n= 6); or (AM251 + JWH-018, ■, n= 5). The HRs (A) and MAPs (B) of the rats were monitored via an implanted telemetry device as described in *Materials and Methods*. The values plotted on the graph represent mean ± SEM for all of the rats in each of the indicated test groups. Statistical significance was determined using the Holm-Sidak method. *, vehicle + vehicle vs. vehicle + JWH-018; #, vehicle + vehicle vs. AM251 + JWH-018; †, vehicle + JWH-018 vs. AM251 + JWH-018. #, $P < 0.05$; ##, $P < 0.01$; ###, $P < 0.001$; ####, $P < 0.0001$.

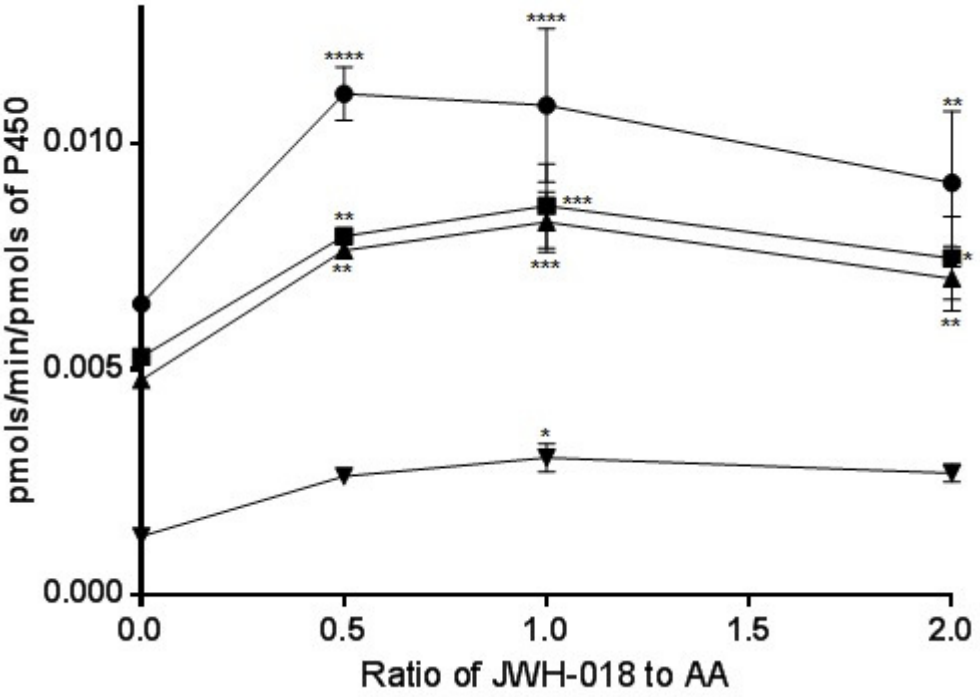

Figure 4.5. Competition between JWH-018 and AA for metabolism by CYP2J2. Recombinant CYP2J2 was reconstituted with reductase (1:2 ratio) and DLPC for 60 min on ice. AA (20 μM) was combined with JWH-018 (0, 10, 20, and 40 μM) for 30 min at 37°C, as described in *Materials and Methods.* The metabolites formed are: 14,15-EET (●); 11,12-EET (■); 8,9-EET (▲); 5,6-EET (▼). The data are the average of two separate experiments done in duplicate and the error bars represent SEM values. *, $P < 0.05$; **, $P < 0.01$; ***, $P < 0.001$; ****, $P < 0.0001$.

shows the effect of JWH-018 on the metabolism of AA by CYP2J2. Surprisingly, rather than causing inhibition of the metabolism of AA, the presence of JWH-018 significantly increased the production of three of the four epoxide metabolites, the 14,15-, 11,12-, and 8,9-EETs. It also caused a slight increase in the formation of 5,6-EET, but this increase only reached significant levels when there were equal amounts of JWH-018 and AA. The presence of AA had no effect on JWH-018 metabolism (data not shown).

The Metabolism of JWH-018 by Rat Heart and Liver Microsomes. In order to better understand the *in vivo* effects of JWH-018, the metabolism of JWH-018 was investigated utilizing rat heart and liver microsomes. Pooled heart and liver microsomes were prepared as described in *Materials and Methods* and used for metabolism studies of JWH-018. Several different extracted ion chromatograms were used for the analysis, including those at *m/z* 358, 374, and 390 corresponding to the mono-, di-, and trihydroxy metabolites, respectively. The mass-to-charge ratio that corresponds to the terminal carboxylated metabolite, *m/z* 372, was monitored as well. Figure 4.6 shows the total ion chromatogram (TIC) and the three different extracted ion chromatograms (*m/z* 338, 358, and 376) for the products formed by rat heart microsomes (RHM). Figure 4.7 shows the TIC and the extracted ion chromatograms for the products peaks at *m/z* values of 358, 372, 374, 376, and 392 formed by rat liver microsomes (RLM). RHM and RLM both formed products that were unique to their respective tissues, but some metabolites such as M4, M5, M6, M8, and M9 were formed by both heart and liver microsomes. The monohydroxylated metabolites were the major products formed by both RHM and RLM. The peak observed at *m/z* 338 (M3) was a major product formed by RHM; however, its formation by RLM was not NADPH-dependent (data not shown). The 1,2-diol products

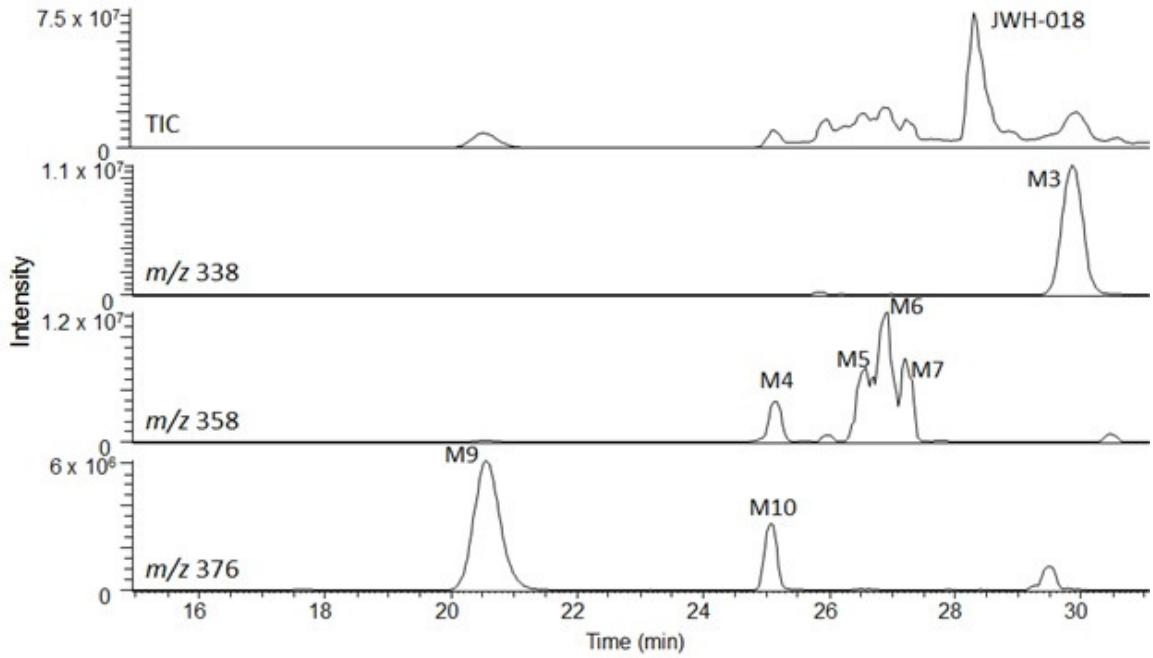

Figure 4.6. JWH-018 metabolism by rat heart microsomes. Rat heart microsomal protein (0.8 mg/mL) was combined with JWH-018 (100 µM) in 0.1 M phosphate buffer containing $MgCl_2$. After the addition of NADPH (1.3 mM) the reaction was incubated for 45 min at 37°C with shaking. The reaction was terminated and the samples were prepared as described in *Materials and Methods*. Based on previous studies, the metabolite M3 is probably a 1,2-diol formed by the addition of two hydroxyl groups with the loss of the carbon chain, see Figure 4.8 (Zhang et al., 2006). While the identity of M4 is unknown, M5-M7 probably corresponds to hydroxyl substitutions on the indole ring of JWH-018. M9 and M10 are most likely the diols of hydrolyzed epoxides on the naphthalene rings (Figure 4.8).

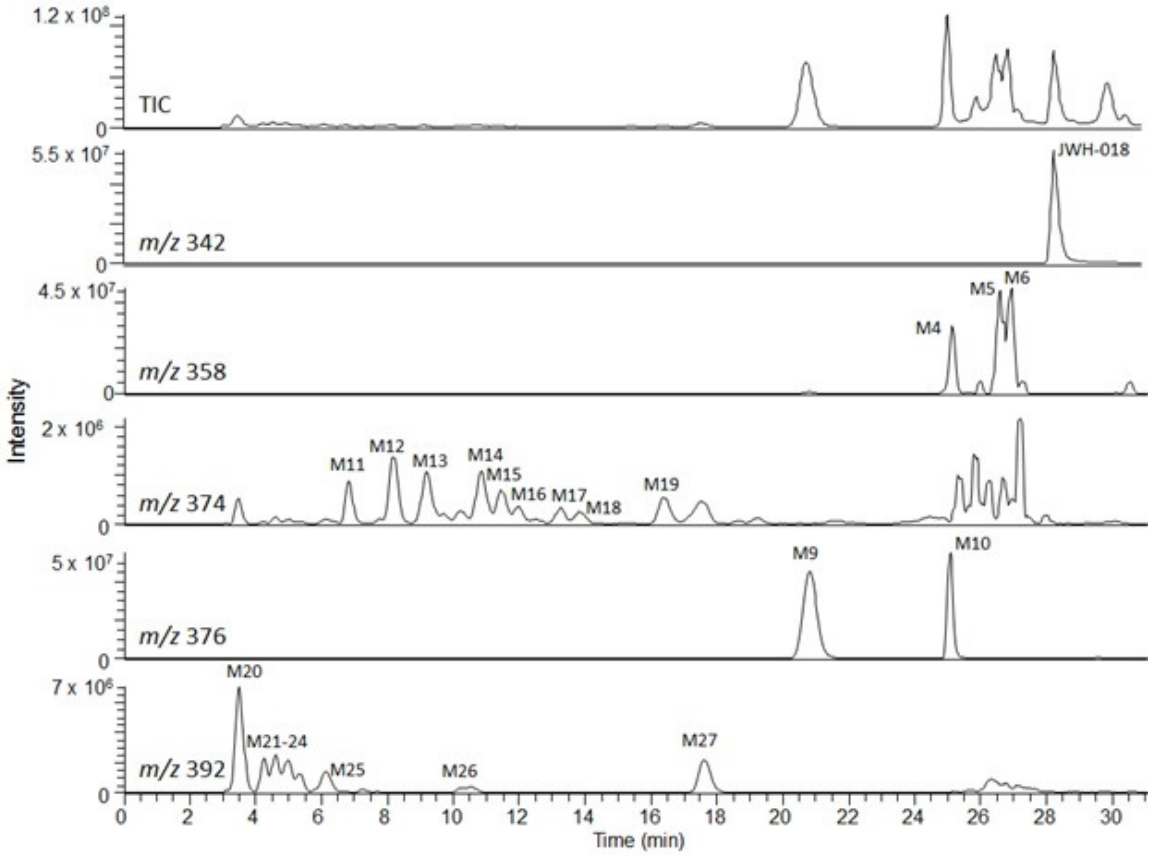

Figure 4.7. JWH-018 metabolism by rat liver microsomes. Rat liver microsomal protein (0.8 mg/mL) was incubated with JWH-018 (100 μM) for 20 min at 37°C under the standard reaction conditions stated previously in *Materials and Methods*. The reaction was performed and the metabolites were extracted as previously described in *Materials and Methods*. About 22 different metabolites of JWH-018 were formed by RLM. Three monohydroxylated (*m/z* 358) and nine dihydroxylated (*m/z* 374) products were formed. The products observed at *m/z* 376 are 1,2-diols and the peaks observed at *m/z* 392 are 1,2-diols with an additional hydroxyl group on the indole ring or the carbon side chain (Wintermeyer et al., 2010). See Figure 4.8 for potential structures of JWH-018 metabolites.

observed at *m/z* 376 (M9 and M10), were formed by both RHM and RLM. These metabolites were minor products with RHM whereas with RLM the amount of these products formed corresponded to a major portion of the total metabolites produced. Postulated structures for these unidentified products are shown in Figure 4.8.

JWH-018 Metabolism by Human Liver Microsomes and Human Intestine Microsomes. In order to better understand any possible correlations with respect to JWH-018 metabolism between rats and humans, human liver microsomes (HLM) were also used to compare the product profiles to those seen in RLM. Metabolites formed in the intestine can be absorbed by the intestinal wall and enter the systemic circulation via the portal vein (Gao et al., 2013). This may be why JWH-018 is known to cause severe toxicities after ingestion (Lapoint et al., 2011). As a result, JWH-018 metabolism by human intestinal microsomes (HIM) was investigated as well. Because of the large amount of diols formed by RHM and RLM, metabolites with *m/z* values at 376 were monitored for product peak formation. Figure 4.9 shows the chromatograms for the products formed by HLM metabolism of JWH-018 and Figure 4.10 shows the chromatograms for ESI-LC/MS analysis of the metabolism of JWH-018 by HIM. In addition, the product profiles for the HIM and the HLM were different, the intestinal microsomes catalyzed less product formation from JWH-018 when compared to the liver microsomes when normalized for the amount of the microsomal proteins used for the reactions, but this decrease in activity is in accordance with other reports (Chhabra et al. 1974).

Human Recombinant CYP2C9 Metabolism of JWH-018. Due to its expression levels in the liver and its efficiency for the metabolism of JWH-018, CYP2C9 was

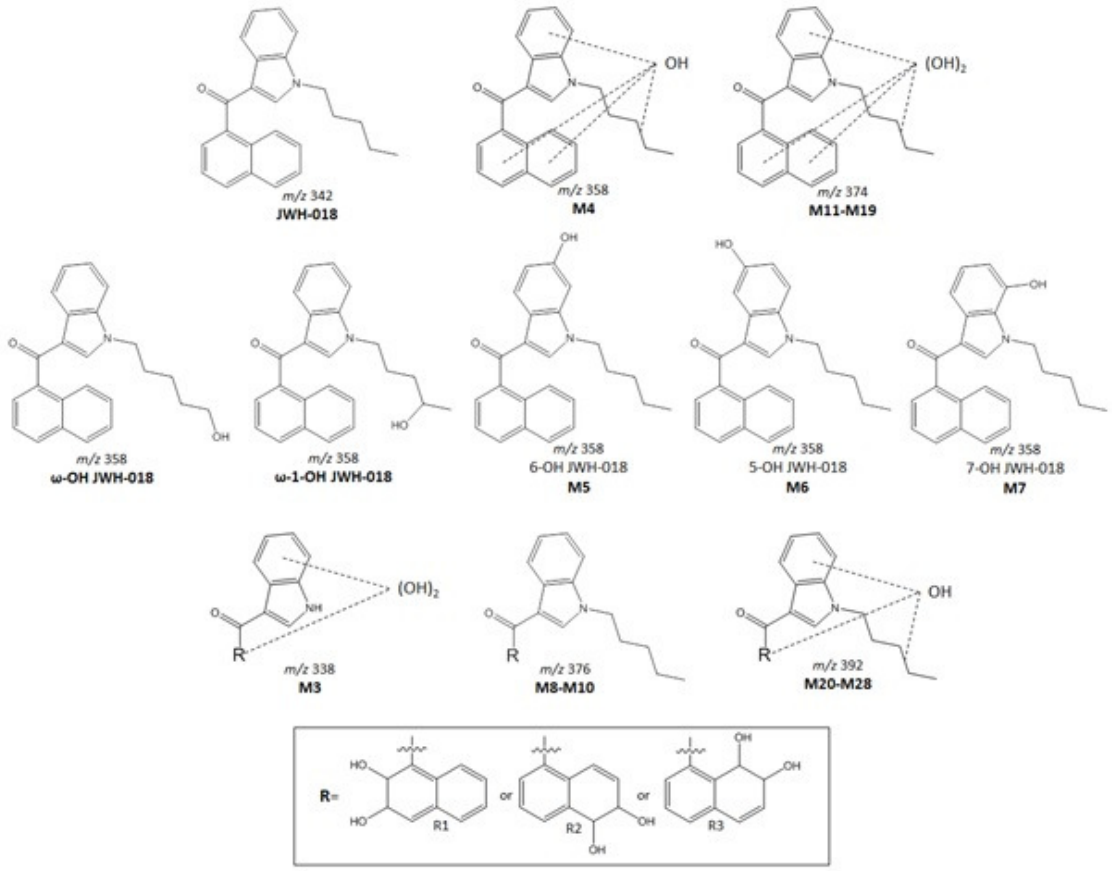

Figure 4.8. Postulated structures for the metabolites formed from JWH-018. The top row shows the structures of the parent compound JWH-018 along with potential sites for oxygenation. The M4 product is mono-oxygenated and could have a hydroxyl group at any of the suggested positions except for on the indole ring or at the ω and ω-1 positions of the carbon chain because these products have already been identified. The M11-M19 products are di-oxygenated and can have hydroxyl groups at any combination of two hydroxylation sites. The middle row shows the mono-oxygenated metabolites with confirmed structural identities for ω-OH and ω-1-OH JWH-018 metabolites. The other confirmed structures are the 5-, 6-, and 7-OH indole JWH-018 metabolites corresponding to M6, M5, and M7, respectively. The bottom row shows the hypothesized structures and potential hydroxylation sites for the products containing 1,2-diols (M3, M8-M10, and M20-M28). Although there are four potential sites for epoxide formation and subsequent hydrolysis to diols, only three products were identified, M8, M9, and M10. The three likely positions for the 1,2-diols are shown in box. Diol formation at the fourth potential position is probably limited by steric effects (adapted from Wintermeyer et al., 2010; Zhang et al., 2006).

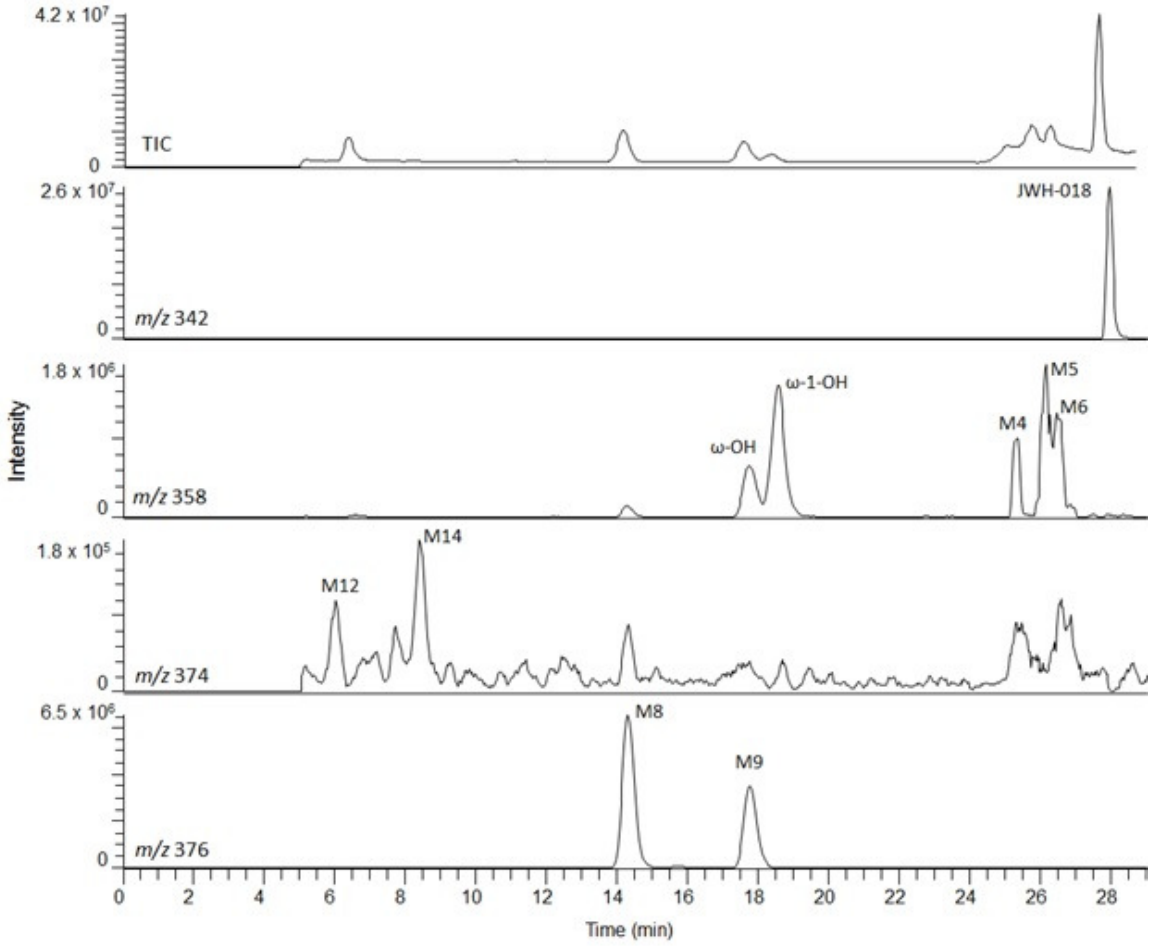

Figure 4.9. JWH-018 metabolism by human liver microsomes. To determine the products formed by the metabolism of JWH-018 by the liver, HLM protein (80 µg) was incubated with JWH-018 (20 µM) in phosphate buffer, pH 7.4. After the addition of NADPH, the reaction was incubated with shaking for 30 min at 37°C. The reaction was stopped with ethyl acetate, extracted and prepared for LC/MS analysis as stated in *Materials and Methods.* The ω-OH and the ω-1-OH metabolite eluted after 17.4 and 18.6 min, respectively at *m/z* 358. Other metabolites observed at *m/z* 358 are the unidentified M4 (25.3 min) and some unresolved peaks designated as M5 and M6 that eluted after 26 min, most likely corresponding to the JWH-018 6- and 5-hydroxyindole metabolites, respectively, based on the elution times of commercial standards. At *m/z* 374, there were two peaks representative of a metabolite with two separate hydroxylation sites, M12 (6 min) and M14 (8.4 min). The extracted ion chromatogram at *m/z* 376 contained the major diol metabolites, M8: (14.3 min) and M9 (17.8 min). See Figure 4.8 for metabolite structures.

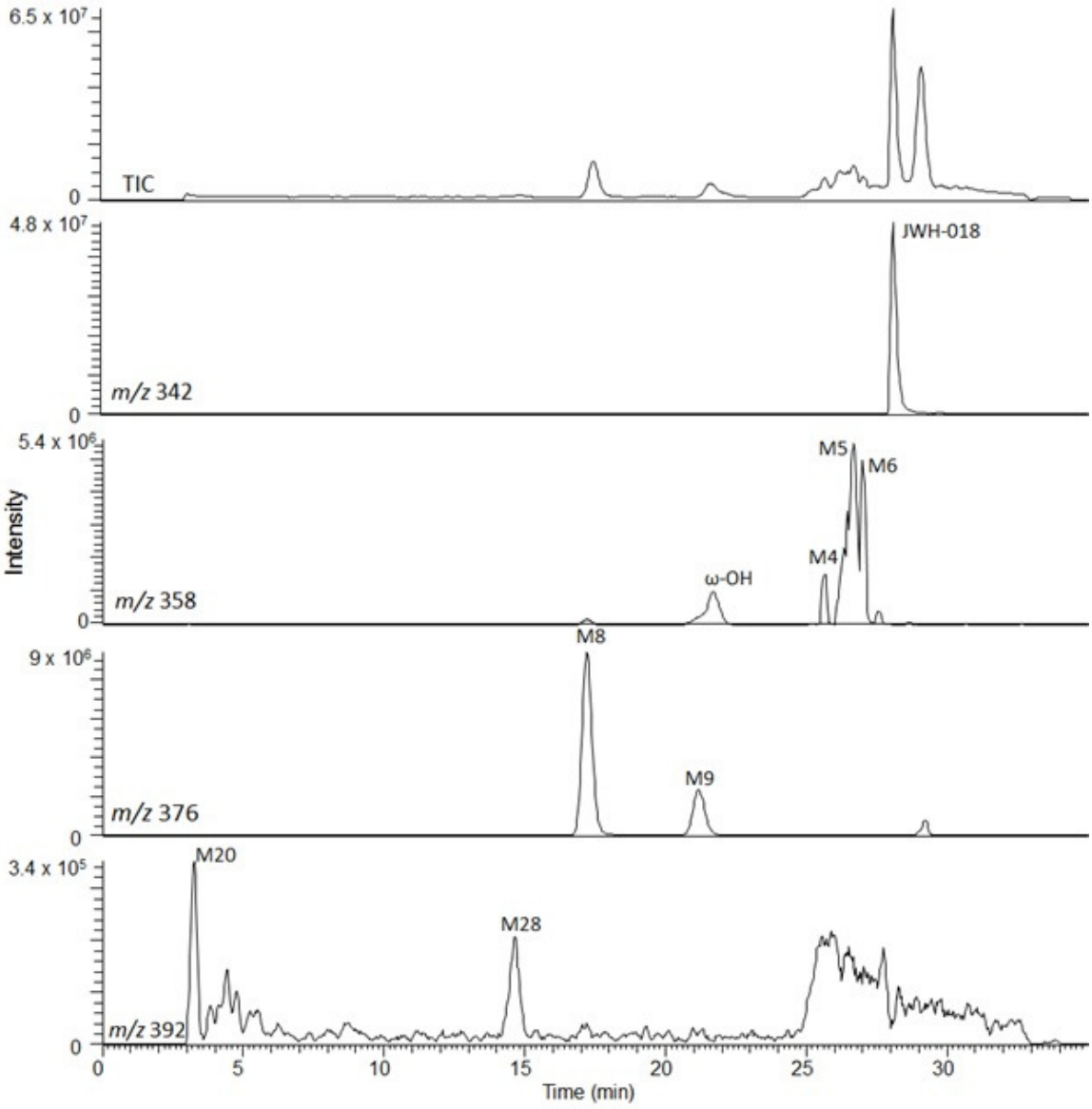

Figure 4.10. JWH-018 metabolism by human intestine microsomes. To identify the metabolites formed byJWH-018 metabolism in the intestine, HIM protein (200 µg) was incubated with JWH-018 (100 µM) in 100 mM of phosphate buffer, pH 7.4. NADPH was added and the reaction was incubated for 30 min at 37°C with shaking. The samples were prepared for ESI-LC/MS as previously described in *Materials and Methods.* The extracted ion chromatogram for products with *m/z* 358 exhibited several metabolite peaks: the ω-OH metabolite (21 min), M4 (25 min), and a jagged mass of peaks M5 and M6 that are representative of 6- and 5-hydroxylation on the indole ring of JWH-018 (c. 26 min), respectively. At *m/z* 376, M8 (17 min) and M9 (21 min), the 1,2-diols were the major metabolites formed. The metabolites M20 (3 min) and M28 (14 min) observed at *m/z* 392 correspond to hydroxylated diols. See Figure 4.8.

previously reported to be one of the major P450s involved in JWH-018 metabolism in the liver (Chimalakonda et al., 2012). As a result, its ability to catalyze the metabolism of JWH-018 was investigated and its efficiency was compared to that of CYP2J2. The ESI-LC/MS chromatograms of the products formed (Figure 4.11) showed that CYP2C9-mediated metabolism of JWH-018 produced four products. Three products are seen in the extracted ion chromatogram at *m/z* 358 representing the ω-OH and ω-1-OH metabolites of JWH-018 which eluted after approximately 23 and 24 min, respectively, and a third peak eluting at about 27 min possibly corresponding to M4 or a hydroxylation on the indole ring. Different from CYP2J2 metabolism, the major product formed by CYP2C9-catalyzed metabolism of JWH-018 was the ω-OH metabolite. Moreover, recombinant CYP2C9 also catalyzed the formation of M8 which has an *m/z* of 376 and eluted after 19 min, but metabolites M9 and M10 were not formed.

The Michaelis-Menton kinetic curves for the formation of the ω-OH and ω-1-OH metabolites of JWH-018 by CYP2C9 can be seen in Figure 4.12. The K_M, k_{cat}, and k_{cat}/K_M values for CYP2C9 metabolism of JWH-018 were calculated form these data and are presented in Table 4.1. The data for CYP2J2 are also provided for comparison. It can be seen that CYP2C9 is better at metabolizing JWH-018 than CYP2J2.

Discussion

The use of K2 has been linked to numerous deaths and emergency room visits in the United States alone (Lapoint et al., 2011; Pant et al., 2012; Simmons et al., 2011a; Simmons et al., 2011b). Due to increasing evidence that JWH-018 is becoming a major

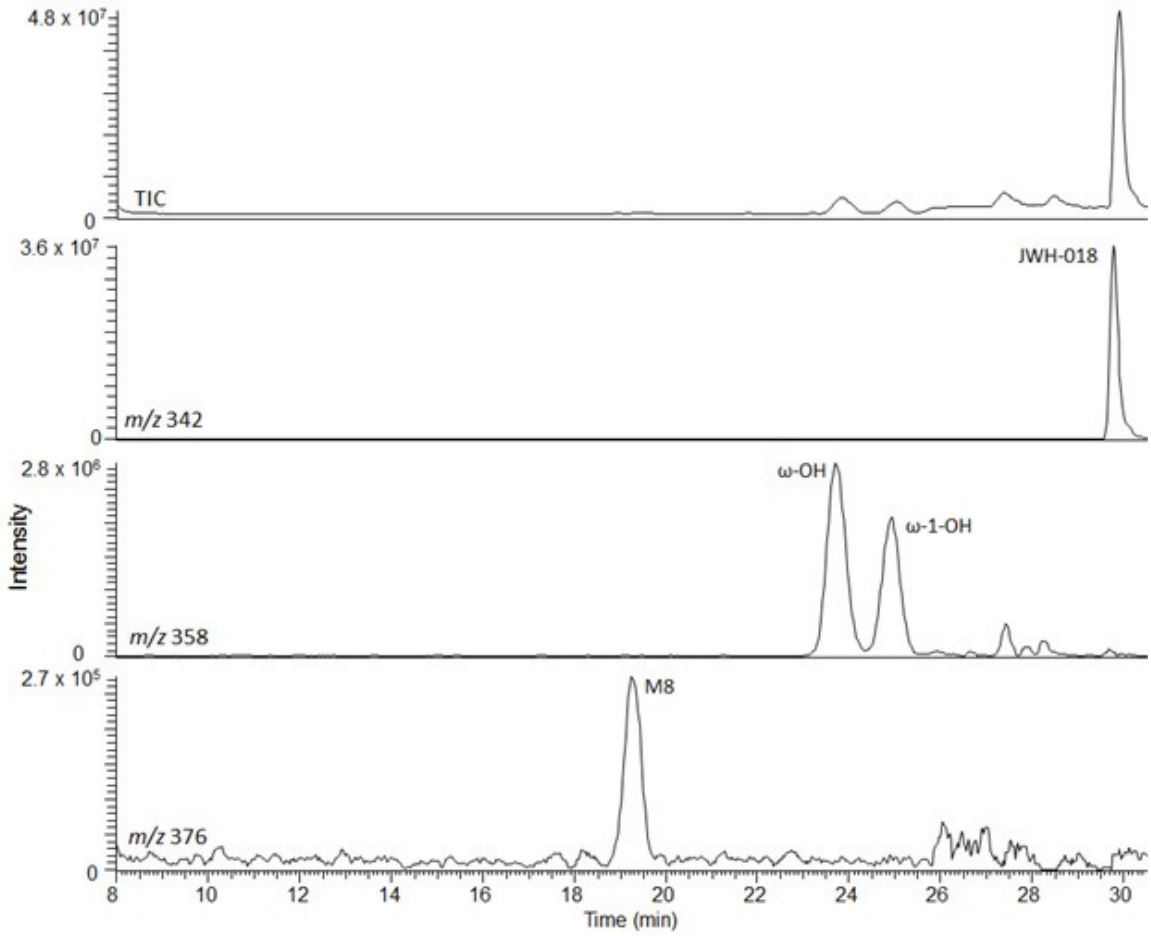

Figure 4.11. JWH-018 metabolism by recombinant CYP2C9. Purified CYP2C9 was reconstituted with reductase and cytochrome b_5 (1:2:1 ratio) in lipid (L-α-dilauroyl-phosphocholine) on ice for at least 30 min. This enzyme source (9 µL) was then added to the incubation mixture (0.25 mL) containing 100 mM potassium phosphate buffer (pH 7.4), JWH-018 (25 µM), and catalase. The reaction was initiated by the addition of 1.2 mM of NADPH and allowed to continue for 15 min at 37°C. The reaction was stopped and sample extraction performed as described in *Materials and Methods*. The second chromatogram shows the parent ion which eluted after 29.8 min at *m/z* 342. The extracted ion chromatogram observed at *m/z* 358 shows monooxygenated product peaks which elute at approximately 23.7, 24.9, and 27.4 min corresponding to JWH-018 ω-OH, JWH-018 ω-1-OH, and an unknown metabolite, respectively. An additional unknown resolved diol metabolite (M8) eluted after 19.2 min with an *m/z* values of 376, see Figure 4.8 for potential structure. Product identity was verified by comparing the retention times and fragmentation patterns of the products formed with their respective commercial standards.

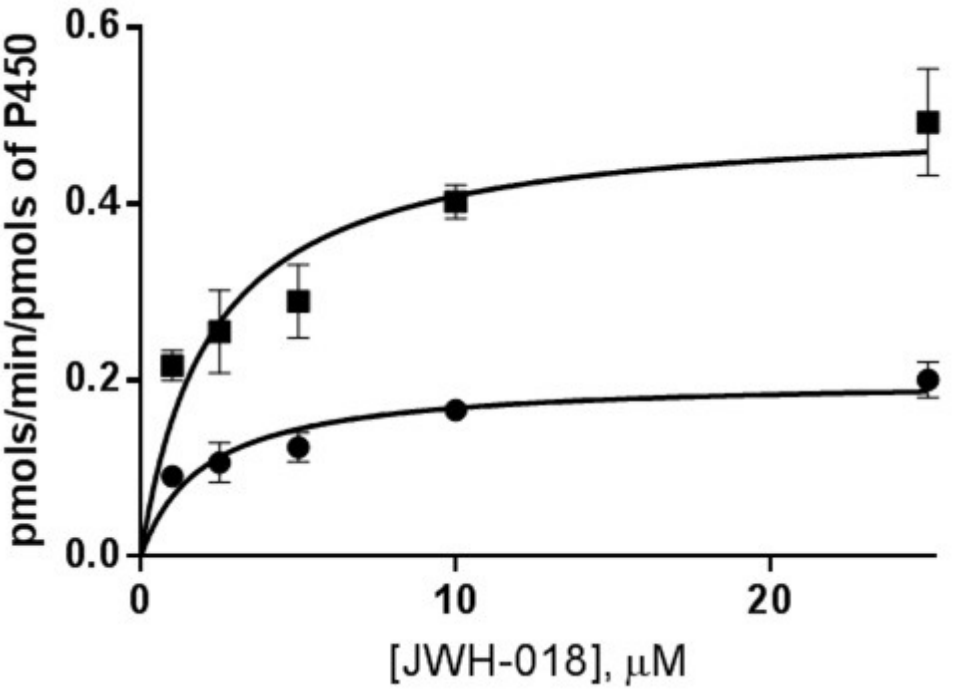

Figure 4.12. Kinetic analysis for the metabolism of JWH-018 by purified CYP2C9. Varying amounts of JWH-018 (1-25 μM) were added to the reaction mixtures containing rCYP2C9 (25 pmol) and the standard reagents required for the reconstitution mixture. After adding NADPH, the reaction mixture was incubated for 15 min at 37°C with shaking. The reaction conditions and sample preparation were performed as described in *Materials and Methods.* The graph shows the kinetic curves for the ω-1-OH (●) and ω-OH (■) JWH-018 metabolites. The data points represent the mean ± SEM (n = 3).

	K_M (μM)	k_{cat} (pmol/min/pmol of P450)	k_{cat}/K_M ($\mu M^{-1}min^{-1}$)
CYP2J2			
ω-1-OH	10 ± 3	0.2 ± 0.02	0.02 ± 0.007
ω-OH	11 ± 3	0.03 ± 0.003	0.003 ± 0.001
CYP2C9			
ω-1-OH	2 ± 0.5	0.2 ± 0.01	0.1 ± 0.02
ω-OH	2 ± 0.6	0.5 ± 0.04	0.25 ± 0.07
CYP1A2			
ω-1-OH	4.7 ± 0.49	1.438 ± 0.032	0.306 ± 0.065
ω-OH	5.3 ± 0.74	0.833 ± 0.025	0.16 ± 0.034
CYP2C19			
ω-1-OH	106	5.157	0.0487
ω-OH	82	0.535	0.00652
CYP2D6			
ω-1-OH	3.2 ± 0.7	0.043 ± 0.002	0.013 ± 0.0029
ω-OH	2.8 ± 0.52	0.026 ± 0.00	0.0093 ± 0.001

Table 4.1. . Comparison of Kinetic Constants for CYP2J2 and CYP2C9. Kinetic parameters were calculated from the data in Figures 4.3 (CYP2J2) and 4.12 (CYP2C9). Numerical values represent the mean ± SEM (CYP2J2, $n = 9$; CYP2C9, $n = 3$). Data for CYP1A2, CYP2C19, and CYP2D6 adapted from Chimalakonda et al. (2012).

drug of abuse in the U.S. (Ginsburg et al., 2012; Gunderson et al., 2012; Seely et al., 2011), it is important to study the metabolism of this drug in order to understand the metabolism and toxicology of this compound. Most reports indicate that inhalation of SCs produce side effects similar to marijuana including an alteration in mood, increased pulse rate, dry mouth and red eyes to name a few (Auwarter et al., 2009; Pant et al., 2012). Some adverse side effects associated with SC usage that are atypical for marijuana usage include hypertension, nausea, vomiting, and hyperventilation (Auwarter et al., 2009; Gunderson et al., 2012; Pant et al., 2012). Serious central nervous system effects include loss of consciousness, confusion, agitation, seizures, and psychosis (Every-Palmer, 2011; Peglow et al., 2012; Simmons et al., 2011a; Simmons et al., 2011b). One suicide has been reported due to intolerable anxiety after K2 ingestion (Pant et al., 2012). Cardiovascular effects associated with synthetic cannabinoid toxicity include supraventricular tachycardia and myocardial infarction (Mir et al., 2011; Simmons et al., 2011a).

Several JWH-018 metabolites have been shown to retain their affinities and activities for the cannabinoid receptors *in vitro* and *in vivo*. (Brents et al., 2011; Chimalakonda et al., 2012; Rajasekaran et al., 2013). While the parent compound, JWH-018, is an extremely potent agonist at the CB1R (K_i = 1.3 nM), its ω-OH and ω-1-OH metabolites also have good affinities at this receptor with K_i values of 35 nM and 15.4 nM, respectively (Chimalakonda et al., 2012). In addition, all three compounds induce G-protein activation with equal or greater efficacy than Δ^9-THC (Brents et al., 2011; Chimalakonda et al., 2012). Rajasekaran and associates studied the affinity of 4-, 5-, and 6-hydroxyindole JWH-018 metabolites, the JWH-018 *N*-pentanoic acid metabolite (ω-

COOH), and the ω-OH and the ω-1-OH JWH-018 metabolites for the CB2R (Rajasekaran et al., 2013). They reported that all of the metabolites, with the exception of the carboxylic acid, bind to the CB2R with K_i values ranging from 20 to 115 nM (Rajasekaran et al., 2013). Moreover, these metabolites showed activities ranging from partial to full agonists for the CB2R because they activate associated G-proteins and inhibit adenylyl cyclase activity (Rajasekaran et al., 2013). Due to the organ specific expression of the cannabinoid receptors and the ability of the parent and its mono-oxygenated metabolites to activate both cannabinoid receptors, it is important to investigate the metabolism of JWH-018 in tissues that exhibit high expression of a particular CYP compared to other P450s. CYP2J2 is the most abundant P450 in the human heart (Michaud et al., 2010; Wu et al., 1996). It is likely that the main route of JWH-018 administration is inhalation of smoke. As a result, it would not undergo traditional first pass metabolism in the intestine and liver, but would enter the circulation through the lungs and then circulate to the heart. Michaud et al. (2010) reported that cardiomyocytes can participate in drug metabolism and that cardiovascular CYPs are responsible for the clearance of drugs from the heart (Michaud et al., 2010). Since CYP2J2 is expressed in the human lung and is the most abundant P450 expressed in the human heart (Wu et al., 1996; Zeldin et al., 1996), it is important to investigate the ability of members of the CYP2J family to catalyze the metabolism of the SC of abuse, JWH-018.

In the reconstituted system, recombinant CYP2J2 metabolized JWH-018 primarily to give the ω-1-OH metabolite with the concomitant formation of a small amount of the ω-OH product. Purified CYP2C9 metabolized JWH-018 to give the same

two metabolites as CYP2J2, but the metabolite profile was extremely different. The ratios of ω-OH to ω-1-OH for CYP2C9 and CYP2J2 were 2.5:1 and 1:5, respectively. Although the k_{cat} values for the formation of the ω-1-OH metabolite of JWH-018 were the same for the CYP2J2 and CYP2C9 catalyzed reactions, CYP2C9 was approximately five times more efficient than CYP2J2 at catalyzing the formation of the ω-1-OH JWH-018 metabolite and 83 times more efficient at forming the ω-OH JWH-018 metabolite based on the k_{cat}/K_M values. When discussing purified protein, the order of efficiency goes from CYP1A2 > CYP2C9 > CYP2C19 > CYP2J2 > CYP2D6. Interestingly, we found that the addition of JWH-018, rather than acting as a competitive inhibitor, significantly increased the CYP2J2-catalyzed metabolism of AA, its endogenous substrate, leading to the formation of all four EETs, especially at equimolar ratios. Although the ratios of JWH-018 to AA will probably never reach equimolar ratios *in vivo*, a ratio of 0.5 to 1 still significantly increased the formation of 8,9-, 11,12-, and 14,15-EETs. It is unlikely that an increase in EET formation during exposure to JWH-018 will cause an increase in blood pressure, but a decrease in circulatory resistance caused by EET-induced vasodilation might possibly trigger baroreceptor activation.

Administration of JWH-018 to rats had little to no effect on HR; however, it did cause a significant increase in MAP compared to the vehicle control. Because the CB1R antagonist AM251 partially blocked the increase in blood pressure elicited by JWH-018 administration, these studies suggest the involvement of the CB1 receptor in altering the MAP in response to JWH-018. Moreover, during the 30 min pretreatment with AM251 there was a significant increase in HR and MAP when compared to the vehicle pretreatment. Activation of presynaptic CB1 receptors is known to inhibit noradrenaline

release resulting in a decrease in HR and MAP (Niederhoffer et al., 2003). This is in agreement with what we observed during pretreatment of the rats with AM251. However, our results also suggest that JWH-018 may cause some of the increase in MAP independent of CB1 receptor activation since pretreatment of the rats with AM251 only partially blocked the decrease in blood pressure. It is unlikely that JWH-018 is acting at the CB2 receptor because its activation is usually devoid of cardiovascular effects, but this area remains largely unexplored (Pacher and Mechoulam, 2011).

Several reports describe an increase in blood pressure after smoking marijuana which can be attributed to centrally mediated effects of CB1 receptor activation (Rudz et al., 2012). This may explain the increase in MAP after JWH-018 administration since centrally mediated effects, which are opposite of the peripheral effects of cannabinoids, override the peripherally mediated effects (Rudz et al., 2012). Another possibility could be that JWH-018 or one of its metabolites act as antagonists at either PPARγ or PPARδ to increase blood pressure. It has been shown that agonists of either of these receptors can decrease blood pressure (Cheang et al., 2013; Walker et al., 1999; Zarzuelo et al., 2011). As such, it is important to understand the metabolism of JWH-018 in order to identify the compound responsible for the adverse cardiovascular effects.

Several product peaks were observed at *m/z* 358 following metabolism by human and rat microsomes. The ω-OH and ω-1-OH JWH-018 metabolites were only observed in human intestine and liver microsomal samples; however, the ω-1-OH JWH-018 metabolite was only observed from certain lots of HIM (data not shown). The HIM used in these experiments were purchased from BD Biosciences and two separate lots were

used. Microsomal protein from Lot # 05886 formed the ω-1-OH metabolite, while the HIM from Lot # 3077535 did not (data not shown).

The M4, M5, and M6 metabolites were observed in all samples following metabolism by human and rat microsomes, whereas the M7 metabolite was only seen in RHM preparations. The product peaks M5, M6, and M7 are likely to correspond to 6-, 5-, and 7-hydroxyindole metabolites of JWH-018, respectively, based on the elution times of the commercially available standards. A reference standard compound was not commercially available for the M4 metabolite. This product could either have a hydroxyl group on the carbon side chain at a position other than the ω or the ω-1 carbon or it could be on the naphthyl group (Figure 4.8).

The possible carboxylic acid metabolite, which would be observed at *m/z* 372, could not be detected in any of the preparations. Two peaks (M12 and M14) were identified at *m/z* 374 in the human liver microsomal samples, but nine separate peaks with *m/z* values of 374 were observed in RLM preparations corresponding to M11-M19. Because no standards are available, these metabolites could not be positively identified. Based on their molecular weights and potential substitution sites, these metabolites are probably dihydroxylated metabolites containing two hydroxyl groups on the indole ring, the naphthalene group, and/or the carbon side chain (Figure 4.8) (Wintermeyer et al., 2010; Zhang et al., 2006).

The peaks present in the extracted ion chromatograms with *m/z* values of 376 suggest the formation of dihydroxylated products originating from epoxides. Recombinant CYP2C9 formed M8 only, while the microsomes showed the formation of three different diol structures (M8, M9 and M10). Two compounds fitting this description

have been extracted from urine samples of subjects who smoked JWH-018 (Sobolevsky et al., 2010). Likewise, phase I metabolism studies of JWH-018 by HLM conducted by Wintermeyer and coworkers demonstrated the formation of these two metabolites (Wintermeyer et al., 2010). Moreover, the metabolism of two other SCs, JWH-015 and WIN55212-2, showed the formation of only two reduced 1,2-diols even though there are four possibilities for the dihydroxylation of the naphthyl ring (Zhang et al., 2006; Zhang et al., 2002). These diols were then further hydroxylated to give several other metabolites which could be observed at *m/z* 392 (Wintermeyer et al., 2010). The ability of these products to form *in vivo* is likely since M20-M28 were formed in the HIM and/or the RLM. Likewise, the M3 metabolite isolated from RHM that was observed at *m/z* 338, probably originated from a 1,2-diol that lost its carbon side chain in a rearrangement and was subsequently dihydroxylated on the indole ring and/or the naphthalene group (Figure 4.8).

In conclusion, JWH-018 was metabolized by CYP2J2 to two metabolites that were hydroxylated on the side chain with the ω-1-hydroxylated compound as the major metabolite. In human intestine and liver microsomes, all products observed at *m/z* values of 358 and 376 were formed in large quantities and could be considered major products as opposed to the minor products observed at *m/z* 374 and 392 for the liver and intestinal microsomes, respectively. For incubations with RHM, the metabolites observed at *m/z* 358 and 338 were formed in the highest amounts while the diol products at *m/z* 376 were formed to lesser extinct. However, in RLM the 1,2-diols (*m/z* 376) were a major product along with the mono-oxygenated metabolites observed at *m/z* 358. Although there was substantial formation of the metabolites having *m/z* values at 374 and 392, it was still

relatively less than the products observed at *m/z* 358 and 376. Because the rats experienced some of the same cardiovascular side effects as humans, these effects may be caused by the same compounds. It is possible that JWH-018 is responsible for these effects but major metabolites formed by RLM and HLM including the diols observed at *m/z* 376 in addition to M4, M5, and M6 can potentially be responsible as well. The potential targets and activities of the most of the mono-oxygenated products have been previously studied (Brents et al., 2011; Chimalakonda et al., 2012), but the receptor targets and the effects of the 1,2-diols (*m/z* 376), the other major metabolites, have not. It is important to determine whether these diols and their secondary metabolites (e.g. compounds with *m/z* values at 338 and 392) bind to the cannabinoid receptors or another receptor family with an appreciable affinity and efficacy. It is possible that the adverse effects associated with the use of SCs are mediated by the parent, one or more metabolites, or a synergistic interaction between the metabolites and the parent compound. Combining two or more SCs has been reported to result in synergistic effects (Brents et al., 2013). Moreover, although the one biologically active metabolite of Δ^9-THC exhibits less affinity for the CB1R (Kochanowski and Kala, 2005), this is not the case for synthetic cannabinoid metabolites which can contribute to the effects of the parent synthetic compounds (Brents et al., 2011; Chimalakonda et al., 2012; Rajasekaran et al., 2013).

References

Atwood, B.K., Huffman, J., Straiker, A., and Mackie, K. (2010). JWH018, a common constituent of 'Spice' herbal blends, is a potent and efficacious cannabinoid CB receptor agonist. Br J Pharmacol *160*, 585-593.

Aung, M.M., Griffin, G., Huffman, J.W., Wu, M., Keel, C., Yang, B., Showalter, V.M., Abood, M.E., and Martin, B.R. (2000). Influence of the N-1 alkyl chain length of cannabimimetic indoles upon CB(1) and CB(2) receptor binding. Drug Alcohol Depend *60*, 133-140.

Auwarter, V., Dresen, S., Weinmann, W., Muller, M., Putz, M., and Ferreiros, N. (2009). 'Spice' and other herbal blends: harmless incense or cannabinoid designer drugs? J Mass Spectrom *44*, 832-837.

Brents, L.K., Reichard, E.E., Zimmerman, S.M., Moran, J.H., Fantegrossi, W.E., and Prather, P.L. (2011). Phase I hydroxylated metabolites of the K2 synthetic cannabinoid JWH-018 retain in vitro and in vivo cannabinoid 1 receptor affinity and activity. PLoS One *6*, e21917.

Brents, L.K., Zimmerman, S.M., Saffell, A.R., Prather, P.L., and Fantegrossi, W.E. (2013). Differential Drug-Drug Interactions of the Synthetic Cannabinoids Jwh-018 and Jwh-073: Implications for Drug Abuse Liability and Pain Therapy. J Pharmacol Exp Ther.

Cheang, W.S., Fang, X., and Tian, X.Y. (2013). Pleiotropic effects of peroxisome proliferator-activated receptor gamma and delta in vascular diseases. Circ J *77*, 2664-2671.

Chhabra, R.S., Pohl, R.J., and Fouts, J.R. (1974). A comparative study of xenobiotic-metabolizing enzymes in liver and intestine of various animal species. Drug Metab Dispos *2*, 443-447.

Chimalakonda, K.C., Bratton, S.M., Le, V.H., Yiew, K.H., Dineva, A., Moran, C.L., James, L.P., Moran, J.H., and Radominska-Pandya, A. (2011a). Conjugation of synthetic cannabinoids JWH-018 and JWH-073, metabolites by human UDP-glucuronosyltransferases. Drug Metab Dispos *39*, 1967-1976.

Chimalakonda, K.C., Moran, C.L., Kennedy, P.D., Endres, G.W., Uzieblo, A., Dobrowolski, P.J., Fifer, E.K., Lapoint, J., Nelson, L.S., Hoffman, R.S., James, L.P., Radominska-Pandya, A., and Moran, J.H. (2011b). Solid-phase extraction and quantitative measurement of omega and omega-1 metabolites of JWH-018 and JWH-073 in human urine. Anal Chem *83*, 6381-6388.

Chimalakonda, K.C., Seely, K.A., Bratton, S.M., Brents, L.K., Moran, C.L., Endres, G.W., James, L.P., Hollenberg, P.F., Prather, P.L., Radominska-Pandya, A., and Moran, J.H. (2012). Cytochrome P450-mediated oxidative metabolism of abused synthetic

cannabinoids found in K2/Spice: identification of novel cannabinoid receptor ligands. Drug Metab Dispos *40*, 2174-2184.

ElSohly, M.A., Gul, W., Elsohly, K.M., Murphy, T.P., Madgula, V.L., and Khan, S.I. (2011). Liquid chromatography-tandem mass spectrometry analysis of urine specimens for K2 (JWH-018) metabolites. J Anal Toxicol *35*, 487-495.

Enayetallah, A.E., French, R.A., Thibodeau, M.S., and Grant, D.F. (2004). Distribution of soluble epoxide hydrolase and of cytochrome P450 2C8, 2C9, and 2J2 in human tissues. J Histochem Cytochem *52*, 447-454.

Every-Palmer, S. (2011). Synthetic cannabinoid JWH-018 and psychosis: an explorative study. Drug Alcohol Depend *117*, 152-157.

Galiegue, S., Mary, S., Marchand, J., Dussossoy, D., Carriere, D., Carayon, P., Bouaboula, M., Shire, D., Le Fur, G., and Casellas, P. (1995). Expression of central and peripheral cannabinoid receptors in human immune tissues and leukocyte subpopulations. Eur J Biochem *232*, 54-61.

Gao, Y., Shao, J., Jiang, Z., Chen, J., Gu, S., Yu, S., Zheng, K., and Jia, L. (2013). Drug enterohepatic circulation and disposition: constituents of systems pharmacokinetics. Drug Discov Today.

Ginsburg, B.C., Schulze, D.R., Hruba, L., and McMahon, L.R. (2012). JWH-018 and JWH-073: Delta(9)-tetrahydrocannabinol-like discriminative stimulus effects in monkeys. J Pharmacol Exp Ther *340*, 37-45.

Glass, M., and Felder, C.C. (1997). Concurrent stimulation of cannabinoid CB1 and dopamine D2 receptors augments cAMP accumulation in striatal neurons: evidence for a Gs linkage to the CB1 receptor. J Neurosci *17*, 5327-5333.

Gunderson, E.W., Haughey, H.M., Ait-Daoud, N., Joshi, A.S., and Hart, C.L. (2012). "Spice" and "K2" herbal highs: a case series and systematic review of the clinical effects and biopsychosocial implications of synthetic cannabinoid use in humans. Am J Addict *21*, 320-326.

Hanna, I.H., Teiber, J.F., Kokones, K.L., and Hollenberg, P.F. (1998). Role of the alanine at position 363 of cytochrome P450 2B2 in influencing the NADPH- and hydroperoxide-supported activities. Arch Biochem Biophys *350*, 324-332.

Howlett, A.C. (2005). Cannabinoid receptor signaling. Handb Exp Pharmacol, 53-79.

Hudson, S., Ramsey, J., King, L., Timbers, S., Maynard, S., Dargan, P.I., and Wood, D.M. (2010). Use of high-resolution accurate mass spectrometry to detect reported and previously unreported cannabinomimetics in "herbal high" products. J Anal Toxicol *34*, 252-260.

Huffman, J.W., Dai, D., Martin, B.R., and Compton, D.R. (1994). Design, synthesis, and pharmacology of cannabimimetic indoles. Bioorg Med Chem Lett *4*, 4.

Jutkiewicz, E.M., Rice, K.C., Carroll, F.I., and Woods, J.H. (2013). Patterns of nicotinic receptor antagonism II: cardiovascular effects in rats. Drug Alcohol Depend *131*, 284-297.

Kochanowski, M., and Kala, M. (2005). Tetrahydrocannabinols in clinical and forensic toxicology. Przegl Lek *62*, 576-580.

Lapoint, J., James, L.P., Moran, C.L., Nelson, L.S., Hoffman, R.S., and Moran, J.H. (2011). Severe toxicity following synthetic cannabinoid ingestion. Clin Toxicol (Phila) *49*, 760-764.

Lauckner, J.E., Hille, B., and Mackie, K. (2005). The cannabinoid agonist WIN55,212-2 increases intracellular calcium via CB1 receptor coupling to Gq/11 G proteins. Proc Natl Acad Sci U S A *102*, 19144-19149.

Lin, H.L., Roberts, E.S., and Hollenberg, P.F. (1998). Heterologous expression of rat P450 2E1 in a mammalian cell line: in situ metabolism and cytotoxicity of N-nitrosodimethylamine. Carcinogenesis *19*, 321-329.

Matsuda, L.A., Lolait, S.J., Brownstein, M.J., Young, A.C., and Bonner, T.I. (1990). Structure of a cannabinoid receptor and functional expression of the cloned cDNA. Nature *346*, 561-564.

Mechoulam, R., and Hanus, L. (2000). A historical overview of chemical research on cannabinoids. Chem Phys Lipids *108*, 1-13.

Michaud, V., Frappier, M., Dumas, M.C., and Turgeon, J. (2010). Metabolic activity and mRNA levels of human cardiac CYP450s involved in drug metabolism. PLoS One *5*, e15666.

Mir, A., Obafemi, A., Young, A., and Kane, C. (2011). Myocardial infarction associated with use of the synthetic cannabinoid K2. Pediatrics *128*, e1622-1627.

Moran, C.L., Le, V.H., Chimalakonda, K.C., Smedley, A.L., Lackey, F.D., Owen, S.N., Kennedy, P.D., Endres, G.W., Ciske, F.L., Kramer, J.B., Kornilov, A.M., Bratton, L.D., Dobrowolski, P.J., Wessinger, W.D., Fantegrossi, W.E., Prather, P.L., James, L.P., Radominska-Pandya, A., and Moran, J.H. (2011). Quantitative measurement of JWH-018 and JWH-073 metabolites excreted in human urine. Anal Chem *83*, 4228-4236.

Munro, S., Thomas, K.L., and Abu-Shaar, M. (1993). Molecular characterization of a peripheral receptor for cannabinoids. Nature *365*, 61-65.

Niederhoffer, N., Schmid, K., and Szabo, B. (2003). The peripheral sympathetic nervous system is the major target of cannabinoids in eliciting cardiovascular depression. Naunyn Schmiedebergs Arch Pharmacol *367*, 434-443.

Ortiz de Montellano, P.R. (2005). Cytochrome P450s: structure, mechanism, and biochemistry, third edn (New York, Kluwer Press).

Pacher, P., and Mechoulam, R. (2011). Is lipid signaling through cannabinoid 2 receptors part of a protective system? Prog Lipid Res *50*, 193-211.

Pant, S., Deshmukh, A., Dholaria, B., Kaur, V., Ramavaram, S., Ukor, M., and Teran, G.A. (2012). Spicy seizure. Am J Med Sci *344*, 67-68.

Peglow, S., Buchner, J., and Briscoe, G. (2012). Synthetic cannabinoid induced psychosis in a previously nonpsychotic patient. Am J Addict *21*, 287-288.

Pertwee, R.G. (2005). Pharmacological actions of cannabinoids. Handb Exp Pharmacol, 1-51.

Pertwee, R.G. (2008). The diverse CB1 and CB2 receptor pharmacology of three plant cannabinoids: delta9-tetrahydrocannabinol, cannabidiol and delta9-tetrahydrocannabivarin. Br J Pharmacol *153*, 199-215.

Poklis, J.L., Amira, D., Wise, L.E., Wiebelhaus, J.M., Haggerty, B.J., and Poklis, A. (2012). Detection and disposition of JWH-018 and JWH-073 in mice after exposure to "Magic Gold" smoke. Forensic Sci Int *220*, 91-96.

Rajasekaran, M., Brents, L.K., Franks, L.N., Moran, J.H., and Prather, P.L. (2013). Human metabolites of synthetic cannabinoids JWH-018 and JWH-073 bind with high affinity and act as potent agonists at cannabinoid type-2 receptors. Toxicol Appl Pharmacol *269*, 100-108.

Robson, P. (2005). Human studies of cannabinoids and medicinal cannabis. Handb Exp Pharmacol, 719-756.

Roman, R.J. (2002). P-450 metabolites of arachidonic acid in the control of cardiovascular function. Physiol Rev *82*, 131-185.

Rudz, R., Schlicker, E., Baranowska, U., Marciniak, J., Karabowicz, P., and Malinowska, B. (2012). Acute myocardial infarction inhibits the neurogenic tachycardic and vasopressor response in rats via presynaptic cannabinoid type 1 receptor. J Pharmacol Exp Ther *343*, 198-205.

Seely, K.A., Brents, L.K., Radominska-Pandya, A., Endres, G.W., Keyes, G.S., Moran, J.H., and Prather, P.L. (2012). A major glucuronidated metabolite of JWH-018 is a neutral antagonist at CB1 receptors. Chem Res Toxicol *25*, 825-827.

Seely, K.A., Prather, P.L., James, L.P., and Moran, J.H. (2011). Marijuana-based drugs: innovative therapeutics or designer drugs of abuse? Mol Interv *11*, 36-51.

Simmons, J., Cookman, L., Kang, C., and Skinner, C. (2011a). Three cases of "spice" exposure. Clin Toxicol (Phila) *49*, 431-433.

Simmons, J.R., Skinner, C.G., Williams, J., Kang, C.S., Schwartz, M.D., and Wills, B.K. (2011b). Intoxication from smoking "spice". Ann Emerg Med *57*, 187-188.

Smith, H.E., Jones, J.P., 3rd, Kalhorn, T.F., Farin, F.M., Stapleton, P.L., Davis, C.L., Perkins, J.D., Blough, D.K., Hebert, M.F., Thummel, K.E., and Totah, R.A. (2008). Role of cytochrome P450 2C8 and 2J2 genotypes in calcineurin inhibitor-induced chronic kidney disease. Pharmacogenet Genomics *18*, 943-953.

Snider, N.T., Kornilov, A.M., Kent, U.M., and Hollenberg, P.F. (2007). Anandamide metabolism by human liver and kidney microsomal cytochrome p450 enzymes to form hydroxyeicosatetraenoic and epoxyeicosatrienoic acid ethanolamides. J Pharmacol Exp Ther *321*, 590-597.

Sobolevsky, T., Prasolov, I., and Rodchenkov, G. (2010). Detection of JWH-018 metabolites in smoking mixture post-administration urine. Forensic Sci Int *200*, 141-147.

Uchiyama, N., Kikura-Hanajiri, R., Ogata, J., and Goda, Y. (2010). Chemical analysis of synthetic cannabinoids as designer drugs in herbal products. Forensic Sci Int *198*, 31-38.

von Weymarn, L.B., Blobaum, A.L., and Hollenberg, P.F. (2004). The mechanism-based inactivation of p450 2B4 by tert-butyl 1-methyl-2-propynyl ether: structural determination of the adducts to the p450 heme. Arch Biochem Biophys *425*, 95-105.

Walker, A.B., Chattington, P.D., Buckingham, R.E., and Williams, G. (1999). The thiazolidinedione rosiglitazone (BRL-49653) lowers blood pressure and protects against impairment of endothelial function in Zucker fatty rats. Diabetes *48*, 1448-1453.

Wiley, J.L., Compton, D.R., Dai, D., Lainton, J.A., Phillips, M., Huffman, J.W., and Martin, B.R. (1998). Structure-activity relationships of indole- and pyrrole-derived cannabinoids. J Pharmacol Exp Ther *285*, 995-1004.

Wintermeyer, A., Moller, I., Thevis, M., Jubner, M., Beike, J., Rothschild, M.A., and Bender, K. (2010). In vitro phase I metabolism of the synthetic cannabimimetic JWH-018. Anal Bioanal Chem *398*, 2141-2153.

Wu, S., Moomaw, C.R., Tomer, K.B., Falck, J.R., and Zeldin, D.C. (1996). Molecular cloning and expression of CYP2J2, a human cytochrome P450 arachidonic acid epoxygenase highly expressed in heart. J Biol Chem *271*, 3460-3468.

Zarzuelo, M.J., Jimenez, R., Galindo, P., Sanchez, M., Nieto, A., Romero, M., Quintela, A.M., Lopez-Sepulveda, R., Gomez-Guzman, M., Bailon, E., Rodríguez-Gómez, I., Zarzuelo, A., Gálvez, J., Tamargo, J., Pérez-Vizcaíno, F., and Duarte, J. (2011). Antihypertensive effects of peroxisome proliferator-activated receptor-beta activation in spontaneously hypertensive rats. Hypertension *58*, 733-743.

Zeldin, D.C., Foley, J., Ma, J., Boyle, J.E., Pascual, J.M., Moomaw, C.R., Tomer, K.B., Steenbergen, C., and Wu, S. (1996). CYP2J subfamily P450s in the lung: expression, localization, and potential functional significance. Mol Pharmacol *50*, 1111-1117.

Zhang, Q., Ma, P., Cole, R.B., and Wang, G. (2006). Identification of in vitro metabolites of JWH-015, an aminoalkylindole agonist for the peripheral cannabinoid receptor (CB2) by HPLC-MS/MS. Anal Bioanal Chem *386*, 1345-1355.

Zhang, Q., Ma, P., Iszard, M., Cole, R.B., Wang, W., and Wang, G. (2002). In vitro metabolism of R(+)-[2,3-dihydro-5-methyl-3-[(morpholinyl)methyl]pyrrolo [1,2,3-de]1,4-benzoxazinyl]-(1-naphthalenyl) methanone mesylate, a cannabinoid receptor agonist. Drug Metab Dispos *30*, 1077-1086.

Zuba, D., Byrska, B., and Maciow, M. (2011). Comparison of "herbal highs" composition. Anal Bioanal Chem *400*, 119-126.

CHAPTER V

Conclusions and Future Directions

Cytochrome P450 2J2 (CYP2J2) is believed to be the P450 most responsible for the metabolism of AA and other polyunsaturated fatty acids (Arnold et al., 2010; Moran et al., 2000; Wu et al., 1996). The highest expression levels of CYP2J2 are in the cardiovascular system, but it is also found at lower levels in other tissues including the liver, gastrointestinal tract, monocytes, macrophages, and brain (Bystrom et al., 2011; Chen et al., 2011; Jiang et al., 2005; Wu et al., 1996; Zeldin et al., 1997; Zeldin et al., 1996)). Interestingly, all of these tissues also express some or all of the components of the endocannabinoid system (ECS) (Han et al., 2009; Pacher et al., 2006; Wright et al., 2008). In order to try to investigate the possible functional relevance of the colocalization of CYP2J2 and the ECS, AEA, an endogenous cannabinoid, and JWH-018, a synthetic cannabinoid, were investigated as possible substrates for CYP2J2.

The data presented in Chapter II characterized the metabolism of AEA by CYP2J2. When incorporated into the standard reconstituted system, recombinant CYP2J2 metabolizes AEA to produce 20-HETE-EA and 5,6-, 8,9-, 11,12-, and 14,15-EET-EAs. Data on the metabolism of AEA by human intestinal microsomes (HIM) were also presented. The metabolites formed during the metabolism of AEA by HIM were the same as those formed by CYP2J2 in the reconstituted system with the additional formation of 19-HETE-EA. The physiological relevance of CYP2J2 activity in the intestine has

previously been suggested by reports of its contribution to the intestinal metabolism of certain drugs (Hashizume et al., 2002; Matsumoto et al., 2002). However, our studies reported in Chapter II suggest that CYP2J2 does not contribute significantly to the intestinal metabolism of AEA. However, in Chapter IV we reported that different lots of commercially available HIM exhibited different product profiles for the metabolism of JWH-018. As a result, the lack of significant involvement of CYP2J2 in intestinal AEA metabolism reported here may not be entirely true and needs to be investigated further with additional lots of HIM.

Our lab has previously studied the metabolism of AEA by human kidney and liver microsomes, HKM and HLM, respectively (Snider et al., 2007). HKM incubated with AEA only yield the 20-HETE-EA, whereas HLM and HIM incubations with AEA produce 19- and 20-HETE-EAs (Snider et al., 2007). Liver microsomes are 2 and 44 times more efficient at catalyzing the formation of 20-HETE-EA than kidney and intestine microsomes, respectively, based on V_{max}/K_m values. HLM produced all four EET-EAs in the presence of AEA, but HIM failed to produce the 14,15-EET-EA, although the other three epoxides were formed. The absence of 14,15-EET-EA formation in HIM is reversed by the addition of an epoxide hydrolase inhibitor to reaction mixtures. Liver microsomes were several orders of a magnitude more efficient at catalyzing the formation of 5,6-, 8,9-, and 11,12-EET-EAs when compared to HIM (Snider et al., 2007). In HLM, the 8,9-EET-EA metabolite is the major epoxide formed in respect to quantity and efficiency, but this is not the case for HIM (Snider et al., 2007). The 5,6-EET-EA metabolite was the major product formed from AEA by HIM based on quantity and efficiency. This metabolite has been reported to activate the CB2 receptor in the

nanomolar range (Snider et al., 2009). As such, there may be some potential physiological relevance for this metabolite in the human gastrointestinal (GI) tract.

Inflammatory bowel diseases (IBD) are characterized by chronic inflammation of all or part of the digestive tract. Crohn's disease is an IBD typically confined to the lower end of the small intestine (Di Carlo and Izzo, 2003). Patients suffer intestinal cramps and spasms, severe diarrhea, rectal bleeding, nausea and vomiting, and loss of appetite and weight that can lead to malnutrition (Britton and Peppercorn, 1997). Some reports indicate that people suffering from Crohn's disease get symptomatic relief by smoking marijuana (Di Carlo and Izzo, 2003). This effect has been attributed to the ability of marijuana to stimulate appetite, alleviate nausea, control spasms, and potentially reduce inflammation (Grinspoon and Bakalar, 1997; Nocerino et al., 2000). Some of these salutatory effects may result from activation of the CB2 receptor by Δ^9-THC. If this is true, there may be a pathophysiological relevance for the 5,6-EET-EA in the inflamed gut.

All of the components of the ECS have been detected in the GI system (Wright et al., 2008). The CB1 receptor is colocalized with choline acetyltransferase in neurons and nerve fibers of the stomach, small intestine, and colon (Kulkarni-Narla and Brown, 2000, 2001). As a result, activation of presynaptic CB1 receptors in myenteric nerves and the submucosal plexus neurons decreases intestinal motility as well as the secretion of gastric acid and intestinal fluids (Di Carlo and Izzo, 2003; Mascolo et al., 2002; Pinto et al., 2002; Wilson and Nicoll, 2002). It is widely known that CB2 receptors are expressed on immune cells and the gut has an abundant supply of immune cells (Cabral and Staab,

2005; Klein, 2005; Lunn et al., 2006). However, the physiological function of the CB2 receptor in the gut has not been well studied.

In inflammatory disorders the ECS becomes overstimulated in the small and large intestine (Di Marzo and Izzo, 2006). Evidence suggests that the levels of endocannabinoids (ECBs) and CB1 receptors are significantly increased during intestinal inflammation (D'Argenio et al., 2006; Izzo et al., 2001). It is believed that the ECBs activate the CB1 receptors to protect against both the epithelial damage and the increased motility observed with intestinal inflammation (Izzo et al., 2003; Massa et al., 2004). However, although intestinal motility is attributed to CB1 receptor activation, in an inflammatory state the CB2 receptor may predominate. In a rat model where the animals are exposed to lipopolysaccharide (LPS) to stimulate inflammation and cause an increase in GI transit, activation of the CB2 receptor exhibited a dose-dependent inhibition of the LPS-induced increase in GI transit to control levels; however, the control of basal GI activity was attributed the to the CB1 receptor activity (Mathison et al., 2004). Moreover, activation of the CB2 receptor has been shown to inhibit the release of inflammatory mediators that are known to encourage intestinal peristalsis (Izzo, 2004; Mathison et al., 2004). The activation of CB2 receptors expressed on human colonic epithelial cells has been found to inhibit the TNF-α-induced release of the inflammatory cytokine interleukin-8 (Ihenetu et al., 2003). Because we identified 5,6-EET-EA as the major AEA metabolite formed in intestinal microsomes and it can activate the CB2 receptor at nanomolar concentrations, these observations may indicate a physiological function for 5,6-EET-EA in the inflamed GI system. However, more studies are needed to confirm this hypothesis.

Data were also presented in Chapter II describing the effect of obesity and a junk food diet on the ability of rat liver microsomes (RLM) to metabolize AEA. Somewhat surprisingly, the RLM did not produce any of the traditional metabolites such as the EET-EAs and HETE-EAs observed in studies of human liver metabolism. However, we were able to identify and monitor the formation of three new metabolites to observe for any influence of obesity and diet on AEA metabolism. Because the identity of these products is unknown, we were unable to quantify the amount of the products formed. To compensate, we used the peak area ratio (unknown metabolite peak area/internal standard peak area) to determine relative amounts of formation. The formation of the two products observed at *m/z* 356 was dramatically increased in the microsomes of livers from obese rats as compared to lean controls fed a normal diet. The junk food diet seemed to have no effect on the formation of these metabolites, but this conclusion will need to be confirmed using liver microsomes prepared from diet-induced obese rats on a junk food diet. On the other hand, the formation of the product monitored at *m/z* 380 was significantly decreased as a result of obesity and even more so as a result of the junk food diet. Completing studies to investigate AEA metabolism by liver microsomes prepared from diet-induced obese rats fed a junk food diet are needed to validate this conclusion. Identification of these products observed at *m/z* 356 and 380 and their biological actions would be the most important step to determine the physiological relevance of altered AEA metabolism in response to diet and obesity.

Due to the opposing patterns of formation for the products observed at *m/z* 356 with regard to the product observed at *m/z* 380, it will be of interest to determine the structures of these compounds, their stabilities in biological systems, and their

interactions with the CB1 and CB2 receptors in order to fully understand the possible physiological relevance of these data. If the compounds observed at *m/z* 356 contain terminal hydroxyl groups and the metabolite at *m/z* 380 contains an epoxide, it would strongly suggest that junk food diets and obesity increase inflammation by a mechanism involving the ECS because terminally hydroxylated fatty acids are believed to be proinflammatory and epoxygenated fatty acids are considered to be anti-inflammatory (Imig, 2012; Morisseau and Hammock, 2013; Spector, 2009; Williams et al., 2010). Thus, it would be necessary to complete similar metabolism studies using some of the essential ω-3 and ω-6 fatty acids such as EPA or AA especially because of their potential involvement in obesity-related inflammation (Kim et al., 2013; Tilley et al., 2001).

The studies conducted in Chapter III investigated AEA metabolism by human liver S9 fractions. The liver S9 fractions formed the same metabolites as those previously reported to be produced by human liver microsomes (Snider et al., 2007). Because soluble epoxide hydrolase inhibitors (sEHIs) have proven to be extremely beneficial in determining the biological activities of the EETs *in vivo*, the potent sEHIs AUDA, APAU, and TPPU were tested for their ability to inhibit the hydrolysis of the EET-EAs by soluble epoxide hydrolases in the S9 preparations. AUDA inhibited the hydrolysis of 14,15-EET-EA with an EC_{50} value of 5.6 μM. At nanomolar concentrations, AUDA increased the levels of 11,12-EET-EA, but at concentrations of 10 μM or higher, AUDA decreased the levels of 5,6-, 8,9-, and 11,12-EET-EA in a dose-dependent manner. APAU increased the levels of all of the EET-EAs; however, only 11,12- and 14,15-EET-EAs exhibited a sigmoidal trend with respect to metabolite levels vs. concentration and their respective EC_{50} values were calculated to be 4.7 and10.4 μM. The significant increases

in the levels of 8,9-, 11,12-, and 14,15-EET-EAs induced by TPPU only occurred sporadically, as a result, the EC_{50} values could not be calculated for this sEHI. Our results suggest that it may be necessary to design sEHIs specific for the EET-EAs, since none of the three sEHIs investigated were able to inhibit sEH-mediated hydrolysis of the four EET-EAs equally. Using siRNA to knockdown sEH and mEH activity in hepatocytes in the presence of AEA would be a more efficient approach and would allow for observation of the biological actions of EET-EAs in a closed cell system. It is possible that this approach may be useful *in vivo*, but several other epoxides are likely to be effected as well making the results difficult to interpret. The development of sEHIs to increase the half-life of the EET-EAs will be extremely useful for determining their biological actions.

The work described in Chapter IV demonstrated that purified human CYP2J2 metabolizes the synthetic cannabinoid JWH-018 primarily to give the ω-1-OH JWH-018 metabolite. Human intestine and liver microsomes were also investigated for their ability to metabolize JWH-018. The products formed by these systems included mono- and di-oxygenated metabolites as well as two 1,2-diol products. It was determined that recombinant CYP2C9 catalyzed the formation of one of the diol products. The same products as well as several more were observed following metabolism by rat heart and liver microsomes. A total of 24 different metabolites were shown to be formed as a result of NADPH-dependent metabolism of JWH-018; however, most of those metabolites were observed in rat microsomes and are not applicable to human metabolism. Additional studies will be required to identify the major hydroxydiol metabolites and determine their affinity and potency at the cannabinoid receptors in order to gain further insights into

their potential relevance as products of this commonly abused substance with a wide array of adverse side effects. If the mechanisms behind these side effects can be elucidated, perhaps treatments to reverse the effects can be developed as well.

Studies on the effects of JWH-018 *in vivo* indicated that although it did not have much of an effect on heart rate, it significantly increased blood pressure in rats. This increase in blood pressure was only partially blocked by pretreatment with the CB1 receptor antagonist AM251. This was not surprising since centrally mediated effects of cannabinoids have previously been shown to dominate over peripheral effects (Rudz et al., 2012). Centrally administered cannabinoids cause an increase in blood pressure, but a decrease in heart rate (Niederhoffer and Szabo, 1999). Because JWH-018 binds to both CB1 and CB2 receptors (Aung et al., 2000), it is possible that the lack of effect on heart rate may have something to do with the CB2 receptor activation or the activation of a non-cannabinoid receptor. Future studies focused on the cardiovascular effects of JWH-018 using a CB2 receptor antagonist may provide information as to the biological relevance of CB2 receptor expression in the cardiovascular system. In addition, a non-selective cannabinoid receptor antagonist will be of interest to investigate the possible involvement of another receptor unrelated to the ECS.

In conclusion, CYP2J2 catalyzes the metabolism of the endogenous cannabinoid AEA and the synthetic cannabinoid JWH-018 to give a variety of hydroxylated and epoxygenated products. It is known that cannabinoids, especially CB2 receptor agonists, can inhibit inflammation (Hanus et al., 1999). Studies investigating the effect of JWH-018 on the metabolism of AA revealed that JWH-018 actually increased CYP2J2-catalyzed formation of the anti-inflammatory EETs. If future studies investigating the

interaction between cannabinoid-based substrates of CYP2J2 and AA have similar effects as JWH-018, this may suggest an alternative mechanism for the anti-inflammatory actions of the ECS, especially since inhibition of CYP2J2 activates inflammatory responses *in vivo* (Deng et al., 2011). Due to the overlap in the expression and functions of CYP2J2 and the ECS, in conjunction with the ability of CYP2J2 to metabolize cannabinoids, there is a potential for CYP2J2 to play a critical role in the metabolic fates of some endogenous ligands of the CB1 and CB2 receptors and thereby modulate the physiological effects of the ECS.

References

Arnold, C., Markovic, M., Blossey, K., Wallukat, G., Fischer, R., Dechend, R., Konkel, A., von Schacky, C., Luft, F.C., Muller, D.N., D.N., Rothe, M., and Schunck, W.H. (2010). Arachidonic acid-metabolizing cytochrome P450 enzymes are targets of {omega}-3 fatty acids. J Biol Chem *285*, 32720-32733.

Aung, M.M., Griffin, G., Huffman, J.W., Wu, M., Keel, C., Yang, B., Showalter, V.M., Abood, M.E., and Martin, B.R. (2000). Influence of the N-1 alkyl chain length of cannabimimetic indoles upon CB(1) and CB(2) receptor binding. Drug Alcohol Depend *60*, 133-140.

Britton, A., and Peppercorn, M.A. (1997). Medical Management of Crohn's Disease (Philadelphia, Lippincott-Raven).

Bystrom, J., Wray, J.A., Sugden, M.C., Holness, M.J., Swales, K.E., Warner, T.D., Edin, M.L., Zeldin, D.C., Gilroy, D.W., and Bishop-Bailey, D. (2011). Endogenous epoxygenases are modulators of monocyte/macrophage activity. PLoS One *6*, e26591.

Cabral, G.A., and Staab, A. (2005). Effects on the immune system. Handb Exp Pharmacol, 385-423.

Chen, C., Wei, X., Rao, X., Wu, J., Yang, S., Chen, F., Ma, D., Zhou, J., Dackor, R.T., Zeldin, D.C., and Wang, D.W. (2011). Cytochrome P450 2J2 is highly expressed in hematologic malignant diseases and promotes tumor cell growth. J Pharmacol Exp Ther *336*, 344-355.

D'Argenio, G., Valenti, M., Scaglione, G., Cosenza, V., Sorrentini, I., and Di Marzo, V. (2006). Up-regulation of anandamide levels as an endogenous mechanism and a pharmacological strategy to limit colon inflammation. FASEB J *20*, 568-570.

Deng, Y., Edin, M.L., Theken, K.N., Schuck, R.N., Flake, G.P., Kannon, M.A., DeGraff, L.M., Lih, F.B., Foley, J., Bradbury, J.A.,Graves, J.P., Tomer, K.B., Falck, J.R., Zeldin, D.C., and Lee, C.R. (2011). Endothelial CYP epoxygenase overexpression and soluble epoxide hydrolase disruption attenuate acute vascular inflammatory responses in mice. FASEB J *25*, 703-713.

Di Carlo, G., and Izzo, A.A. (2003). Cannabinoids for gastrointestinal diseases: potential therapeutic applications. Expert Opin Investig Drugs *12*, 39-49.

Di Marzo, V., and Izzo, A.A. (2006). Endocannabinoid overactivity and intestinal inflammation. Gut *55*, 1373-1376.

Grinspoon, L., and Bakalar, J.B. (1997). Marihuana, the forbidden medicine, Rev. and exp. edn (New Haven, Yale University Press).

Han, K.H., Lim, S., Ryu, J., Lee, C.W., Kim, Y., Kang, J.H., Kang, S.S., Ahn, Y.K., Park, C.S., and Kim, J.J. (2009). CB1 and CB2 cannabinoid receptors differentially

regulate the production of reactive oxygen species by macrophages. Cardiovasc Res *84*, 378-386.

Hanus, L., Breuer, A., Tchilibon, S., Shiloah, S., Goldenberg, D., Horowitz, M., Pertwee, R.G., Ross, R.A., Mechoulam, R., and Fride, E. (1999). HU-308: a specific agonist for CB(2), a peripheral cannabinoid receptor. Proc Natl Acad Sci U S A *96*, 14228-14233.

Hashizume, T., Imaoka, S., Mise, M., Terauchi, Y., Fujii, T., Miyazaki, H., Kamataki, T., and Funae, Y. (2002). Involvement of CYP2J2 and CYP4F12 in the metabolism of ebastine in human intestinal microsomes. J Pharmacol Exp Ther *300*, 298-304.

Ihenetu, K., Molleman, A., Parsons, M.E., and Whelan, C.J. (2003). Inhibition of interleukin-8 release in the human colonic epithelial cell line HT-29 by cannabinoids. Eur J Pharmacol *458*, 207-215.

Imig, J.D. (2012). Epoxides and soluble epoxide hydrolase in cardiovascular physiology. Physiol Rev *92*, 101-130.

Izzo, A.A. (2004). Cannabinoids and intestinal motility: welcome to CB2 receptors. Br J Pharmacol *142*, 1201-1202.

Izzo, A.A., Capasso, F., Costagliola, A., Bisogno, T., Marsicano, G., Ligresti, A., Matias, I., Capasso, R., Pinto, L., Borrelli, F., Cecio, A., Lutz, B., Mascolo, N., and Di Marzo, V. (2003). An endogenous cannabinoid tone attenuates cholera toxin-induced fluid accumulation in mice. Gastroenterology *125*, 765-774.

Izzo, A.A., Fezza, F., Capasso, R., Bisogno, T., Pinto, L., Iuvone, T., Esposito, G., Mascolo, N., Di Marzo, V., and Capasso, F. (2001). Cannabinoid CB1-receptor mediated regulation of gastrointestinal motility in mice in a model of intestinal inflammation. Br J Pharmacol *134*, 563-570.

Jiang, J.G., Chen, C.L., Card, J.W., Yang, S., Chen, J.X., Fu, X.N., Ning, Y.G., Xiao, X., Zeldin, D.C., and Wang, D.W. (2005). Cytochrome P450 2J2 promotes the neoplastic phenotype of carcinoma cells and is up-regulated in human tumors. Cancer Res *65*, 4707-4715.

Kim, J., Li, Y., and Watkins, B.A. (2013). Fat to treat fat: emerging relationship between dietary PUFA, endocannabinoids, and obesity. Prostaglandins Other Lipid Mediat *104-105*, 32-41.

Klein, T.W. (2005). Cannabinoid-based drugs as anti-inflammatory therapeutics. Nat Rev Immunol *5*, 400-411.

Kulkarni-Narla, A., and Brown, D.R. (2000). Localization of CB1-cannabinoid receptor immunoreactivity in the porcine enteric nervous system. Cell Tissue Res *302*, 73-80.

Kulkarni-Narla, A., and Brown, D.R. (2001). Opioid, cannabinoid and vanilloid receptor localization on porcine cultured myenteric neurons. Neurosci Lett *308*, 153-156.

Lunn, C.A., Reich, E.P., and Bober, L. (2006). Targeting the CB2 receptor for immune modulation. Expert Opin Ther Targets *10*, 653-663.

Mascolo, N., Izzo, A.A., Ligresti, A., Costagliola, A., Pinto, L., Cascio, M.G., Maffia, P., Cecio, A., Capasso, F., and Di Marzo, V. (2002). The endocannabinoid system and the molecular basis of paralytic ileus in mice. FASEB J *16*, 1973-1975.

Massa, F., Marsicano, G., Hermann, H., Cannich, A., Monory, K., Cravatt, B.F., Ferri, G.L., Sibaev, A., Storr, M., and Lutz, B. (2004). The endogenous cannabinoid system protects against colonic inflammation. J Clin Invest *113*, 1202-1209.

Mathison, R., Ho, W., Pittman, Q.J., Davison, J.S., and Sharkey, K.A. (2004). Effects of cannabinoid receptor-2 activation on accelerated gastrointestinal transit in lipopolysaccharide-treated rats. Br J Pharmacol *142*, 1247-1254.

Matsumoto, S., Hirama, T., Matsubara, T., Nagata, K., and Yamazoe, Y. (2002). Involvement of CYP2J2 on the intestinal first-pass metabolism of antihistamine drug, astemizole. Drug Metab Dispos *30*, 1240-1245.

Moran, J.H., Mitchell, L.A., Bradbury, J.A., Qu, W., Zeldin, D.C., Schnellmann, R.G., and Grant, D.F. (2000). Analysis of the cytotoxic properties of linoleic acid metabolites produced by renal and hepatic P450s. Toxicol Appl Pharmacol *168*, 268-279.

Morisseau, C., and Hammock, B.D. (2013). Impact of soluble epoxide hydrolase and epoxyeicosanoids on human health. Annu Rev Pharmacol Toxicol *53*, 37-58.

Niederhoffer, N., and Szabo, B. (1999). Effect of the cannabinoid receptor agonist WIN55212-2 on sympathetic cardiovascular regulation. Br J Pharmacol *126*, 457-466.

Nocerino, E., Amato, M., and Izzo, A.A. (2000). Cannabis and cannabinoid receptors. Fitoterapia *71 Suppl 1*, S6-12.

Pacher, P., Batkai, S., and Kunos, G. (2006). The endocannabinoid system as an emerging target of pharmacotherapy. Pharmacol Rev *58*, 389-462.

Pinto, L., Izzo, A.A., Cascio, M.G., Bisogno, T., Hospodar-Scott, K., Brown, D.R., Mascolo, N., Di Marzo, V., and Capasso, F. (2002). Endocannabinoids as physiological regulators of colonic propulsion in mice. Gastroenterology *123*, 227-234.

Rudz, R., Schlicker, E., Baranowska, U., Marciniak, J., Karabowicz, P., and Malinowska, B. (2012). Acute myocardial infarction inhibits the neurogenic tachycardic and vasopressor response in rats via presynaptic cannabinoid type 1 receptor. J Pharmacol Exp Ther *343*, 198-205.

Snider, N.T., Kornilov, A.M., Kent, U.M., and Hollenberg, P.F. (2007). Anandamide metabolism by human liver and kidney microsomal cytochrome p450 enzymes to form hydroxyeicosatetraenoic and epoxyeicosatrienoic acid ethanolamides. J Pharmacol Exp Ther *321*, 590-597.

Snider, N.T., Nast, J.A., Tesmer, L.A., and Hollenberg, P.F. (2009). A cytochrome P450-derived epoxygenated metabolite of anandamide is a potent cannabinoid receptor 2-selective agonist. Mol Pharmacol *75*, 965-972.

Spector, A.A. (2009). Arachidonic acid cytochrome P450 epoxygenase pathway. J Lipid Res *50 Suppl*, S52-56.

Tilley, S.L., Coffman, T.M., and Koller, B.H. (2001). Mixed messages: modulation of inflammation and immune responses by prostaglandins and thromboxanes. J Clin Invest *108*, 15-23.

Williams, J.M., Murphy, S., Burke, M., and Roman, R.J. (2010). 20-hydroxyeicosatetraeonic acid: a new target for the treatment of hypertension. J Cardiovasc Pharmacol *56*, 336-344.

Wilson, R.I., and Nicoll, R.A. (2002). Endocannabinoid signaling in the brain. Science *296*, 678-682.

Wright, K.L., Duncan, M., and Sharkey, K.A. (2008). Cannabinoid CB2 receptors in the gastrointestinal tract: a regulatory system in states of inflammation. Br J Pharmacol *153*, 263-270.

Wu, S., Moomaw, C.R., Tomer, K.B., Falck, J.R., and Zeldin, D.C. (1996). Molecular cloning and expression of CYP2J2, a human cytochrome P450 arachidonic acid epoxygenase highly expressed in heart. J Biol Chem *271*, 3460-3468.

Zeldin, D.C., Foley, J., Goldsworthy, S.M., Cook, M.E., Boyle, J.E., Ma, J., Moomaw, C.R., Tomer, K.B., Steenbergen, C., and Wu, S. (1997). CYP2J subfamily cytochrome P450s in the gastrointestinal tract: expression, localization, and potential functional significance. Mol Pharmacol *51*, 931-943.

Zeldin, D.C., Foley, J., Ma, J., Boyle, J.E., Pascual, J.M., Moomaw, C.R., Tomer, K.B., Steenbergen, C., and Wu, S. (1996). CYP2J subfamily P450s in the lung: expression, localization, and potential functional significance. Mol Pharmacol *50*, 1111-1117.